

GLOBAL MEF2 TARGET GENE ANALYSIS IN SKELETAL AND CARDIAC MUSCLE

STEPHANIE ELIZABETH WALES

A DISSERTATION SUBMITTED TO THE FACULTY OF GRADUATE STUDIES IN  
PARTIAL FULFILLMENT OF THE REQUIREMENTS FOR THE DEGREE OF

DOCTOR OF PHILOSOPHY

GRADUATE PROGRAM IN BIOLOGY  
YORK UNIVERSITY  
TORONTO, ONTARIO

FEBRUARY 2016

© Stephanie Wales 2016

## ABSTRACT

A loss of muscle mass or function occurs in many genetic and acquired pathologies such as heart disease, sarcopenia and cachexia which are predominantly found among the rapidly increasing elderly population. Developing effective treatments relies on understanding the genetic networks that control these disease pathways. Transcription factors occupy an essential position as regulators of gene expression. Myocyte enhancer factor 2 (MEF2) is an important transcription factor in striated muscle development in the embryo, skeletal muscle maintenance in the adult and cardiomyocyte survival and hypertrophy in the progression to heart failure. We sought to identify common MEF2 target genes in these two types of striated muscles using chromatin immunoprecipitation and next generation sequencing (ChIP-seq) and transcriptome profiling (RNA-seq). Using a cell culture model of skeletal muscle (C2C12) and primary cardiomyocytes we found 294 common MEF2A binding sites within both cell types. Individually MEF2A was recruited to approximately 2700 and 1600 DNA sequences in skeletal and cardiac muscle, respectively. Two genes were chosen for further study: DUSP6 and Hspb7. DUSP6, an ERK1/2 specific phosphatase, was negatively regulated by MEF2 in a p38MAPK dependent manner in striated muscle. Furthermore siRNA mediated gene silencing showed that MEF2D in particular was responsible for repressing DUSP6 during C2C12 myoblast differentiation. Using a p38 pharmacological inhibitor (SB 203580) we observed that MEF2D must be phosphorylated by p38 to repress DUSP6. This established a unique model whereby MAPK signaling results in repression of a MAPK phosphatase. The second MEF2 target gene studied was Hspb7, a small heat shock protein that is highly expressed in striated muscle. Using a combination of bioinformatic and biochemical analysis we found that AP-1 can inhibit Hspb7 transcription, in contrast to MEF2 which activates it. Additionally, the glucocorticoid receptor (GR) regulates Hspb7 in a manner dependent on the presence of MEF2. We also demonstrate an *in vivo* role for Hspb7 in autophagy which has significant implications in skeletal muscle wasting. Overall we found that MEF2A regulates distinct gene networks in skeletal and cardiac muscle, yet important shared target genes such as DUSP6 and Hspb7 also illustrate that MEF2A regulates some common gene programs that are critical to striated muscle health.

## **ACKNOWLEDGEMENTS**

This was a lot of fun but also a lot of hard work! I couldn't have done it without my parents, Genevieve and Stephen, who taught me to value education and encouraged me to pursue science and learning (and still do!). I wouldn't be who I am without their love. To my husband, Mike, for keeping me laughing even when things got (seemingly) overwhelming. Also to Amanda, Al, Mike Sr., Heather, Leah and Kristyn: your encouragement and friendship have been so important to me!

I would like to thank my supervisor, Dr. McDermott, for training me in all of the different aspects of science and academia. I would also like to thank Dr. Blais for teaching me how to do bioinformatic analyses and my committee members Dr. Scheid and Dr. Cheung for giving me direction during my PhD.

There is no way I could have made it through six years without great lab members – Thank you for your support and criticism over the years. In particular I'd like to thank Nezeke for training me from the beginning and helping me talk through my problems. Also, thank-you Sara for being so great to work with on all of our collaborations.

# TABLE OF CONTENTS

<b>ABSTRACT .....</b>	<b>ii</b>
<b>ACKNOWLEDGEMENTS .....</b>	<b>iii</b>
<b>TABLE OF CONTENTS .....</b>	<b>iv</b>
<b>LIST OF TABLES .....</b>	<b>vi</b>
<b>LIST OF FIGURES .....</b>	<b>vii</b>
<b>LIST OF ABBREVIATIONS .....</b>	<b>ix</b>
<b>CHAPTER I: Literature Review .....</b>	<b>1</b>
1. Development of striated muscle.....	1
1.1 Early development of the mesodermal lineages.....	1
1.2 Skeletal myogenesis.....	2
1.3 Cardiogenesis.....	7
1.4 Striated muscle contraction.....	9
2. The role and regulation of MEF2.....	11
2.1 Overview of MEF2 .....	11
2.2 Role of MEF2 during vertebrate development and adult tissue maintenance.....	13
2.3 MEF2 protein:protein interactions .....	15
2.4 MEF2 and chromatin remodelling .....	17
2.5 Regulation of MEF2 by post-translational modifications .....	22
2.6 MEF2 and miRNA gene silencing .....	23
3. Therapeutic relevance of MEF2 in skeletal and cardiac muscle disease .....	24
3.1 Metabolic disease.....	24
3.1a: <i>Diabetes</i> .....	25
3.1b: <i>Pathways regulating muscle atrophy</i> .....	28
3.2 Role of MEF2 in skeletal muscle regeneration .....	33
3.3 Role of MEF2 in cell death and muscle atrophy.....	37
3.4 Cardiac hypertrophy.....	39
4. Summary of Literature Review.....	42

<b>CHAPTER II: Statement of Purpose.....</b>	<b>43</b>
<b>CHAPTER III: Global MEF2 target gene analysis in cardiac and skeletal muscle reveals novel regulation of DUSP6 by p38MAPK-MEF2 signaling.....</b>	<b>44</b>
<b>CHAPTER IV: Regulation of Hspb7 by MEF2 and AP-1 in muscle atrophy.</b>	<b>73</b>
<b>CHAPTER V: Summary of Dissertation.....</b>	<b>106</b>
<b>CHAPTER VI: Future Directions and Conclusions.....</b>	<b>108</b>
<b>REFERENCES.....</b>	<b>111</b>
<b>APPENDIX .....</b>	<b>149</b>
Expanded Material and Methods .....	149
Bioinformatic Analysis .....	156

## **LIST OF TABLES**

### **Chapter I: Literature Review**

Table 1. MEF2 and human disease.....	34
--------------------------------------	----

### **Chapter IV: Regulation of Hspb7 by MEF2 and AP-1 in muscle atrophy**

Table S1. MEF2A target genes that contain AP-1 consensus sequences within the enriched DNA fragment.....	104
--	-----

Table S2. siRNA oligonucleotides.....	105
---------------------------------------	-----

Table S3. Primers used in qRT-PCR and ChIP-qPCR.....	105
--	-----

# LIST OF FIGURES

## **Chapter I: Literature Review**

Figure 1. Mesoderm specification during embryogenesis.....	2
Figure 2. Somite specification.....	3
Figure 3. Embryonic myogenesis.....	4
Figure 4. Satellite cell activation.....	6
Figure 5. The formation of cardiogenic mesoderm during embryogenesis.....	8
Figure 6. The regulation of MEF2 by upstream factors.....	13
Figure 7. The role of MEF2 in epigenetic gene regulation.....	21
Figure 8. Mechanisms of glucose storage.....	25
Figure 9. Insulin signaling in metabolic tissue.....	26
Figure 10. Protein ubiquitination and degradation in muscle.....	30
Figure 11. Pathways of autophagy.....	31
Figure 12. Transcriptional regulators of muscle atrophy.....	33
Figure 13. Structure of the sarcomere and DAG complex.....	36
Figure 14. The role of MEF2 in the progression to heart failure.....	39
Figure 15. MEF2 and $\beta$ -adrenergic signaling.....	41

## **Chapter III: Global MEF2 target gene analysis in cardiac and skeletal muscle reveals novel regulation of DUSP6 by p38MAPK-MEF2 signaling**

Figure 1. Identification of MFE2A target genes in myoblasts and cardiomyocytes using ChIP-exo.....	53
Figure 2. RNA-seq analysis of MEF2A depleted skeletal myoblasts.....	56
Figure 3. Functional analysis of MEF2A target genes.....	60
Figure 4. siRNA mediated gene silencing of MEF2 in cardiomyocytes or myoblasts induces DUSP6 expression.....	63
Figure 5. MEF2D inhibits DUSP6 in a p38MAPK dependent manner in myoblasts.....	65
Figure S1. MEF2A and MEF2D protein expression during C2C12 differentiation.....	69
Figure S2. Efficiency of siRNA mediated gene silencing.....	70
Figure S3. Effect of p38MAPK inhibition on MEF2 expression.....	70
Figure S4. siRNA catalog numbers (Sigma-Aldrich).....	71
Figure S5. Primers used in ChIP-qPCR.....	72

Figure S6. Primers used in qRT-PCR.....72

**Chapter IV: Regulation of Hspb7 by MEF2 and AP-1 in muscle atrophy**

Figure 1. A comparison of MEF2A and AP-1 target genes in skeletal muscle.....81

Figure 2. Differential recruitment of MEF2A and AP-1 to actin cytoskeletal target genes.....84

Figure 3. MEF2A and AP-1 regulation of actin cytoskeletal genes.....87

Figure 4. Aging and dexamethasone-induced atrophy cause changes in MEF2A/AP-1  
cytoskeletal target genes.....90

Figure 5. MEF2 and AP-1 regulate atrophy induced Hspb7 expression.....92

Figure 6. Role of Hspb7 in skeletal muscle atrophy.....95

Figure 7. Hspb7 expression is associated with autophagy.....97

Figure 8. Hspb7 expression prevents induction of autophagy markers in response to fasting.....98

Figure 9. Model for the regulation and role of Hspb7 in atrophic conditions.....100



## LIST OF ABBREVIATIONS

Akt	Protein Kinase B
ANP	Atrial natriuretic peptide
AP-1	Activator protein 1
Ash2L	Ash2 (absent, small or homeotic)-like
ATF	Activating transcription factor
Bag3	Bcl-2-associated athanogene 3
bHLH	Basic helix loop helix
CaMKII	calcium/calmodulin-dependent protein kinase II
CASA	Chaperone assisted selective autophagy
CHIP	Carboxy-terminus of Hsc70 interacting protein
ChIP-seq	Chromatin immunoprecipitation sequencing
CM	Cardiomyocyte
CMA	Chaperone mediated autophagy
DAG	Dystrophin associated glycoprotein
Dex	Dexamethasone
DM	Differentiation medium
DM1	Myotonic dystrophy 1
DMD	Duchenne muscular dystrophy
DUSP6	Dual specificity phosphatase 6
ERK	Extracellular signal regulated kinase
FIRE	Fast intronic regulatory element
FGF	Fibroblast growth factor
FKHR	Forkhead
FoxO	Forkhead box protein
Fra	Fos related antigen
Glut4	Glucose transporter 4
GM	Growth medium
GO	Gene ontology
GSK3- $\beta$	Glycogen synthase- $\beta$
HAT	Histone acetyltransferase
HDAC	Histone deacetylase
HMT	Histone methyltransferase
HP1	Heterochromatin protein 1
Hspb7	Heat shock protein family B (small) member 7
ICM	Inner cell mass
IGF	Insulin-like growth factor
IGFR	Insulin-like growth factor receptor
iPSC	Induced pluripotent stem cell
JNK	c-Jun N-terminal kinase

lncRNA	Long non-coding RNA
Lmod3	Leiomodin 3
LSD1	Lysine specific demethylase 1
MADS	MCM1, agamous, deficiens, serum response factor
MB	Myoblast
MCK	Muscle creatine kinase
MEF2	Myocyte enhancer factor 2
MAPK	Mitogen-activated protein kinase
miRNA	microRNA
MLL	Mixed lineage leukemia
MRF	Myogenic regulatory factor
MT	Myotube
mTOR	Mammalian target of rapamycin
MyHC	Myosin heavy chain
MyLC	Myosin light chain
MyoG	Myogenin
ncRNA	Non-coding RNA
NMJ	Neuromuscular junction
NURF	Nucleosome remodeling factor
Pax	Paired box protein
PRC2	Polycomb repressive complex 2
PGC-1 $\alpha$	Peroxisome proliferative activated receptor gamma coactivator-1 $\alpha$
PI3K	Phosphatidylinositol-4,5-bisphosphate 3-kinase
PKA	Protein kinase A
PKC	Protein kinase C
PTM	Post-translational modification
RNA-seq	RNA sequencing
RSRF	Related serum response factor
RyR	Ryanodine receptor
SERCA	SR Ca <sup>2+</sup> -ATPase
Six	Sine oculis homeobox homolog
SRF	Serum response factor
SURE	Slow upstream regulatory element
SWI/SNF	Switch/sucrose non-fermenting
TA	Tibialis anterior
TAC	Transverse aortic constriction
TAD	Transcriptional activation domain
TGF- $\beta$	Transforming growth factor- $\beta$
TSA	Trichostatin A
TSS	Transcription start site
T-tubules	Transverse tubules

## **CHAPTER I: Literature Review**

### **1. Development of striated muscle**

#### **1.1 Early development of the mesodermal lineages**

Early embryonic patterning is complex and relies on the strict co-ordination of gene expression. The processes that occur during development often follow a similar pattern during adult cell differentiation, therefore understanding developmental processes may improve our understanding and treatment of post-natal diseases. The earliest differentiation of cells in mammals is at the transition from the 16-cell stage, when the collection of cells referred to as the morula, transition to become the blastocyst (1, 2). At this point, the blastocyst consists of two types of specialized cells: trophoblast cells that make up the outer layer of cells, called the trophectoderm, and the inner cell mass (ICM), a group of pluripotent cells (2). The blastocyst also contains an empty cavity called the blastocoel. The ICM will separate into two cell types, the hypoblast, a layer of cells in contact with the blastocoel, and the epiblast, a collection of cells adjacent to the hypoblast (2). The hypoblast will not contribute to the embryo but it is critical in the formation of extraembryonic tissues that contribute to the yolk sac (2, 3). One of the most important processes to occur during development is gastrulation, development of the three germ layers (endoderm, mesoderm and ectoderm), all of which arise from the epiblast (4). The movement of epiblast cells to a region called the primitive streak sets up gastrulation and initiates cell commitment in a posterior to anterior direction (4). The primitive streak is formed between the epiblast and hypoblast. As cells migrate from the epiblast to the primitive streak they become committed to the endoderm and mesoderm lineages. The first cells that migrate to the primitive streak become endodermal cells, and move anterior alongside the primitive streak towards the hypoblast, displacing it (5). As the primitive streak moves toward the anterior end, cells become committed to different mesodermal lineages and migrate to a space between the new endodermal layer and the existing epiblast. Finally, the ectoderm is derived from the remaining cells of the epiblast that do not migrate to the primitive streak (5).

During gastrulation the neural tube also develops in a process called neurulation which is critical as it sets up the anterior-posterior axis (6, 7). The dorsal cells that do not migrate to the primitive streak are ectodermal cells and form a structure called the neural plate which will fold inward and form the neural tube, as well as neural crest cells, and surface ectoderm. The neural crest cells (discussed below) that arise from neurulation are often referred to as the fourth germ

layer since they give rise to fundamental tissues including connective tissue of the face, arteries, smooth muscle, the peripheral nervous system and other tissues (8). As the neural tube is formed, the mesoderm can be separated into four independent regions: lateral plate mesoderm, paraxial mesoderm, chordamesoderm and intermediate mesoderm (**Figure 1**), which are formed in a posterior-anterior direction as the primitive streak moves anterior (1, 9). Each type of mesoderm will contribute to distinct tissues. Lateral plate mesoderm will form the heart (cardiac muscle), other visceral organs, and connective tissue. Paraxial mesoderm will form skeletal muscle, bones, cartilage and dermis of the back. The notochord is derived from chordamesoderm and will assist in neural tube formation. Intermediate mesoderm will form kidneys, gonads and ducts.

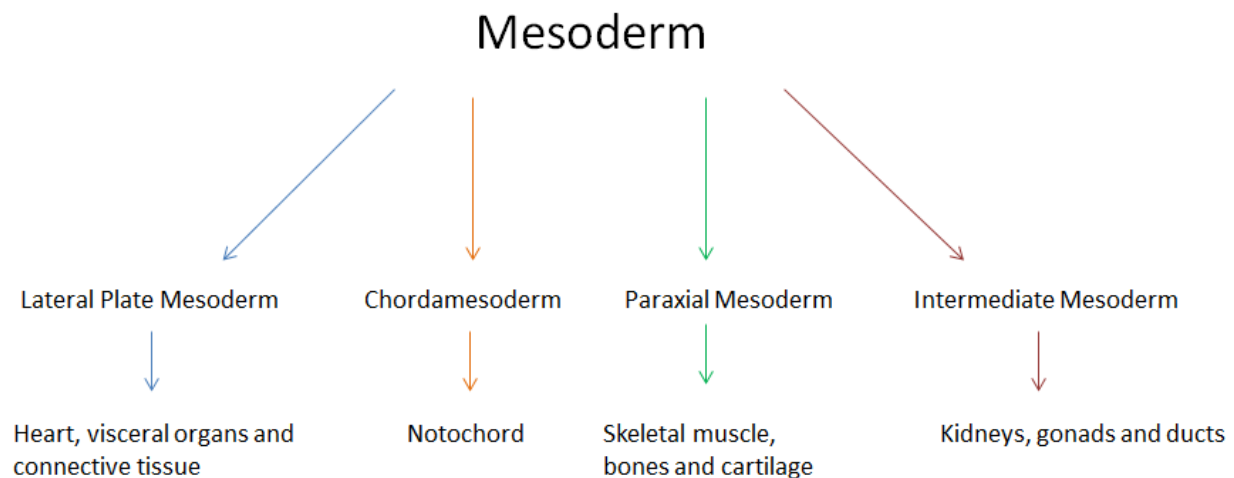


**Figure 1.** Mesoderm specification during embryogenesis. Mesoderm will become specified into four sub-types: Lateral plate mesoderm, chordamesoderm, paraxial mesoderm and intermediate mesoderm.

## 1.2 Skeletal myogenesis

Paraxial mesoderm runs alongside the notochord and neural tube. Upon receiving the proper cues, paraxial mesoderm becomes segmented into blocks of mesoderm called somites, from which all skeletal muscle is derived, in a process called somitogenesis (10). This occurs in an anterior-posterior direction and is dependent first on Notch signaling and then on Hox signaling (11, 12). Notch signaling triggers paraxial mesoderm to separate at specific segments along the anterior-posterior axis, forming the somites (11). Then, somites become specialized depending on the Hox transcription factors they express (9, 13). The first derivative to form is the sclerotome, and then the dermomyotome (**Figure 2**). Cells on the ventral side of the somite and

closest to the neural tube will form the sclerotome and then become bones and tendon (9). The dermomyotome will form several different tissue including skeletal muscle, endothelial cells, and brown fat (9, 14).

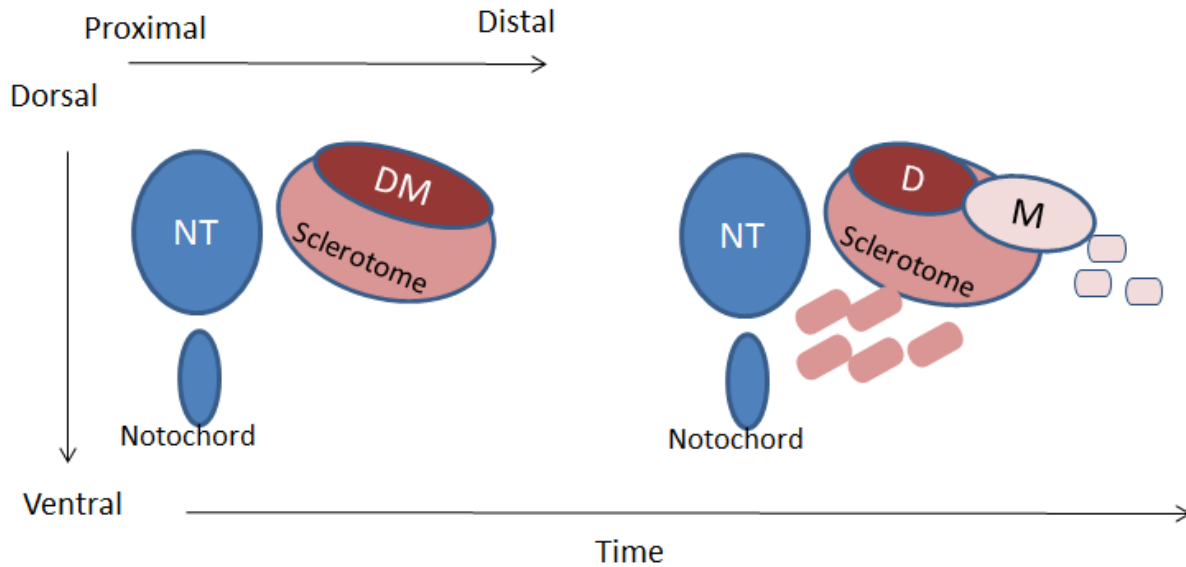


**Figure 2.** Somite specification. During development the somite is initially composed of the sclerotome and dermomyotome (DM). As cells of the sclerotome migrate away, the distal myotome (M) and dorsal dermatome (D) become distinct regions.

The cells of the sclerotome will migrate toward the neural tube and at this point the dermomyotome begins to differentiate into the myotome and dermatome. The remaining parts of the somite are made of three cell types and are arranged such that the myotome is between the migrating sclerotome (ventral) and the dermatome (dorsal). The dermatome will form connective tissue, skin and fat. The dorsal-most region of the myotome (epaxial myotome) will pattern muscles of the back (15). Cells of the ventral myotome (hypaxial myotome) will begin to migrate toward early limb buds (15) and interact with migrating neural crest cells in a “kiss and run” manner that is Notch-signaling dependent (16). Neural crest cells express the Notch ligand Delta, which interacts with the Notch receptor in migrating muscle precursor cells of the myotome. Activation of Notch signaling in these precursor cells leads to expression of the first myogenic commitment marker, Myf5 (16).

In general there are two main myogenic events: during development and in the adult in the form of skeletal muscle satellite stem cells. Although there are some differences, both of these

processes promote myogenesis by initiating a three step process: Determination, Commitment, and Differentiation (**Figure 3**). Determination of cells to mesodermal origin during somitogenesis begins with expression of paired domain transcription factors Pax3 and Pax7. Loss of Pax3 activity results in various defects in neural tube closure and heart development that result in perinatal and *in utero* lethality (17, 18). Pax3 mutants also develop a severe limb muscle phenotype caused by a failure for cells to migrate to the limb buds (19–22). Pax7<sup>-/-</sup> mice have normal muscle development but die perinatally and lack satellite cells (23, 24). Dominant fusion mutants of the DNA binding domain of Pax3 and Pax7 to the transcriptional activation domains of Forkhead/Foxo1 (Pax3-FKHR and Pax7-FKHR) are found in rhabdomyosarcoma, a cancer with skeletal muscle properties (25, 26). Pax3 is expressed as early as unsegmented paraxial mesoderm and expression is maintained until commitment markers are expressed (21). Pax7 expression, however, is delayed until somites are formed and is predominantly localized to the dermomyotome (27, 28).

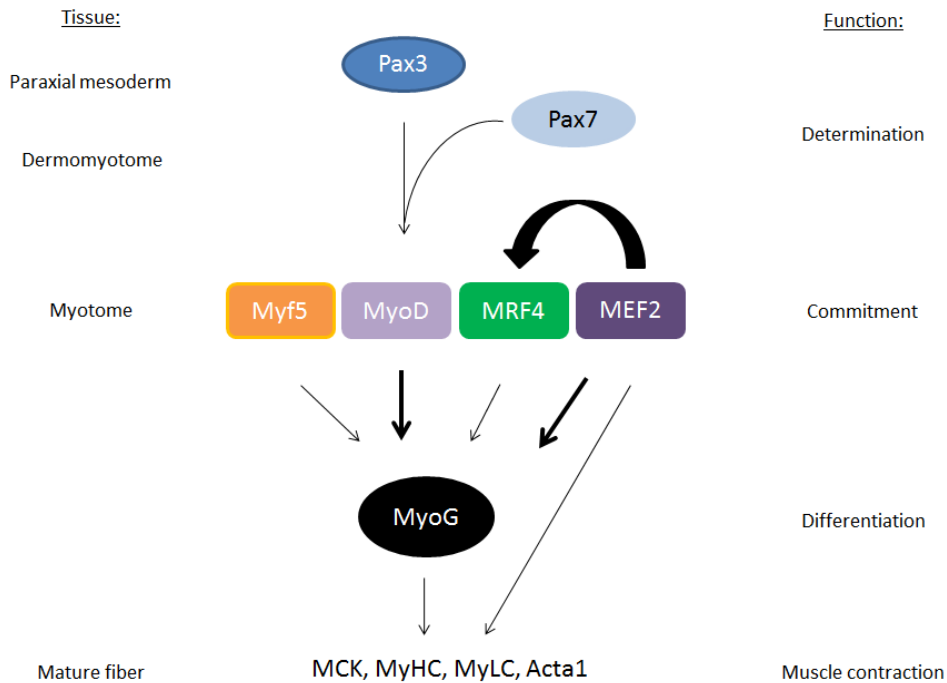


**Figure 3.** Embryonic myogenesis. Pax3 is expressed in the unsegmented paraxial mesoderm and specifies mesoderm fate. Pax3<sup>+</sup> cells can produce other types of mesodermal-derived cells. Pax7 is not detected until the dermomyotome is formed and Pax7<sup>+</sup> cells can form only cells of the myogenic lineage. Three MRFs (Myf5, MyoD and MRF4) and MEF2 are expressed in the myotome in committed muscle precursor cells. MyoD and MEF2 in particular induce MyoG, the fourth MRF which together with MEF2 activates genes related to muscle contraction. MEF2 can also contribute to expression of MRF4.

Commitment to myogenesis is initiated by the expression of Myf5, MRF4 and MyoD which are three of four members of the family of basic helix-loop-helix (bHLH) Muscle Regulatory Factors (MRFs) and regulate transcription through recognition of an E-box consensus sequence (CANNTG) in combination with E proteins E12/E47 (29). Individual deletion of Myf5 but not MyoD or MRF4 in genetic mouse models is lethal yet muscle is able to develop relatively unaffected in all cases (30–33). If Myf5 and MyoD are simultaneously deleted from the genome, muscles are unable to form (34). Similarly loss of MRF4 in combination with either Myf5 or MyoD results in improper commitment and differentiation of muscle (35, 36). This indicates a redundant function of some MRFs. Expression of MRFs is regulated by upstream factors such as Pax3/7. Initially, Pax3 directly regulates Myf5 expression in combination with other upstream signaling such as Notch, Wnt and Sonic hedgehog that are dependent on the compartment of the somite (epaxial, hypaxial or dermomyotome) relative to the notochord (37, 38). As the cells of the myotome migrate to the limb buds Pax3 and Pax7 expression becomes reduced, however a population of Pax3+Pax7+ cells persists and resides adjacent to developing fibers beneath the basal lamina (39). MyoD is expressed downstream of Pax3/7 and Myf5 however the precise mechanism during somitogenesis is unclear. One possible mechanism regulating MyoD expression is Notch signaling as there is evidence that Notch represses MyoD expression in Myf5+ cells (40). Additionally, Notch can block the transcriptional activity of MyoD (41). It is not until expression of a fourth MRF, Myogenin (MyoG) that myoblasts begin to terminally differentiate, which other MRFs cannot compensate for as it activates functional myogenic genes that contribute to muscle contraction (42).

Additional regulation of myogenesis both in the embryo and adult are Six transcription factor (Six1,4) and their co-factor Eya1/2, which have a role upstream of Pax3 during somitogenesis (43, 44) but can also regulate myogenesis via MRF expression in the embryo (45) and in adult muscle regeneration (46). Myocyte Enhancer Factor 2 (MEF2; see The role and regulation of MEF2) is a transcription factor that is also expressed in the somites that is necessary for muscle development (47). microRNA (48), epigenetic regulation (49) and co-factor recruitment (e.g. by histone deacetylases class I and II) have also been shown to have a role in muscle specification (50).

Mature skeletal muscle has regenerative capacity due to quiescent muscle precursor cells called satellite cells that reside atop the myofibers between the basal lamina and sarcolemma

**(Figure 4).** These adult stem cells were derived from Pax3+/Pax7+ cells from the dermomyotome, localize between the basal lamina and sarcolemma during embryonic development and eventually become Pax7+/Pax3- (39, 51, 52). Following injury, myofibers can be repaired through activation of satellite cells which may differentiate and contribute to the myofiber or asymmetrically divide and retain quiescence. Single myofiber isolation has been a useful method that allows *ex vivo* detection of satellite cell activation. Polarity of satellite cell division determines whether cells will become part of the myofibers or remain quiescent. In an apical-basal division, Myf5 is the first commitment marker activated (28) and this is through Pax7 recruitment to the *Myf5* gene (53). As the satellite cell divides asymmetrically, the cell closest to the sarcolemma becomes Pax7+Myf5+ while the apical cell, in contact with the basal lamina remains Pax7+Myf5- (54). Shortly thereafter Pax7+Myf5+ cells will begin to express MyoD however Pax7 and MyoD toggle between quiescence and myogenesis as Pax7 can inhibit MyoD transcriptional activity (55), indicating additional factors are required to trigger full commitment to myogenesis. Finally, as terminal differentiation begins all Pax7 expression is lost, MyoD becomes fully active, and MyoG is expressed. This decrease in Pax7 is hypothesized to be due in part because of Myogenin expression but the mechanism remains unclear (56).

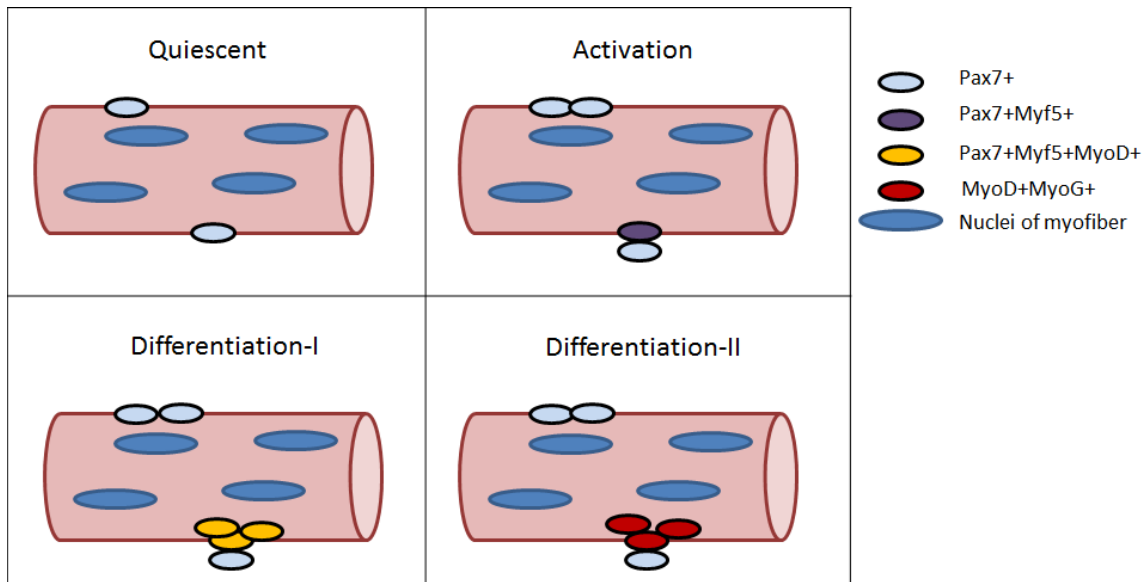


**Figure 4.** Satellite cell activation. In uninjured muscle Pax7+ cells are quiescent and reside between the sarcolemma of the myofiber and the basal lamina. Activation of Pax7+ cells can result in symmetric or asymmetric division. In asymmetric division the cell closest to the sarcolemma will express Myf5. These cells will proliferate to expand the myoblast population and activate commitment marker MyoD. When Pax7 expression becomes reduced, MyoD can activate terminal differentiation marker MyoG, which further reduces Pax7 expression.



Wnt and Notch signaling have been implicated in early skeletal muscle development and recent research has assessed how these pathways may regulate the satellite cell niche to assist in the treatment of various myopathies. Canonical Wnt signaling has been shown to promote Type I (slow-oxidative) muscle fiber formation and differentiation of satellite cells (57, 58). Non-canonical Wnt signaling regulated by Wnt7a and the receptor Fzd7, however, maintain the satellite cell population by encouraging symmetric cell division (59). This is in part accomplished by fibronectin, an extracellular matrix protein co-operates with Wnt7a signaling to create a satellite cell niche (60). Asymmetric division has been documented to be regulated by Notch signaling (61) and miRNAs, such as microRNA-489 (62). In aged muscle, which have reduced regenerative capability, satellite cell activation is impaired because of reduced Delta-1 expression (63).

### **1.3 Cardiogenesis**

The heart is one of the most complex organs in the body, and it is the first to be formed during embryogenesis. The mammalian heart is made of four chambers: the right and left atria, and the right and left ventricles. Within the heart there are different types of specialized cells including smooth muscle, endothelial cells, fibroblasts, pacemaker cells, purkinje fibers, myocardial (cardiac muscle) cells and epicardial cells that are distributed within one of three layers: the endocardium (endothelial cells; interior layer), myocardium (contractile cardiomyocytes) and epicardium (connective tissue; exterior layer) (64). Furthermore, there are different types of myocardial cells, atrial and ventricular myocytes, which adds further complexity to heart development. This section of the review will focus on development of the myocardium (cardiogenic mesoderm).

Lateral plate mesoderm will form somatic and splanchnic mesodermal cells from which connective tissue and visceral organs (e.g. the heart) are derived, respectively (65). Cells that make up lateral plate mesoderm must migrate through the primitive streak to either side of the neural tube, at the distal most regions of the embryo, adjacent to the somites and intermediate mesoderm (66, 67) (**Figure 5**). Once here, cells on the dorsal region adjacent to the ectoderm are somatic mesoderm while adjacent to the endoderm is splanchnic mesoderm on the ventral region. In the anterior region of the gastrula, splanchnic mesoderm will become committed towards cardiogenic mesoderm (endocardial endothelial cells, atrial and ventricular myocytes) while hemangiogenic mesoderm (blood and blood vessels) will form in the posterior region (67).

Cardiogenic mesoderm is shaped into two paired endocardial tubes in a region referred to as the primary or first heart field (FHF), adjacent to the developing gut and ventral to the neural tube, and will quickly develop into the early heart tube and left ventricle (68). A second wave of cardiac progenitors known as the secondary heart field (SHF) arises near the FHF and will form the right ventricle and outflow tract (69). These cardiac progenitors in both the FHF and SHF express early cardiac markers such as Gata4, Nkx2-5 and Tbx5 which are all transcription factors required for commitment to the heart lineage (70–73). Each endocardial tube will move towards the midline and fuse into the primitive heart tube. Since these genes are only expressed in early cardiac progenitors, staining or lacZ reporter mice containing the promoters of these genes can be visualized as a crescent shape in the embryo, therefore, the region in which the earliest cardiac progenitor cells are found are often referred to as the cardiac crescent (74). Gata4 is one of the earliest markers required in heart development as homozygous null mice do not develop a heart tube (71, 73). From here a series of sophisticated processes occur including heart looping and chamber formation under the direction of differentiation factors such as Hand1 and Hand2 (which are found in the left and right ventricle, respectively (75, 76)), Nodal and Lefty-1/2 (77). MEF2 and serum response factor (SRF) are also required in heart development (78, 79). In mice the cardiac crescent is detected at E7 and a fully functional heart is formed by E14.5 (80).

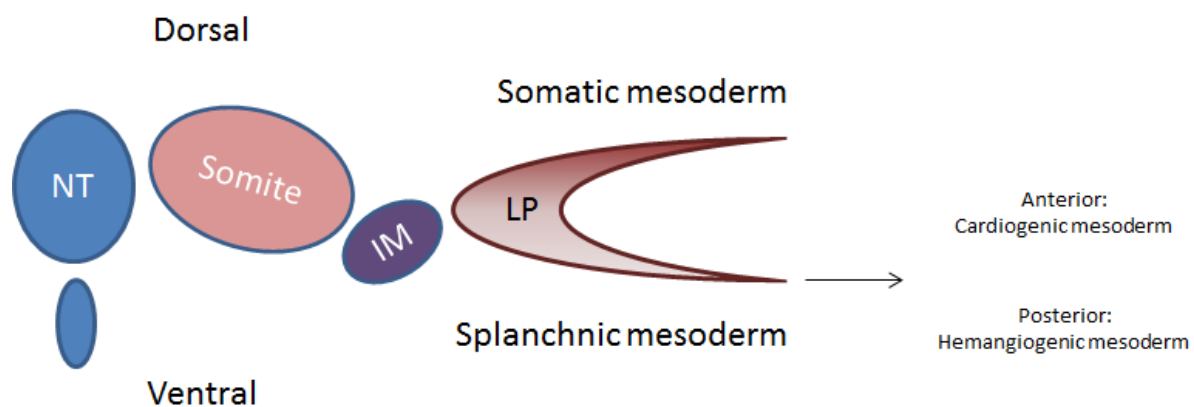


**Figure 5.** The formation of cardiogenic mesoderm during embryogenesis. Somatic and splanchnic mesoderm develops from the dorsal and ventral regions of lateral mesoderm, respectively. Splanchnic mesoderm then becomes cardiogenic mesoderm in the anterior compartment of the embryo or hemangiogenic mesoderm in the posterior end. NT: Neural tube; IM: Intermediate mesoderm; LP: Lateral plate mesoderm.

Cardiac and skeletal muscles differ in their regenerative capacity as the heart does not contain a significant source of precursor cells that may replenish the cardiomyocyte pool (81–84). Therefore, little can be done intrinsically to recover heart function following cardiac stress or myocardial infarction (heart attack), which results in significant cardiomyocyte death (85). Instead the adult heart compensates for loss of cardiomyocytes by undergoing cardiac hypertrophy, resulting in left ventricle thickening to increase blood flow output (86). This compensatory mechanism depends on a gene program similar to what is observed during development and is therefore referred to as activation of the fetal cardiac gene program (87). This hypertrophic response is ultimately debilitating to the organism and results in heart failure (see Therapeutic relevance of MEF2).

#### **1.4 Striated muscle contraction**

Formation of functional skeletal and cardiac muscle is characterized by the sarcomere which is the fundamental unit of contraction. It is made up of polymers of contractile proteins,  $\alpha$ -actin and myosin, which are organized into thin and thick filaments, respectively. Blocks of sarcomeres form myofibrils, which in skeletal muscle are then bundled to form myofibers or multi-nucleated muscle cells. In cardiac muscle, cells remain mononucleated and branched. Connecting each sarcomere to the sarcolemma and the extracellular matrix (ECM) are protein complexes called costameres, which provide stability to myofibers and mediate signaling from the extracellular space (88, 89) (see Therapeutic relevance of MEF2). Myosin is an ATPase hexamer composed of two myosin heavy chains (MyHC) and four myosin light chains (MyLC) that utilize ATP energy to pull actin scaffolds to produce a muscle contraction (90–92). In a non-contracted muscle, myosin binding sites on actin are hidden by tropomyosin. Troponin is a protein that interacts with and controls the location of tropomyosin on actin and contains regulatory calcium binding sites. Contraction can only be induced in the presence of intracellular calcium, which displaces inhibitory tropomyosin-troponin complexes from the myosin binding sites on actin (93).

Skeletal muscle contraction may be elicited by  $\beta$ -adrenergic signaling or nervous regulation. Skeletal muscles are innervated and when a nerve elicits an action potential it secretes acetylcholine from the terminal cleft into the space between the nerve and the muscle fiber, termed the neuromuscular junction (NMJ). Acetylcholine receptors on the muscle fibers will then activate ligand-gated sodium channels, allowing entry of sodium to the muscle fibers and

depolarization of the skeletal muscle fiber (94). Invaginations of the sarcolemma into the muscle fiber are called transverse-tubules (T-tubules), which allow the action potential to trigger contraction efficiently. The sarcoplasmic reticulum will release calcium into the intracellular space upon muscle depolarization. This is regulated by a class of calcium channels on the sarcoplasmic reticulum called Ryanodine Receptors (RyR1 in skeletal muscle) (95, 96) and dihydropyridine receptors (voltage gated L-type calcium channels) on the sarcolemma (97). Once released, intracellular calcium migrates to troponin and initiates tropomyosin relocation, allowing myosin to bind to actin. In a relaxed state, myosin is poised for contraction and contains ADP and phosphate. If myosin is able to bind actin, a power stroke or contraction occurs and ADP and the phosphate group are released from myosin. ATP is required to allow myosin to be released from actin, resulting in relaxation and the formation of ADP and phosphate, and myosin is then placed in an active position. Flight of fight molecules such as adrenaline and epinephrine can also cause contraction of skeletal muscle through  $\beta$ -adrenergic signaling which mediates intracellular calcium release (98, 99).

Skeletal myofibers in vertebrates can be grouped into four main fiber types (I, IIa, IIb and IIx) which correspond to the expression of various isoforms of myosin. These fiber types vary in the rate of contraction, twitch duration, morphology and metabolism (100). Differences in metabolism are dependent on whether a muscle fiber uses glycolysis or oxidative phosphorylation as a primary source of ATP production (101). Type I muscle is referred to as slow twitch (slow-oxidative) muscle since it contracts more slowly, but can have longer twitch duration because it uses oxidative phosphorylation as the source of ATP. These muscle types have an abundance of mitochondria. On the other hand, Type II fibers are fast twitch (fast-oxidative or fast-glycolytic), since they are able to contract much faster and with more power but for shorter periods of time. Type II fibers therefore rely less on mitochondria and glycolytic Type IIb and IIx have the least amount. The factor that determines Type I fiber type formation over Type II is Peroxisome proliferative activated receptor gamma coactivator-1 $\alpha$  (PGC-1 $\alpha$ ) (102), a transcriptional regulator that drives a number of cell processes, including mitochondrial biogenesis (see Therapeutic relevance of MEF2). The heart primarily relies on oxidative phosphorylation for energy production but differences between atrial and ventricular cardiomyocytes can be seen in gene expression and physiological assays (103).

Unlike skeletal muscle, cardiac muscle contraction is involuntary. The depolarization of cardiac cells relies on a combination of sodium and calcium voltage gated channels. First sodium and calcium ions slowly enter cardiomyocytes via leaky ion channels and then into neighbouring cells via gap junctions. This causes the cardiac myocyte to become depolarized and if the cell reaches threshold, voltage gated sodium channels will open (104). Next L-type voltage gated calcium channels, found along cardiac muscle and within T-tubules (105, 106) are activated and further drive depolarization. Calcium is released from the SR via RyR2 and contraction proceeds. The speed of contraction is regulated by pacemaker cells which do not require regulation from the nervous system to function but respond to flight or fight molecules such as adrenaline and acetylcholine which modulate heartrate. Restoration of intracellular calcium stores to the SR in both types of striated muscle is regulated by SR Ca<sup>2+</sup>-ATPase (SERCA) of which there are several isoforms (107, 108).

Generation of skeletal and cardiac muscle from mesoderm is complex and each requires two highly specific gene programs, however, to be functional these tissues rely on the basic unit of the sarcomere for contraction and express many similar contractile genes. Additionally, these diverse gene programs rely on the transcription factor MEF2.

## **2. The role and regulation of MEF2**

### **2.1 Overview of MEF2**

An important transcriptional regulator in cardiac and skeletal muscle formation is Myocyte Enhancer Factor 2 (MEF2). MEF2 is a member of the MADS (MCM1, Agamous, Deficiens, SRF) box family of transcription factors that contain a conserved protein domain and recognize an A/T rich DNA binding sequence (109). MADS-box proteins are found across kingdoms: MCM1 is found in yeast, Agamous and Deficiens are in plants, and SRF and MEF2 are expressed in animals.

MEF2 was originally identified in the late 1980s as a novel transcription factor with high DNA binding affinity to muscle creatine kinase (MCK) (110) and further shown in the early 1990's to have strong sequence similarity to SRF and was therefore termed Related to Serum Response Factor (RSRF) (109). This similarity was identified by the highly conserved consensus sequences between SRF (CC(A/T)<sub>6</sub>GG) and MEF2/RSRF (C/T)TA(AT)<sub>4</sub>TA(G/A) (109, 110). Although these two cis elements are functionally distinct, a hybrid SRF and MEF2 consensus sequence (CCATTTATAG) was characterized by L'honore et al. (111) which is temporally

regulated first by SRF in satellite cells and later by MEF2 in myofibers. Across tissues, MEF2 can have different binding consensus sequences, as observed by Andres et al. (112) who determined that MEF2 consensus sequences in the brain but not striated muscle require an additional five nucleotides upstream of C/TTA. Position weight matrices of MEF2 consensus sequences demonstrate that the A/T rich core is primarily made of adenine (113). MEF2 has been found to share its consensus sequence with the TATA boxes upstream of some genes such as MRF4 (114). This was discovered to have functional significance in *Drosophila* where it was shown that after infection by mycobacterium, MEF2 phosphorylation at T20 is lost, and instead MEF2 is recruited to compound MEF2-TATA box sequences found on immune-responsive promoters (115).

*C. elegans* and *Drosophila* express one MEF2 gene, however in more complex organisms such as vertebrates, MEF2 activity and regulation is more elaborate as there are four MEF2 genes (A-D) (116). Preliminary studies determined that the predominant role for MEF2 was to regulate several muscle specific genes involved in metabolism and muscle structure such as MCK, MyLC, cardiac myosin light chain 2A and later found to also regulate aldolase, troponin, desmin and in skeletal muscle MyoG (110, 117–121). Using mutagenesis in *Drosophila*, MEF2 was shown to be involved in cardiac and smooth muscle development, but necessary for myoblast differentiation not myoblast formation (122). The four MEF2 genes in vertebrates however are involved in a wider range of cell and tissue development such as myogenic cells (including skeletal, cardiac and smooth muscle) as well as various other cell types such as neurons, bone and immune cells (T and B cells) (123–130).

The protein domains within MEF2 can be divided into three sections: The MADS box and MEF2 domain in the N terminus, which together regulate DNA binding, dimerization and co-factor interaction (131), and a transcriptional activation domain (TAD) in its C terminus (**Figure 6**) which can be regulated by a variety of post-translational mechanisms (47). In MEF2C the MADS box is within residues 1-56 and the MEF2 domain is from 57-85 (131). The MADS and MEF2 domains are highly conserved across MEF2 isoforms while the C-terminal is highly divergent. This C-terminal sequence heterogeneity provides the opportunity for MEF2 isoforms to differentially regulate the same genes in response to different cues. Within the C-terminal on all MEF2 isoforms is a nuclear localization sequence (132).

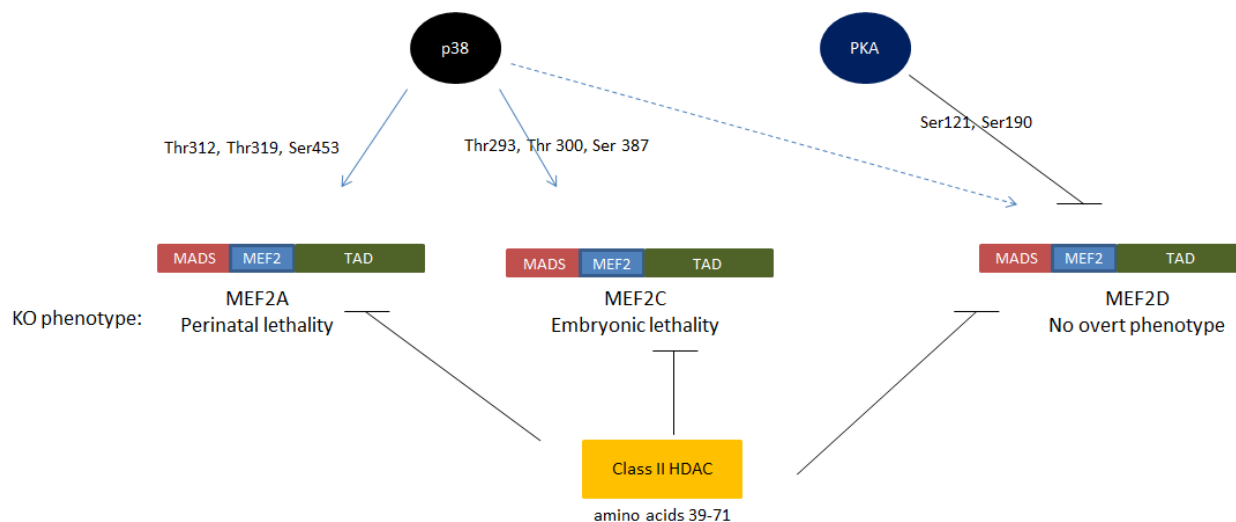


**Figure 6.** The regulation of MEF2 by upstream factors. MEF2 regulation by two kinases, p38 and PKA has been well characterized. Direction phosphorylation of MEF2A and C by p38 has been documented. PKA phosphorylates MEF2D at two sites that mediate MEF2D repression. Class II HDACs directly inhibit MEF2 activity by binding within amino acid 39-71 of MEF2 proteins.

## 2.2 Role of MEF2 during vertebrate development and adult tissue maintenance

MEF2 is essential to development. Using *in situ* hybridization in mouse embryos, *Mef2a-d* can be detected in the early cardiac, skeletal muscle and nervous systems. *Mef2c* is the earliest MEF2 isoform to be expressed in the development of several tissues. For example, *Mef2c* is first expressed in the cardiac mesoderm at day 7.5 post-coitum, then at day 9 in the myotome and later at 11.5 pc in the telencephalon (124, 126). *Mef2c* expression is not detected until *Myf5* and *Myogenin* are expressed in the myotome, followed by *Mef2a* and *Mef2d* (126). In cardiac mesoderm, *Mef2c* is expressed prior to formation of the primitive heart tube (126). *Mef2b* is expressed in a pattern similar to *Mef2c*, and MEF2B can activate the MEF2 consensus sequence, however this isoform does not appear to have a unique role from the other MEF2 isoforms during development as null mice are phenotypically normal (133). MEF2 can also be detected in both the developing and adult brain (124, 127).

Global gene deletion analysis of MEF2 in mice revealed that only MEF2C is embryonic lethal due to impaired left ventricle looping (78). MEF2A null mice survive gestation but die as neonates due to severe cardiac muscle defects but do not show overt skeletal muscle phenotypes (134). MEF2D deficient mice are phenotypically normal unless exposed to cardiac stress, in which they show improved cardiac function (129, 135).

To find tissue-specific roles for MEF2, conditional mutations have been used. Part of the challenge to these experiments, however, is that because MEF2 can function as a hetero- or homodimer, different MEF2 isoforms often have a redundant role and can compensate for each other. Conditional deletion of MEF2A or MEF2D from skeletal muscle results in muscles that are phenotypically normal however skeletal muscle specific deletion of MEF2C results in perinatal lethality and decreased sarcomere integrity (136). This was accomplished using two Cre-lox systems with an early (Myogenin) or late (MCK) myogenic promoter driving recombination. Early deletion of *Mef2c* from skeletal muscle resulted in lethality on post-natal day 1, however, loss of *Mef2c* did not affect viability if deleted later in development under the control of MCK (136). In a parallel study using morpholino knockdown of MEF2C or -D in zebrafish resulted in impaired thick filament formation of the sarcomere (137). Skeletal muscle-specific deletion of MEF2A does not cause any developmental defects (134) but *in vitro*, dominant negative mutations of MEF2A blocks myoblast differentiation indicating MEF2A has a role in skeletal myogenesis (138). Indeed mice with global MEF2A deficiency show impaired muscle regeneration (139). To account for functional redundancy between MEF2 isoforms in skeletal muscle regeneration Liu et al. (140) generated *Mef2a*, *Mef2c* and *Mef2d* muscle specific knockout mice in Pax7+ cells. In contrast to Snyder et al. (139) who saw defects in muscle regeneration in globally deficient MEF2A mice this study concluded that only in the case of triple MEF2 deletion was muscle regeneration reduced and when cultured, myoblasts could not terminally differentiate (140).

Type I muscle fiber type specification is also regulated by MEF2. This has been demonstrated by isolating two regulatory elements from Troponin I slow and fast genes, the slow upstream regulatory element (SURE) and a fast intronic regulatory element (FIRE) which are expressed in slow or fast twitch fibers, respectively (121). MEF2 was only able to activate the SURE enhancer, not the FIRE enhancer (141). Fiber-type specific MCK enhancers have been found in slow and fast twitch muscle but both are regulated by MEF2 (142, 143). Shortly thereafter, it was shown that fiber type switching was primarily governed by PGC-1 $\alpha$  which acts as a co-factor to enhance MEF2 activity (102). Exercise can enhance MEF2 activity in MEF2-lacZ sensor mice, particularly in Type II glycolytic fibers, which the authors hypothesize to indicate a conversion to Type I muscle (144). Additionally Potthoff et al. (145) found that loss of either MEF2C or MEF2D decreased Type I slow oxidative fiber formation.



Based on MEF2 expression during development and knockout experiments, MEF2 proteins have differential roles during development and adulthood. MEF2C is crucial for early cardiac and skeletal muscle development, however MEF2A and MEF2D have a role in post-natal heart function and stress compensation and also in adult skeletal muscle regeneration. Additionally, MEF2 regulates Type I fiber formation. These *in vivo* mutational assays implicate a role for MEF2 in metabolic and striated muscle diseases.

### **2.3 MEF2 protein:protein interactions**

The transcriptional activity of MEF2 is well documented to be heavily influenced by co-factor interactions as well as post-translational modifications, direct targeting by microRNAs, alternate splicing and epigenetic modifications. Like many transcription factors, MEF2 functions as a hetero- or homodimer. In skeletal muscle, a MEF2A homodimer is most prominent although MEF2A:MEF2D heterodimers also exist (146). In the adult heart, MEF2A and MEF2D are predominately expressed (134). The consequences of MEF2 dimer composition can influence gene expression based on differential regulation of MEF2 isoforms by post-translational modification or co-factor interaction. For example, MEF2D is negatively regulated by PKA (147) and alternative splice variants of MEF2D can determine recruitment of HDAC4 (discussed below) (148) which could lead to repression of gene expression. Loss of MEF2D may result in alternative MEF2 dimer composition such as a MEF2A homodimer. Indeed global deletion of MEF2D does not affect development but interestingly provides protection from cardiac stress (135) whereas MEF2A deficient mice develop severe heart defects and paradoxically, expression of MEF2 target genes related to cardiac hypertrophy is enhanced (134). Based on these findings, the composition of MEF2 subunits should be considered in future studies.

Skeletal muscle-specific MEF2 interacting partners MyoD and MyoG, were some of the first proteins documented to interact with MEF2 (149, 150). In a myogenic conversion assay using 10T1/2 cells, MEF2A was shown to synergize with MyoD to promote muscle differentiation but it was not sufficient to induce differentiation on its own (149). Since then the number of MEF2 binding proteins has grown exponentially, and these interactions are often tissue and context dependent. For example, Myocardin is a muscle specific protein that can be modified into two respective splice variants (151). The shorter isoform is expressed in smooth muscle and interacts with SRF exclusively, while the longer isoform is cardiac specific and can also interact with MEF2 in addition to SRF. During embryogenesis Myocardin expression in the

somites represses skeletal muscle differentiation (152). A Myocardin protein family member called MASTR is highly expressed in skeletal muscle and can interact with MEF2 to regulate MyoD expression during satellite cell differentiation (153). MEF2 also interacts with key transcription factors involved in cardiogenesis including Gata4 (154) and Tbx5 (155).

The involvement of MEF2 in several signaling pathways including Wnt, Notch and TGF- $\beta$  has been documented in our lab. Recently, MEF2 and  $\beta$ -catenin, a terminal protein effector in the canonical Wnt pathway, have been shown to directly interact (156, 157). As discussed above, non-canonical Wnt signaling has been associated with satellite cell symmetric division while canonical Wnt signaling has been associated with satellite cell proliferation and differentiation (58, 158). Precocious activation of canonical Wnt signaling via GSK3- $\beta$  inhibitors induces satellite cell differentiation and expression of Follistatin, an antagonist of Myostatin, in a MyoG-dependent manner (58). Similarly, Wnt signaling is involved in several aspects of heart maintenance including cardiomyocyte death (159). Mesenchymal stem cells that are recruited to the damaged heart release Secreted Frizzled receptors (Sfrps) which act as antagonists of Wnt signaling and prevent ischemia-induced cardiomyocyte death (159). Whether MEF2 is directly involved in Wnt signaling during satellite cell regeneration or cardiomyocyte apoptosis has not been determined.

Notch signaling is a unique pathway in that it requires physical cell contact between the cell containing the Notch receptor and the cell expressing the Notch ligand, Delta or Jagged. *In vitro* Notch signaling reduces MEF2C DNA-binding and blocks myogenesis by a direct interaction between the Ankyrin-repeat domains of Notch and MEF2C (160). A downstream Notch co-factor (MAML) can also interact with MEF2, however in this case, MAML promotes MEF2 transcriptional activity (161). Upon Notch signaling, MAML is displaced from MEF2 and is instead recruited to the Notch transcriptional complex (161). Using a yeast two-hybrid screen (162) Strawberry Notch (Sbno1) was found to be a binding partner of MEF2D. Sbno1 was identified using mutational analyses in *Drosophila* which demonstrated phenotypic mutations similar to loss of function mutations in Notch signaling (163). The exact role of Sbno1 remains unclear. In C2C12 myoblasts Sbno1 inhibits MEF2 transcriptional activity and prevents myogenesis (Jahan, S unpublished). In contrast, Notch and MEF2 synergistically contribute to the metastasis of epithelial cells in *Drosophila* (164).

The majority of TGF- $\beta$  signaling results in repression of myogenesis (e.g. TGF $\beta$ -1 (165, 166)) or promotes muscle degradation (e.g. Myostatin (167)). By contrast, a related family member, GDF-11 had been recently shown to activate muscle regeneration and reduce cardiac hypertrophy using heterochronic parabiosis between young and aged mice (168). GDF-11 is very similar to Myostatin and therefore the scientific veracity of GDF-11 as a rejuvenation factor has been called into question (169). The crosstalk between TGF- $\beta$  signaling and MEF2 activity during myogenesis has been unclear. MEF2 was shown to interact with canonical Smad2 *in vitro* in a p38MAPK-dependent manner to promote gene expression (170) but another study showed that Smad3 could repress MEF2 (171). Quinn et al. (170) speculated that MEF2 activity may be repressed by TGF- $\beta$  in high serum conditions and synergize with Smad proteins if TGF- $\beta$  is received after differentiation has begun in low serum conditions.

These examples highlight that MEF2 is implicated in many ubiquitous signaling pathways yet much work remains to be done to decipher the precise protein:protein interactions that mediate these effects.

#### **2.4 MEF2 and chromatin remodelling**

Epigenetics is the sequence independent modification of chromatin that may regulate gene expression. This includes DNA methylation of cytosine and guanine repeats, termed CpG islands, histone modifications and non-coding RNA (ncRNA). It is the combined effect of transcription factors and epigenetics that determine whether or not a gene is transcribed.

DNA packaging is dependent on the nucleosome, a multimeric protein complex around which the DNA double helix is wound. The proteins within a nucleosome are called histones, a basic protein family that facilitate the packaging of DNA. There are five types of histone proteins: H1, a linker histone, and four core histones (H2A, H2B, H3 and H4). The nucleosome core is made up of an octamer of two of each core histone, around which approximately 146 nucleotides are looped (172, 173). Linking each nucleosome is a span of 40-60 additional nucleotides where H1 can bind, which stabilizes the nucleosome by increasing the number of nucleotides coiled around the histone octamer to 166 base pairs (174). H1 also facilitates further DNA packaging and has an affinity for methylated DNA which strengthens the repression of genes (175–177).

Nucleosomes may be repositioned via ATP-dependent chromatin remodelling complexes such as SWI/SNF (switch/sucrose non-fermenting) or NURF (nucleosome remodeling factor)

(178, 179). Nucleosome stability also has implications in gene expression and is regulated by histone modifying enzymes which target specific residues on histones to compress or relax DNA through a variety of PTMs such as ubiquitination, sumoylation, and phosphorylation however, acetylation and methylation are two of the better studied histone modifications. The interaction between histones and DNA is mediated by positively charged residues within histone proteins which are attracted to the negative charges in DNA. Several histone PTMs utilize this electrostatic attraction as a mechanism of control over DNA expression to affect not only chromatin structure, but also the recruitment of other proteins such as transcription factors to DNA. In most cases, histone PTMs target the histone tail, located at the amino terminal in histones. Histone acetylation generally relaxes DNA compaction by neutralizing the positive charges within the basic histone, and therefore this modification is associated with active transcription (180, 181). Histone methylation can indicate active or repressed genes depending on which histone residue is targeted. Two histone methylation markers commonly used in gene expression analyses are H3K4me3 and H3K27me3 for active and repressed gene expression, respectively (182, 183). In some cases the same residue within the histone may be targeted for acetylation or methylation such as H3K9 which is methylated to induce heterochromatin assembly but acetylated to maintain an active chromatin state (184).

Epigenetic and co-factor recruitment to MEF2 target genes is necessary for myogenesis and is implicated in cardiac disease. One of the best studied MEF2 interactions is with class II histone deacetylase (HDAC4, 5, 7 and 9). Among all HDACs, only class II has a MEF2 interacting domain (185) which contacts with MEF2 at the N terminus (amino acid 39-71) where the MADS and MEF2 domains are found. Sub-cellular localization of class II HDACs is regulated by calcium/calmodulin-dependent protein kinase (CaMK) which directly phosphorylates class II HDACs and results in its exportation from the nucleus, and therefore dissociation from MEF2, via chaperone protein 14-3-3 (186–188). Class II HDACs contain a catalytic domain which serves to deacetylate histones, however, their repression of MEF2 transcriptional activity is not dependent on this domain but instead predominantly through steric blockage (185). The nuclear export of class II HDACs is required for skeletal myogenesis in a CaMK dependent manner (189). In cardiac hypertrophy the CaMK-MEF2-HDAC signalling cascade has been studied extensively (86). Constitutively active CaMKIV results in HDAC nuclear exclusion and activates MEF2 in the heart resulting in cardiac hypertrophy (190).

Genetic deletion of HDAC9 also results in cardiac hypertrophy, and when crossed with MEF2-lacZ mice, there is enhanced MEF2 activity (191). HDAC9 has the unique ability to form a negative feedback loop, as MEF2 directly binds to and regulates HDAC9 gene expression (192). HDAC9 also has an alternative splice variant called MEF2-interacting transcriptional repressor (MITR) which interacts with and represses MEF2 but has no catalytic domain (193). In cardiomyocytes Backs et al. (194) presented evidence indicating that the nuclear export of HDAC4 is evaded by alternative splicing in response to PKA signaling, such that only the inhibitory MEF2 binding domain moves to the nucleus, and the domain recognized by 14-3-3 is no longer present (194). In contrast to HDACs, p300/CBP are histone acetyl-transferases that are required for skeletal muscle differentiation and can directly interact with bHLH proteins and MEF2 (195–197). More recently, the MEF2-HDAC interaction has been implicated in mesenchymal-epithelial transition (MET) that happens during somatic cells reprogramming to iPS cells (198). The authors argue that MEF2 prevents MET during reprogramming and that class II HDACs are necessary to inhibit MEF2 signaling and allow reprogramming of fibroblasts to occur.

Trichostatin A (TSA) is an HDAC inhibitor (HDACi) which targets the zinc dependent catalytic domain of Class I, II and IV HDACs to inhibit deacetylase activity. In muscle cell culture, TSA promotes myogenesis (199). BML-210 could be a promising HDACi as it blocks the interaction between MEF2 and HDAC4 (200). Using class II specific HDACi *in vivo*, however, may indirectly target protective effects of HDACs. Using a muscle-specific HDAC4 deficient mouse model, Pax7 and its downstream targets are downregulated, indicating a critical role for HDAC4 in satellite cell activation and regeneration (201).

Histone methylation is found on lysine and arginine residues and can signify active or repressed chromatin, depending on which histones and residues are targeted. An important feature of histone methylation that differs from acetylation is that multiple methyl groups can be added to the targeted residue (mono-, di- or tri-methylated). Histone methylation is regulated by histone methyltransferase (HMT) and histone demethylase. H3K27 trimethylation is regulated by a complex of proteins including Ezh2, Suz12 and Eed which together form a regulatory complex called Polycomb repressive complex 2 (PRC2). In myoblasts H3K27me3 is present on the Myogenin promoter, but Suz12 knockdown decreases this histone modification and results in an increased expression of *Myogenin* RNA (202). Recent studies have identified important HMT

and histone demethylase to be dependent on MEF2 interacting partners, MyoD and class II HDACs. When HDAC4/5 and MITR are associated with MEF2, they recruit Heterochromatin Protein 1 (HP1) which may associate with histone methyltransferase SUV39H1, thereby resulting in H3K9 methylation and gene silencing (**Figure 7A**) (203). H3K4 may be di or trimethylated by the Mixed Lineage Leukemia (MLL) histone methyltransferase complex which corresponds to poised and active transcription, respectively. Using an *in vitro* muscle cell line MEF2D, and to a lesser extent MEF2C, were shown to recruit the MLL subunit Ash2L which provides the transcriptionally permissive mark H3K4me3 in a p38 dependent manner to muscle specific promoters (**Figure 7B**) (204). Brg1, an ATP-dependent helicase and SWI/SNF chromatin remodeling enzyme was shown to be necessary for p38 to induce myogenesis (205) and later MEF2D, Myogenin and Brg1 were shown to interact on late muscle specific promoters (206).

The complexity of epigenetic regulation becomes even more complex when other transcription factors are taken into account. Pax7 is also able to interact with MLL via a Pax3/4 binding protein and also after post-translational methylation of Pax7 by Carm1 (207, 208). Set7, the HMT responsible for monomethylation of H3K4, is required for myogenesis and is able to interact with MyoD (209). Furthermore, the repressive marker, H3K27me3, is maintained in myoblasts by PRC2 and then removed by UTX as the cells differentiate (210).

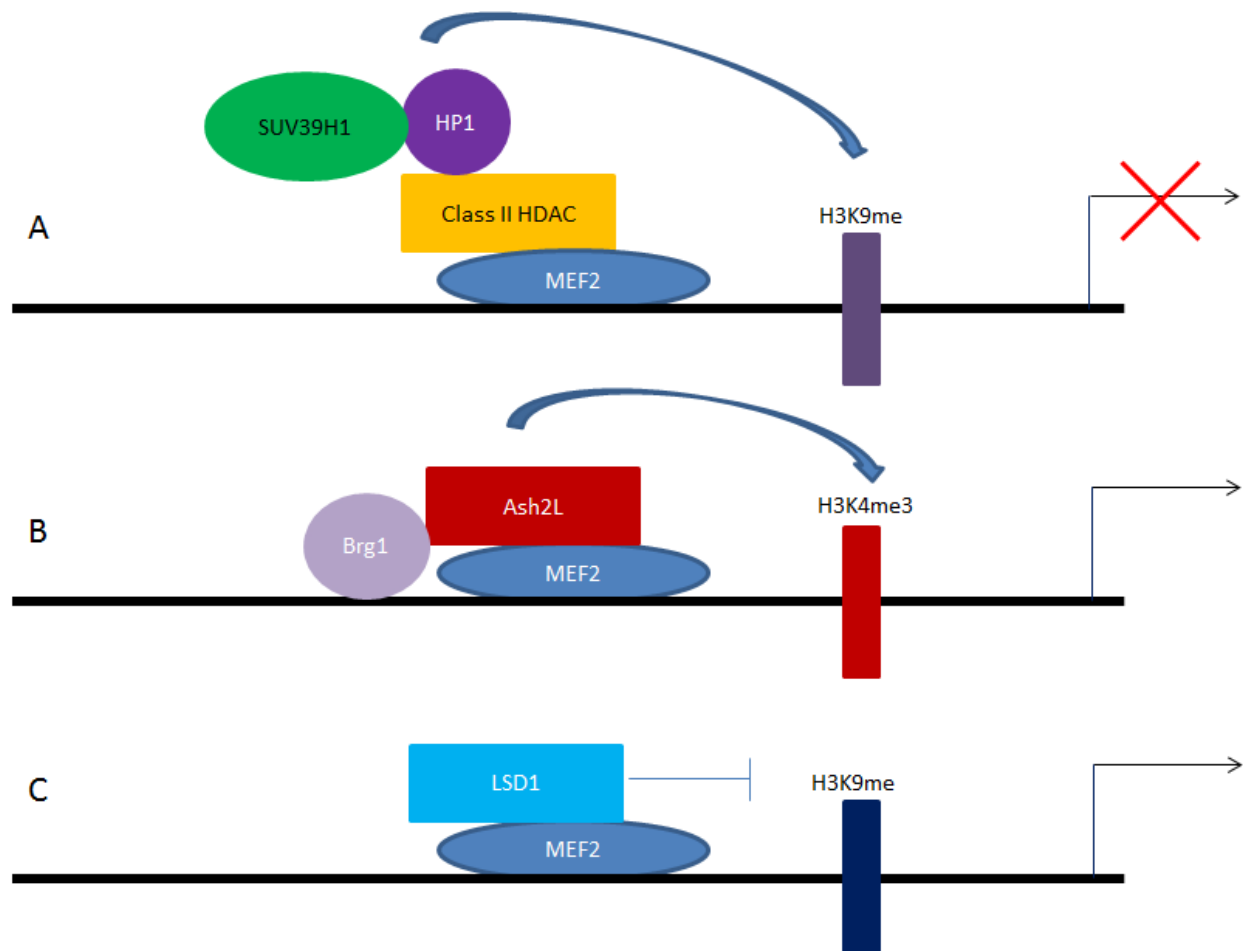


**Figure 7.** The role of MEF2 in epigenetic gene regulation. A) MEF2 strongly interacts with class II HDACs which repress MEF2 function and may also contribute to regional histone deacetylation, but also recruit HP1 and SUV39H1 which methylates H3K9 and represses transcription. B) MEF2 recruitment of histone methyltransferase Ash2L, which places a transcriptionally permissive histone marker, has been well studied in skeletal muscle. Chromatin remodelling factor Brg1 may also be recruited by MEF2 to promote gene expression. C) LSD1 demethylates transcriptionally repressive histone markers to promote gene expression in skeletal muscle.

Histone demethylation of H3K4 and H3K9 is mediated by lysine specific demethylase 1 (LSD1) (211). LSD1 is able to interact with MEF2 to induce myogenesis however it appears that LSD1 only demethylates H3K9 in this context (**Figure 7C**) (212).

Using ChIP methodology in combination with microarray analysis (ChIP-chip) or with sequencing (ChIP-seq) there has been tremendous movement in our understanding of the role of MEF2 in myogenesis. In *Drosophila*, ChIP-chip assays in three stages of the *Drosophila* lifecycle identified multiple pathways of MEF2 involvement in muscle development (213). In C2C12 myoblasts MEF2 and MRF recruitment was assessed also using ChIP-chip which showed in

addition to myogenesis, these factors were involved in the cell cycle, stress pathways and development of the neuromuscular junction (NMJ) (214). In C2C12, MEF2 on CpG islands (ChIP-CpG island-chip) was also shown to be associated with NMJ (215). These ChIP-chip arrays are useful in identifying biological function, but have a limited scope as they contain select regions of DNA. Using ChIP-seq, MyoD was revealed to have thousands of novel binding sites during myogenesis, the majority of these were inter and intragenic regions (216). MyoD recruitment was also found to be correlated to chromatin accessibility as shown in a conversion assay using mouse embryonic fibroblasts, MyoD overexpression induced significant changes in regional histone acetylation (216).

## **2.5 Regulation of MEF2 by post-translational modifications**

MEF2 is also regulated by a variety of kinases such as p38 MAPK (217, 218), ERK5 (162, 219), HIPK2 (220), PKA (147), PKC (218), skMLCK which results in PCAF/p300 recruitment (221) and Nemo-like kinase during early *Xenopus* development (222). Protein phosphatases, although less well-studied, have also been shown to regulate MEF2 activity such as PP1- $\alpha$  (223).

In skeletal muscle the p38MAPK-MEF2 signaling cascade is necessary for myogenesis and has been studied extensively. p38 phosphorylates three locations of MEF2 within the TAD at Threonine 312 and 319 and Serine 453 in MEF2A and in conserved sites in MEF2C at Thr 293, Thr 300, and Ser 387 (**Figure 6**), resulting in enhanced transcriptional activity of myogenic targets (217, 224). ERK5/BMK1 also targets Ser387 in MEF2C and the conserved site in MEF2A (162, 219). MEF2D and MEF2B have not been shown to be directly phosphorylated by p38, however changes in transcriptional activity by activated p38 and MEF2D have been documented (204, 225). *In vitro* p38 blockade using chemical inhibitors that sterically block the catalytic domain prevents skeletal myogenesis (226). In the developing somites and limb buds, p38 and MEF2 are co-expressed and inhibition of p38 results in decreased MEF2 activity as determined in a MEF2-lacZ model (227). One mechanism by which p38 promotes skeletal myogenesis is through targeting SWI/SNF chromatin remodelling complexes to target genes (205). As p38 is a stress activated pathway, it is not surprising to see that p38 activity is upregulated in cardiac hypertrophy (228). A recent study showed that pressure overload-induced hypertrophy was mediated through Adiponectin, p38 and MEF2 (229) but the precise mechanism of p38 activation in cardiac hypertrophy and the downstream consequences require further investigation.



The regulation of MEF2 by PKA phosphorylation has been studied in a variety of tissues including cardiomyocytes, skeletal muscle, vascular smooth muscle and neurons. In myoblasts PKA inhibits MEF2 transcriptional activity in two ways. PKA directly phosphorylates MEF2D at Serine 121 and Serine 190 (**Figure 6**) and indirectly represses MEF2 by promoting HDAC4 nuclear accumulation (147). Interestingly MEF2D has two splice variants, one of which lacks the MEF2D PKA phosphorylation target sites. Full-length MEF2D is expressed in myoblasts and subject to PKA repression, however as cells exit the cell cycle and enter differentiation the alternative splice isoform is present and MEF2D escapes PKA-mediated repression (148). This study also identified different co-factors for MEF2D splice variants. The early MEF2D isoform was able to interact with HDAC4 but the later form interacted with Ash2L. In vascular smooth muscle, PKA signaling enforces a MEF2-HDAC4 interaction indirectly, by phosphorylating SIK1 to lead to HDAC4 nuclear accumulation (230). MEF2 also has a pro-survival role in hippocampal neurons wherein PKA activation results in apoptosis and the repression of MEF2D (231). Similarly, in primary rat cardiomyocytes, activation of PKA increased cell death but PKA resistant mutants of MEF2 rescued this effect (232).

## **2.6 MEF2 and miRNA gene silencing**

The importance of miRNA in developmental and disease pathways has developed at an exponential rate since the first miRNA was characterized in *C. elegans* in the early 1990s. In 2006 Chen et al. (233) used a miRNA microarray to identify miRNA involved in skeletal myogenesis. Two miRNA clusters containing miR-1 and miR-133 stood out as they are induced during myogenesis, abundant in both skeletal and cardiac muscle and they are on the same chromosome and transcribed as one transcript. Two of the initial targets of miR-1 and miR-133 were HDAC4 and SRF, respectively. This comprehensive study also determined that miR-1 promoted myogenesis while miR-133 promotes proliferation. These two clusters have been labelled as miR-1-2 with miR-133-1 and miR-1-1 with miR-133-2. Interestingly both of these independent miRNA clusters contain MEF2 regulatory sites, and miR-1-2/miR133-1 was shown to be directly regulated by MEF2 (234).

Another miRNA cluster contains miR-206 with miR-133b. miR-206 promotes skeletal myogenesis by inhibiting p180 and therefore inhibiting DNA synthesis (235) but it has many other targets including Pax7, HDAC4, and Id, a transcriptional repressor of MyoD (235–237). Another locus containing miR-1/206 appears to be indirectly regulated by MEF2 (238).

A negative feedback loop involving MEF2, miR1/206, p38 and Notch signaling has been characterized in myoblasts. The Notch signaling pathway can affect the MAPK pathway by inducing expression of Dual Specificity Phosphatase 1 (DUSP1, also known as MKP-1) which deactivates p38 and therefore blocks myogenesis (239). Gagan et al. (238) showed that Notch3 inhibits myogenesis by upregulating DUSP1 which decreases p38 activity and therefore downregulates MEF2 transcriptional activity (238). MEF2 can in turn regulate Notch3 expression by inducing expression of mir-1/206.

Long noncoding RNAs (lncRNA) are RNA up to 200 nucleotides long with multiple functions including regulating DNA transcription, interfering with translation and acting as sponges for miRNA. linc-MD1 is one such lncRNA that acts as a sponge to modulate the effect of miR-133 and miR-135 and thereby promote muscle differentiation (240). Although it is likely that MEF2 can regulate lncRNA, none have yet been characterized.

### **3. Therapeutic relevance of MEF2 in skeletal and cardiac muscle disease**

With the aging population set to dramatically increase in the near future, identifying therapeutics for muscle degeneration and wasting as well as heart disease will be of critical importance. Investigation of the role of MEF2 in satellite cell quiescence, activation, proliferation and differentiation and heart failure are necessary to fully understand how to treat these diseases.

#### **3.1 Metabolic disease**

Healthy tissue is sustained by the regulation of energy input and output at the molecular level in a process referred to as metabolism. This involves the combined processes of energy production (catabolism) via the breakdown of molecules such as glucose to produce ATP, and energy consumption (anabolism), which requires ATP to produce new molecules. In muscle the cyclical transition of energy input and output is necessary to sustain everyday tasks such as voluntary movements of the limbs or autonomous beating of the heart. The primary sources of energy production are from the liver and skeletal muscles which respond to insulin and house glycogen stores (**Figure 8**). Therefore, skeletal muscle has a role unlike many other tissues in that it is important not only in the storage of energy but also in energy consumption through the high-energy demand of contraction. Understanding the mechanisms by which muscle is able to regulate metabolic pathways is important in the prevention and treatment of muscle-related diseases. Several metabolic diseases are particularly relevant in muscle including diabetes and

muscle atrophy, which can manifest as a side-effect to aging, cancer or AIDS (referred to as cachexia) or muscle disuse.

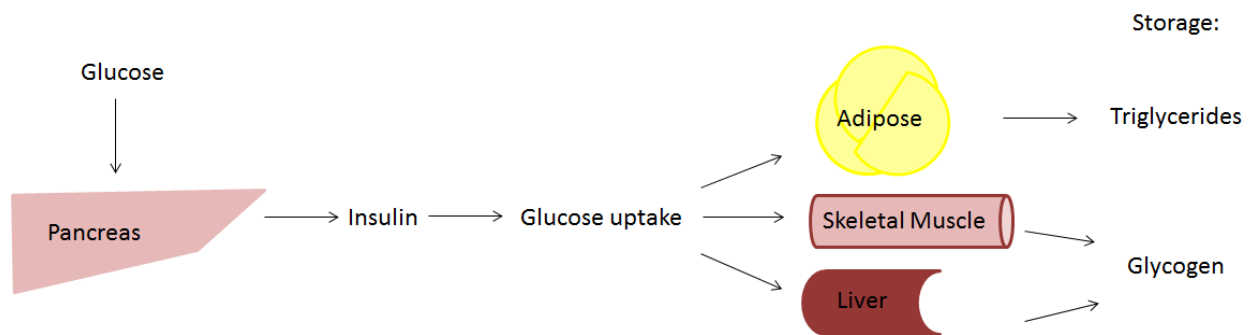


**Figure 8.** Mechanisms of glucose storage. Glucose triggers insulin secretion from the pancreas which results in glucose uptake in various tissues. Shown here are the three main sources of energy: adipose tissue, which store glucose as triglycerides, and skeletal muscle and liver, which store glucose as glycogen.

### 3.1a: Diabetes

After a meal, there is an increase in extracellular glucose that can either be taken up by cells for storage as glycogen, or immediately used for protein synthesis or other processes that require ATP. The body responds to extracellular glucose by secreting insulin from the pancreas to trigger glucose import. The insulin receptor is a receptor tyrosine kinase that responds to insulin or insulin-like growth factor (IGF) I and II by activating downstream effectors that mediate glucose uptake (**Figure 9**). If not needed for immediate energy consumption, glucose is stored as glycogen. Synthesis of glycogen from glucose occurs primarily in the liver and skeletal muscle while adipose tissue stores glucose in the form of triglycerides. Once the insulin signalling cascade is initiated in skeletal muscle and adipose tissues, the primary mechanism of glucose uptake is via insulin-responsive glucose transporter 4 (Glut4) (reviewed in (241)). In the absence of insulin, Glut4 is confined to the interior of the cell, however if insulin signaling is received, Glut4 moves to the plasma membrane. Interestingly, Glut4 mRNA and protein expression is increased following exercise, which in turn leads to enhanced glycogen accumulation (242). In addition the stable overexpression of Glut4 can increase the rate of glycogen made, indicating a critical role for Glut4 in metabolism (243). Glycogen synthesis is mediated by glycogen synthase, which is inhibited by GSK3- $\beta$  in unstimulated cells. Insulin signaling triggers activation of Akt/PKB which phosphorylates and inhibits GSK3- $\beta$ , resulting in glycogen synthesis.

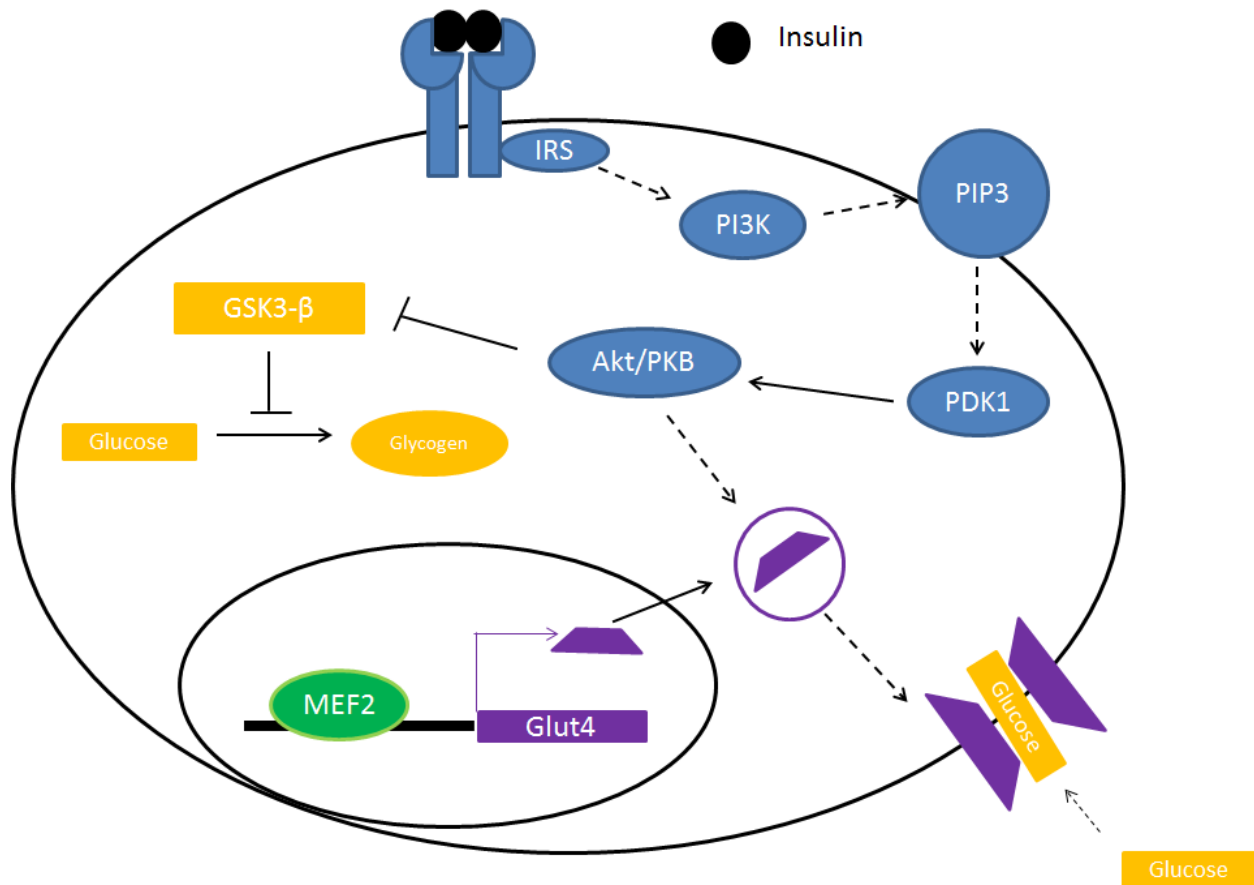


**Figure 9.** Insulin signaling in metabolic tissue. Insulin binds to IGF receptors on the cell surface of metabolic tissues, resulting in Akt/PKB activation which has two main effects on glucose storage: 1) Akt/PKB inhibits GSK3- $\beta$  which results in glycogen synthesis and 2) Promotes Glut4 translocation to the cell membrane which mediates glucose uptake. Glut4, the main glucose transporter, is under the transcriptional control of MEF2.

Diabetes is a metabolic disease in which an individual does not regulate blood-glucose levels properly which can lead to hyperglycemia, severe muscle wasting or death if untreated. There are two primary classes of diabetes. Type I diabetes occurs in individuals who are unable to produce and secrete insulin from the pancreas. This is caused by an autoimmune response in which the insulin producing cells of the pancreas,  $\beta$ -cells, are destroyed. This disease has no cure however it can be treated with insulin injections.

Individuals with Type II diabetes are referred to as insulin resistant, as although insulin is secreted, glucose uptake is impaired. This can occur through various defects in the insulin signal

transduction pathway such as faulty insulin receptors or impaired transportation of glucose into the cell (reviewed in (244)). For example, individuals with Type II diabetes have decreased Glut4 expression in adipocytes but normal expression in skeletal muscle with impaired translocation to the plasma membrane (245, 246). To account for the lack of glucose uptake the body increases insulin secretion and this results in a temporary normal insulin response, yet this compensatory effect is not sustained. It has been reported that Type II diabetes in obese individuals is caused predominantly by diet and exercise, however, there is emerging evidence that the epigenetic events within certain genes may predispose individuals to the development of the disease. Several hypotheses have been proposed to rationalize a genetic reason as to why genes responsible for this disease would be retained in the population. One hypothesis suggests that the environment during early life dictates gene expression as an adult, as modeled through the observed correlation between low birth weight and the development of Type II diabetes (247, 248). There is strong evidence to support this hypothesis using intrauterine growth restricted (IUGR) mouse models and population studies (249).

Since glucose transportation is a critical component of the insulin response, modulating the expression and translocation of Glut4 could be a viable option to treat those who are insulin resistant. Investigation into the molecular events responsible for Glut4 expression revealed that it is dependent on the transcriptional activity of MEF2 and subject to extensive epigenetic control. Initial studies of the Glut4 promoter identified a MEF2 binding sites between -463 and -473 which is required for normal Glut4 expression (**Figure 9**) (250, 251). The MEF2 isoforms believed to be responsible for proper Glut4 expression was a MEF2A/MEF2D heterodimer (252). Glut4 expression also relies on the co-operation between MEF2, MyoD, thyroid hormone, and a novel co-factor, Glut4 enhancer factor (GEF), which binds 300 base pairs upstream of the MEF2 site (253, 254). Interestingly, pregnant mice on a low protein diet produced offspring with increased MEF2A protein, GLUT4 expression and enrichment of H3K4me2 (a transcriptionally permissive mark) and RNA polymerase II on the Glut4 gene (255). Conversely Glut4 expression was decreased if mice were on a low calorie diet (256). In addition, Raychaudhuri et al. (257) found that IUGR leads to an increase in MEF2D but a decrease in MEF2A and MyoD enrichment on Glut4.

Molecular regulation that occurs upstream of MEF2 such as HDACs and p38 are modified by exercise in a concerted effort to produce a cellular environment in which MEF2 is active and

Glut4 is expressed. Examples of this include enhanced DNA interaction between MEF2A/D and GEF, nuclear export of HDAC, strengthened MEF2-p38 interaction and subsequent phosphorylation of MEF2, all of which are exercise-induced events (258, 259). As described in Part 1 of this review (see Striated muscle contraction), there are two main type of energy production in muscle: oxidative phosphorylation (Type I and IIa) and glycolysis (Type IIb and IIx). Type I fiber type is driven by transcription factor PGC-1 $\alpha$  which has several important roles in oxidative phosphorylation and metabolic disease in muscle atrophy and diabetes. The most well studied function of PGC-1 $\alpha$  is to regulate mitochondrial biogenesis, which promotes the oxidative phosphorylation gene program in a calcium dependent manner (260) and, because metabolic preference contributes to fiber type classification, fiber type switching from Type II to Type I is also driven by PGC-1 $\alpha$  (102). MEF2 directly regulates the expression of *Ppargc1a* and it is also able to directly co-operate with PGC-1 $\alpha$  (102, 261). In a microarray screen using human diabetic muscle samples, genes associated with oxidative phosphorylation and driven by PGC-1 $\alpha$  were downregulated (262). In addition, as was seen on the promoters associated with muscle fiber type switching, PGC-1 $\alpha$ , was able to increase Glut4 expression by enhancing MEF2 transcriptional activity (263). Together these studies identify an indirect role for MEF2 in the progression of Type II diabetes.

### ***3.1b: Pathways regulating muscle atrophy***

To gain energy during times of nutrient deprivation, our body takes advantage of energy stores in muscle and fat. In extreme cases, such as starvation, the energy demand outweighs available nutrients and energy stores in the muscle are depleted. This requires the body to produce energy through alternative measures, including degradation of muscle itself. Alternatively, aberrant signaling to the mechanisms that control muscle metabolism can also result in muscle degradation. This muscle wasting phenomena is known as muscle atrophy and can manifest in several diseases including diabetes, cancer, AIDS, aging and muscular dystrophies. The pathways that mediate atrophy are complex but the outcome is simple: reduced protein synthesis and enhanced protein degradation. Exercise is a suggested therapy to regenerate muscle however this is an unrealistic treatment for patients with severe diseases, therefore pharmaceutical treatments to prevent protein degradation or promote muscle regeneration are being pursued. A critical experiment utilized microarray analysis to compare the mRNA levels of mice and rats with muscle wasting induced by fasting, cancer cachexia, diabetes, or renal failure

(264) and identified increased expression of several key factors, termed atrogenes, that mediate protein degradation either through the autophagy or ubiquitin-proteasome pathways.

The ubiquitin-proteasome pathway is a necessary cell process that targets proteins for degradation in the proteasome via mono- or poly-ubiquitin tags that are added to lysine residues (**Figure 10**). Attaching ubiquitin to the target protein happens in a multi-step process in which ubiquitin is transferred by E1 (activating enzyme), to E2 (conjugating enzyme) and finally E3 (ligating enzyme). The E3 ligase has substrate specific activity.

One of the complexes that targets misfolded proteins to the proteasome involves heat shock protein Hsc70, Bcl-2-associated athanogene 1 (Bag1) and carboxy-terminus of Hsc70 interacting protein (CHIP), an E3 ligase (265). Bag1 acts as a co-chaperone with Hsc70 and also interacts with the proteasome, therefore promoting misfolded proteins to be degraded instead of refolded. CHIP expression is enriched in the heart and skeletal muscle (266) and knockout mice develop normally but are more susceptible to myocardial infarction and cardiomyocyte apoptosis after left coronary artery ligation (267).

In times of muscle atrophy two muscle-specific E3 ubiquitin ligases, MAFbx and MURF1, are expressed (268). These proteins are able to target the same proteins such as MyBP-C (269), but evidence exists that they also differentially target proteins such as myosin and other myofibrillar proteins which are targeted by MURF1 (270, 271). MAFbx can target translation protein eIF3-F and MyoD (272, 273).

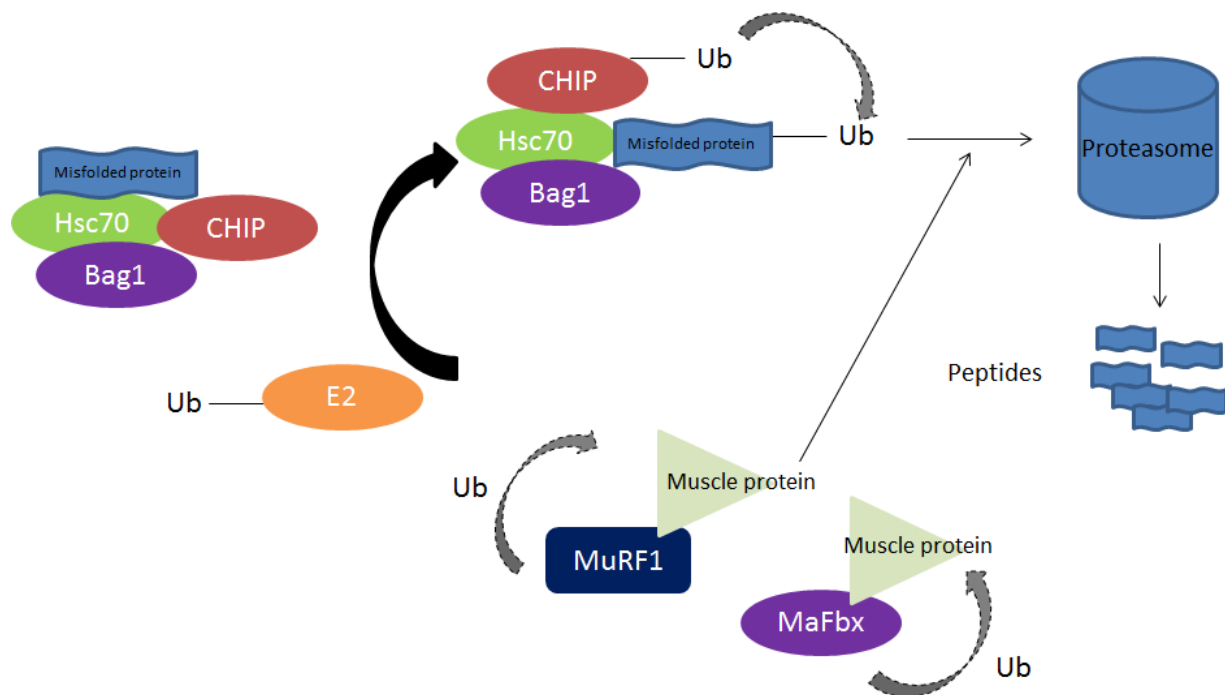


**Figure 10.** Protein ubiquitination and degradation in muscle. The figure highlights two mechanisms protein degradation in muscle. Misfolded proteins are targeted for degradation via a protein complex of Hsc70, Bag1, and E3 ligase CHIP. Under atrophic conditions, muscle-specific E3 ligases MuRF1 and MAFbx are expressed and ubiquitinate muscle proteins.

During classical autophagy, termed macroautophagy, Atg family members contribute to the formation of autophagosomes which will fuse with the lysosome to degrade its contents (**Figure 11**). LC3B (Atg8 in yeast) is integrated into the autophagosome in a step-wise manner. First, full length LC3B is cleaved by cysteine protease Atg4b which produces an exposed glycine residue and results in cytosolic LC3B-I (274). Phosphatidylethanolamine (PE) is added to LC3B-I to produce LC3B-II via Atg7, Atg3 and Atg12-Atg5-Atg16L in a process similar to E1/E2/E3 ubiquitin conjugation (275). Adding this lipid group drives LC3B-II to associate with the membrane of the autophagosome. Substrates are targeted to the autophagosome by autophagy receptors such as p62/Sqstm1 which bind ubiquitinated proteins and bring them to the growing autophagosome via direct interaction with LC3B-II (276). The autophagosome then fuses with the lysosome and the contents are degraded. Macroautophagy includes the degradation of individual proteins and mitophagy, degradation of mitochondria (277). Microautophagy occurs when the lysosome engulf small peptides and lipids. Chaperone mediated autophagy (CMA) requires heat shocks protein Hsc70 (ubiquitous) or Hsp70 (inducible) and co-chaperone proteins



to target peptides to the lysosome via a KFERG motif on the misfolded protein (278, 279). Lamp2A receptors on the surface of lysosomes mediate transfer of the protein into the lysosome (280).

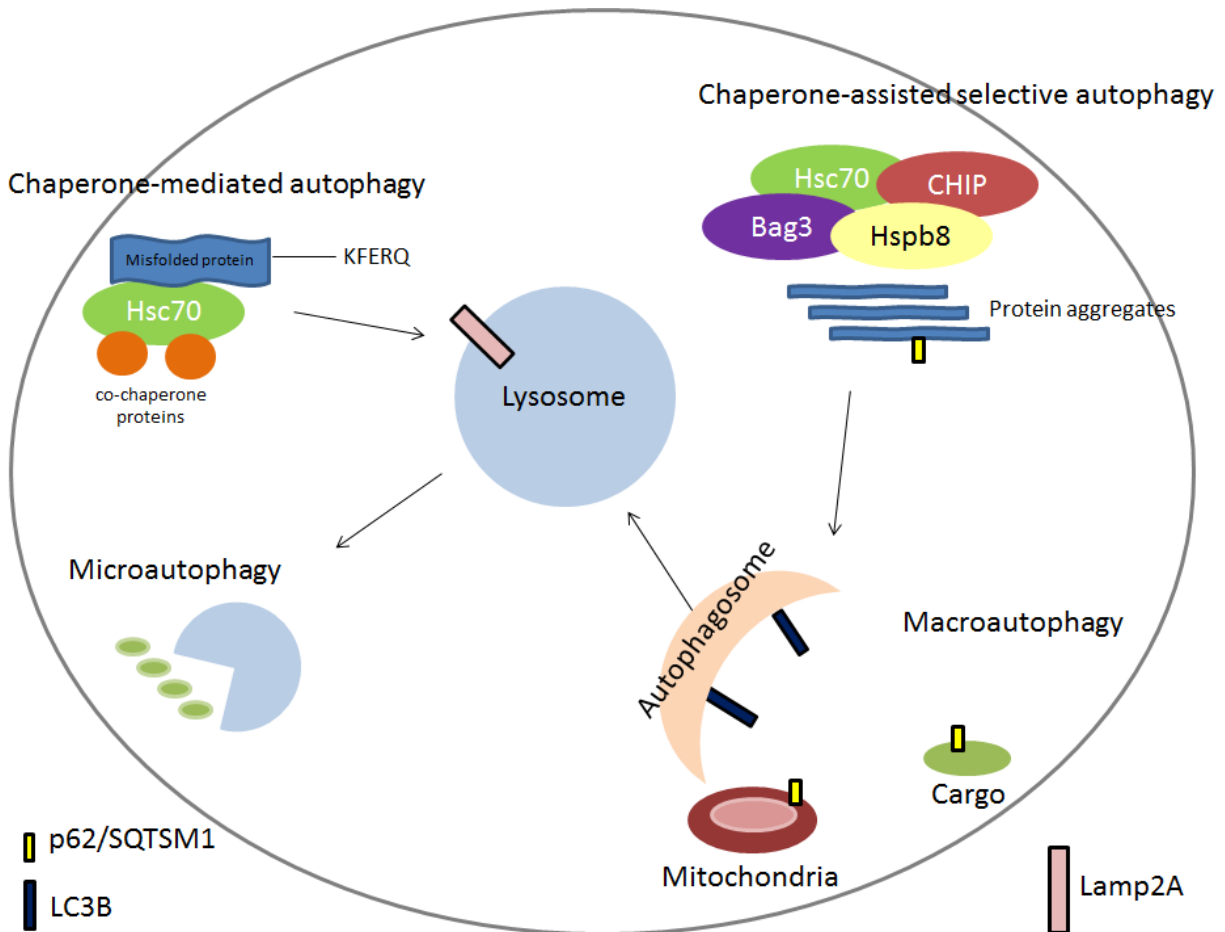


**Figure 11.** Pathways of autophagy. Four methods of autophagy are shown: Chaperone mediated autophagy (CMA), Chaperone-assisted selective autophagy (CASA), Microautophagy and Macroautophagy. CMA degrades misfolded proteins and relies on the protein complex Hsc70 and co-chaperone proteins. The complex then moves to the lysosome where the misfolded protein interacts with Lamp2A on the surface of the lysosome. Microautophagy occurs when the lysosome engulfs small molecules. During macroautophagy p62 binds to ubiquitinated protein cargo or whole organelles (e.g. Mitochondria) and brings them to LC3B in the growing autophagosome. CASA involves Hsc70, Bag3, CHIP and Hspb8 which target protein aggregates to an autophagosome via p62.

The Hsc70-CHIP-Bag1 complex has been known to promote protein degradation via the ubiquitin-proteasome pathway (**Figure 11**) (265), however, Bag3 was found to replace Bag1 in the same complex in aged models and promote autophagy over proteasome-mediated degradation via an interaction with SQSTM1/p62 (281). Another group found that Hsc70, Bag3, CHIP and small heat shock protein Hspb8 (282, 283) form a complex to mediate an alternate mechanism of autophagy which they termed chaperone assisted selective autophagy (CASA). CASA is an intermediate between macroautophagy and chaperone mediated autophagy and primarily targets protein aggregates but has only been described in muscle. The CASA complex localizes to sarcomeric structures in the Z disc, wherein Hsc70, Bag3 and Hspb8 can recognize myofibrillar protein aggregates, CHIP then ubiquitinates the target protein and this recruits the autophagosome via interaction with p62 (282).

Muscle atrophy also depends on the inactivation of pathways which promote muscle formation, which is heavily influence by Akt/PKB and upstream regulation by Myostatin, a member of the TGF- $\beta$  superfamily that activates downstream signaling via Activin Type II receptors (**Figure 12**). Akt signalling represses FoxO family transcription factor members Foxo1 and Foxo3 which are the main drivers of atrophy as they activate the expression of factors that directly contribute to the autophagy and ubiquitin-proteasome pathway. Both Foxo1 and Foxo3 can induce expression of MAFbx and MURF1 however only Foxo3 can activate autophagy by regulating LC3B, Atg4b and other autophagy related genes (284, 285). Foxo3 activity is inhibited by PGC-1 $\alpha$  (286) and Junb in mouse models of muscle atrophy (287).

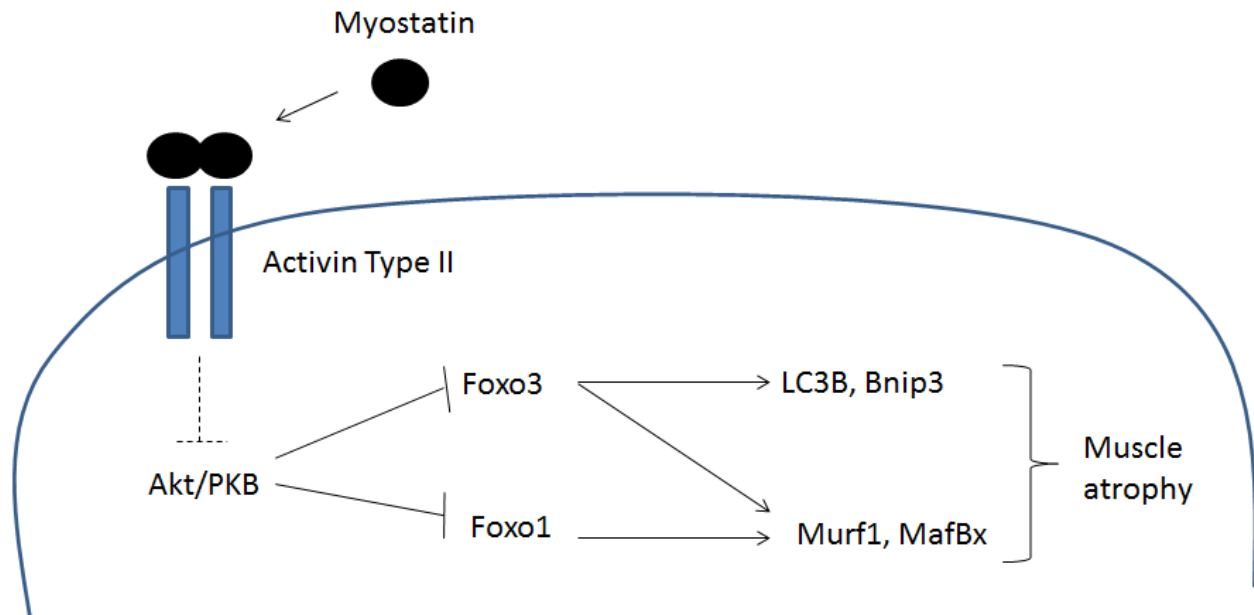


**Figure 12.** Transcriptional regulators of muscle atrophy. Myostatin signaling through the Activin Type II receptors inhibits Akt/PKB and results in activation of transcription factors Foxo3 and Foxo1 which contribute to muscle atrophy.

### 3.2 Role of MEF2 in skeletal muscle regeneration

During muscle regeneration, a process similar to myogenesis occurs in which quiescent Pax7+ cells, called satellite cells, become activated and will express Myf5 and MyoD. This is followed by MyoG and MEF2 and eventually differentiating myoblasts will fuse with the existing myofiber (288) (**Figure 4**). Treatment of genetic and metabolic muscle diseases utilizing satellite cells, either through endogenous activation or satellite cell transplantation, has been an area of active research (289). With age, satellite cell numbers decrease dramatically, therefore regenerative capacity is reduced (290). Inherited skeletal myopathies show dramatic muscle fiber destabilization which signals for constant satellite cell activation until this stem cell pool becomes depleted and regeneration is no longer possible. Harnessing the regenerative potential of satellite cells through transplantation could be a possible treatment option in muscle degeneration. The precise role of MEF2 in satellite cell activation is being explored. Global deletion of MEF2A show impaired skeletal muscle regeneration (139) but since this knockout was not skeletal muscle specific the possibility remained that this deficiency was caused by impairment in the immune response not by defects in satellite cell differentiation. Also gene deletion of individual MEF2 genes during muscle regeneration may be obscured by the redundant function of MEF2 proteins. In 2014 MEF2 was shown to have a role in muscle

regeneration using a skeletal muscle specific MEF2A, C and D triple knockout mouse (140). Some of the implications of MEF2 processes discussed in this review have been associated with human disease (**Table 1**).

**Table 1.** MEF2 and human disease. A compilation of a subset of known MEF2 mutations or functions and the implications in human disease.

Human disease	Evidence	MEF2 function
Alzheimer's; Mental retardation	SNPs or haploinsufficiency of MEF2C (291, 292).	Neuronal targets during development (124). Role in neuronal survival (231, 293).
Bone mineral density	SNPs in MEF2C (294).	MEF2 controls bone hypertrophy (129).
Cachexia	MEF2C is reduced in C26 carcinoma mouse models (295).	MEF2 maintains muscle integrity.
Diabetes (indirect)	i) Promotes Type I fiber formation (slow-oxidative) ii) Mediates glucose uptake	i) PGC-1 $\alpha$ is a MEF2 target gene and co-factor (102, 261). ii) MEF2 binding to Glut4 is reduced in diabetic animal models (250).
Familial hypertrophic cardiomyopathy	Mice carrying MHC <sup>403/+</sup> to model FHC crossed with MEF2-reporter.	MEF2 activity is upregulated with disease progression in MHC <sup>403/+</sup> particularly prior to heart failure (296).
General myopathies (indirect)	Loss of MEF2 results in destabilization of sarcomeres.	i) Regulates costamere-associated gene expression (297). ii) Thick filaments of the sarcomere (137). iii) Disorganized myofibers in MEF2C sk-muscle KO (298).
Heart failure	i) MEF2 activates the fetal gene program. ii) Activity of MEF2 is upregulated in murine models of heart failure (pressure overload).	i) MEF2 upregulates ANF, MHC isoforms, early response genes (86). ii) Alternative splicing of MEF2; regulation of MEF2 by PKA, $\beta$ -blockers and CaMKII, (186, 232, 299).
Myotonic dystrophy (DM1, DM2)	Human samples of DM1 and 2.	MEF2 and downstream targets are downregulated. MEF2 is also alternatively spliced in this disease (300).
Nemaline myopathy	Nemaline myopathy is associated with mutations in Lmod3 (301).	Lmod3 is a MEF2 target gene (225, 302).
Sarcopenia and muscle wasting	Triple MEF2 sk-muscle KO have impaired muscle regeneration (140).	MEF2 has a role in satellite cell differentiation.

Heritable mutations of proteins associated with the sarcomere or muscle structure results in severe disorders in both skeletal and cardiac muscles. Several muscular dystrophies have been characterized to have a strong genetic component. One of the most common and well-studied muscular dystrophies is Duchenne muscular dystrophy (DMD), in which a large scaffolding protein called Dystrophin is mutated (303). Under normal circumstances, Dystrophin is present in the Dystrophin Associated Glycoprotein (DAG) complex of the costamere and anchors muscle Z discs to the sarcolemma to stabilize the muscle during contraction (**Figure 13**). Without

Dystrophin the muscle fiber is weakened and may rupture, allowing calcium to enter the cell and trigger mitochondrial swelling and lysis (304). Mitochondrial dysfunction then triggers activation of the cell death and apoptosis pathways which contribute to muscle atrophy. Resident satellite cells are activated and attempt to replace damaged muscle, however, because of the constant turnover of tissue, the satellite cell pool becomes depleted. Additionally, in this disease Dystrophin is also mutated in the heart, resulting in cardiomyopathy. This is an X-linked mutation that is particularly devastating among young boys who show severe symptoms a young age and succumb to the disease in their twenties by cardiac death (303). Several studies have attempted to do transplantation studies using exogenous satellite stem cells from relatives and while these studies showed some promise, efficiency was low and age was a limiting factor (305). Other groups have used a combination of gene correction and cell reprogramming by using fibroblasts from mice modelling DMD (mdx), correcting the gene using transposons and differentiating the cells into myoblast progenitors (306). An additional consideration to this field is that in mouse models of cancer cachexia, genes associated with muscle membrane integrity, such as Dystrophin, are reduced and E3 ubiquitin ligases, MAFbx and MURF1 are upregulated (307), indicating that therapies that strengthen muscle tissue may be beneficial in other diseases such as cancer.

The Olson lab recently utilized the CRISPR/Cas9 genome editing system to manipulate a mouse embryo of the mdx strain (308). They were successfully able to use CRISPR/Cas9 to edit the germline of mdx mice to rescue this deficiency. This demonstrates that the genetic technology to correct genetic mutations is available, yet the possibility of applying CRISPR/Cas9 editing to human zygotes is seen by most in the scientific community to be dangerous. Several groups have, however, been able to use CRISPR to essentially cure muscular dystrophy in adult mice, without going through the germline which presents our generation with a new frontier of regenerative medicine (309, 310).

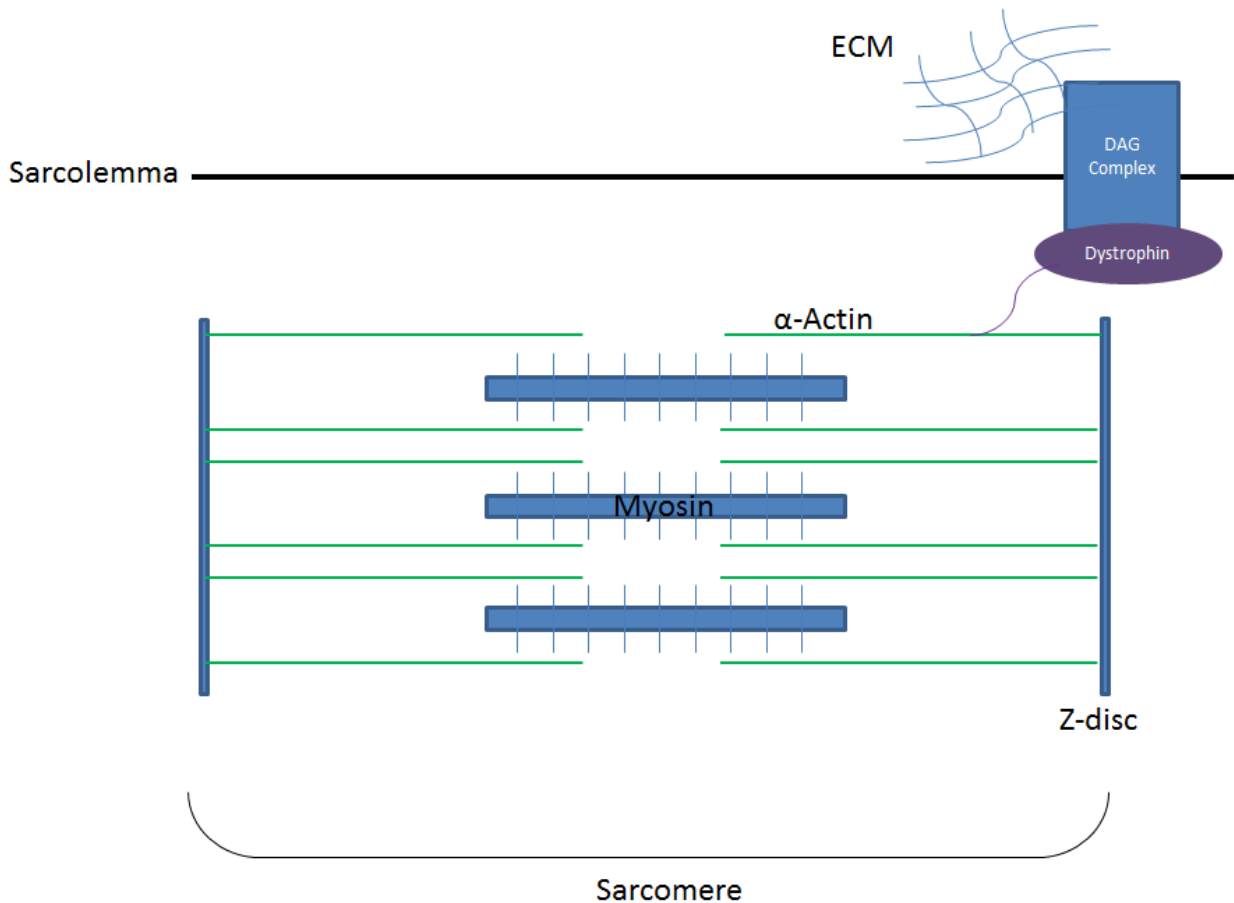


**Figure 13.** Structure of the sarcomere and DAG complex. One sarcomere unit is comprised of actin (thin) and myosin (thick) filaments. At the Z-line are costameres which contain several protein complexes such as the DAG complex that anchors the sarcomere in place and receives signals from the extracellular matrix (ECM).

MEF2 regulates skeletal muscle cell integrity by regulating the expression of a number of sarcomeric and cytoskeletal genes. In the heart, MEF2A knockout mice die post-natally due to defects in the cell structure (134) and in skeletal muscle MEF2C mutants have compromised sarcomeres (136). Ewen et al. (297) showed that MEF2A is strongly linked to cardiac muscle cell integrity by regulating several genes associated with the costamere, and furthermore that loss of MEF2A in cardiomyocytes results in cell death in a cell-adhesion specific manner. In the case of DMD, enhancing expression of Dystrophin is useless if the protein will be non-functional. Interestingly, Utrophin, a highly similar protein to dystrophin that is expressed at the neuromuscular junction, has been investigated as a possible treatment to DMD. PGC-1 $\alpha$  drives Utrophin expression in slow muscle fibers (311). Furthermore, mdx mice that transgenically

express PGC-1 $\alpha$  show improved outcome (312). Whether MEF2 interacts with PGC-1 $\alpha$  to mediate Utrophin expression, or assist PGC-1 $\alpha$  transgenic mice in this improvement remains to be determined.

Involvement of MEF2 has been implicated in other myopathies such as Myotonic dystrophy (DM1 and DM2) that causes muscle wasting and cardiac death. In the DM1 heart, MEF2 is downregulated along with several MEF2-target genes and miRNA (313). In addition, *Mef2* is alternatively spliced in DM and neuromuscular disorder (NMD) (300). Also using a mouse model of Becker syndrome, a disease in which muscle relaxation is delayed, MEF2 activity was enhanced (314).

Nemaline myopathy, an autosomal recessive disease that causes muscle weakness was recently shown to be driven by mutations in Kelch-like family member 40 (KLHL40) and Leoimodin 3 (Lmod3) (301, 315). Both Klhl40 and Lmod3 localize to the thin filament of sarcomeres where Lmod3 functions as an actin-nucleation factor (316). There are three Lmod proteins (1-3) that are differentially expressed among smooth, skeletal and cardiac muscle. Lmod1 is found in smooth muscle and contains an SRF CArG box (317). Lmod2 is found in skeletal and cardiac muscle and also contains a CArG box but this appears to be non-functional. Lmod3 is found in skeletal and cardiac muscle and contain both an SRF and MEF2 binding site which are required for muscle function (318).

### **3.3 Role of MEF2 in cell death and muscle atrophy**

Although MEF2 is traditionally thought of as a differentiation factor, which in itself has implications in restoring muscle fiber mass in various disease conditions, it also has roles in other cellular events such as cell death and survival. The importance of MEF2 in survival has been seen in neurons (223, 231, 293) and cardiomyocytes (232, 319) but many questions related to the mechanism remain. In contrast, MEF2 promotes apoptosis in T cells by regulating the expression of Nur77 (320). Since PKA (231, 232) and PP1- $\alpha$  (223) activity can result in MEF2 transcriptional repression and subsequent cell death, investigating the target genes in this context would reveal the function of MEF2 in survival. Loss of MEF2D in cardiomyocytes led to cell cycle re-entry but also increases in cell death and related genes (e.g. Caspase 8) (319). Wales and Hashemi (manuscript in preparation, 2016) found that loss of MEF2A in primary cardiomyocytes also induced several genes related to apoptosis and cell death using RNA-seq.

The relationship between MEF2 and apoptosis have been investigated but other aspects of cell death may also involve MEF2 including atrophy via the ubiquitin pathway, necrosis and autophagy. While there is no evidence that MEF2 is involved in autophagy, MEF2 is degraded via CMA in neurons (321, 322). Muscle atrophy can be observed in muscle disuse, however in animals that undergo hibernation muscle atrophy is reduced in spite of enhanced MAFbx expression (323). This is associated with enhanced MEF2 expression and adaptive metabolic consequences including increased Glut4 expression and Type I fiber formation (324, 325). Several other correlative analyses indicate MEF2 and atrophy are linked. Transgenic mice overexpressing Foxo1 have enhanced muscle atrophy and reduced MEF2C expression (326) and similarly MEF2 expression and downstream target genes are dysregulated in microgravity-induced muscle atrophy (327). Perhaps the strongest evidence that MEF2 is involved in atrophy is that MURF1 was shown to be a MEF2 target gene in the heart in times of metabolic stress such as nutrient deprivation (328) yet surprisingly little has been done to further characterize this regulation.

After muscle fiber damage, induced by muscular dystrophies or infection, cellular integrity is compromised and an unprogrammed form of cell death known as necrosis occurs. Immune cells are recruited to the site of injury as well as inflammatory cells which together contribute to the clearance of debris, recruitment of additional immune cells and activation of satellite cells (329). Chronic inflammation is seen in muscular dystrophies which further perpetuate muscle damage and this results in fibrosis instead of repair (330). TNF- $\alpha$ , one of the key mediators of inflammation (331), activates the p38 pathway in muscle and induces MAFbx expression (332). While no direct evidence between inflammatory signals and MEF2 in either damaged myofibers or recruited immune cells has been thoroughly explored, it has been shown that cardiotoxin-induced damage of MEF2A knockout muscle results in delayed clearance and repair of necrotic tissue (139) and triple knockout MEF2 mutants (MEF2A,C,D) show regenerative defects (140). Mechanistically, TNF- $\alpha$  and p38 signaling has been shown to activate Ezh2 to repress Pax7 expression, thereby controlling muscle regeneration (333). The significance of TNF- $\alpha$  and p38 signaling on MEF2 signaling could therefore also mediate important downstream consequences on muscle regeneration and the immune response.



### 3.4 Cardiac hypertrophy

Pathological hypertrophy occurs after myocardial infarction (heart attack) which results in cardiomyocyte death. Since there is no significant regenerative mechanism akin to skeletal muscle in the heart, existing cardiomyocytes undergo hypertrophy to compensate for decreased cardiac output (**Figure 14**). This mechanism, however, is not a permanent solution and sustained cardiac hypertrophy will result in heart failure. The paracrine signaling that mediates these processes are via the  $\beta$ -adrenergic signalling cascade which is activated by agonists, such as epinephrine or the drug isoproterenol, that bind to  $\beta$ -adrenergic receptors I or II. The  $\beta$ -II adrenergic receptors appear to have a protective role as it is anti-apoptotic but  $\beta$ -I is associated with maladaptive effects (334). During hypertrophy the distribution of  $\beta$ -II receptors changes from the T-tubules to crest cells, while  $\beta$ -I receptors remain ubiquitous (335).

It is unclear of the *in vivo* activity of MEF2 immediately after myocardial infarction, however *in vitro*  $\beta$ -adrenergic activation reduces MEF2 activity and promotes cell death through PKA (232). Furthermore  $\beta$ -blockers prevent cell death in a MEF2 dependent manner (232) suggesting that post-myocardial infarction *in vivo*, MEF2 activity is low (**Figure 14**). As the heart progresses to cardiac hypertrophy, however, MEF2 activity becomes markedly enhanced and contributes to pathological remodelling with Gata4 and Nkx2-5 (86). PGC-1 $\alpha$  expression also becomes reduced, changing the metabolism of the heart (336).

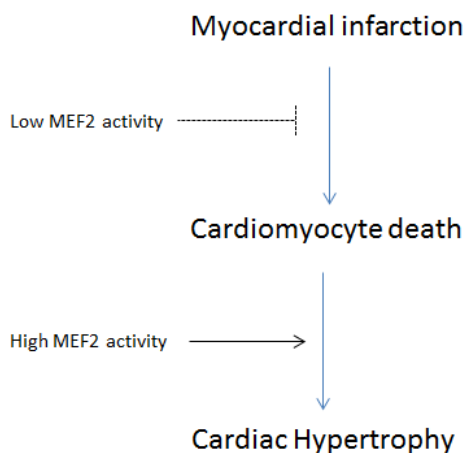


**Figure 14.** The role of MEF2 in the progression to heart failure. MEF2 has two roles in heart failure: 1) MEF2 can prevent cardiomyocyte death, but the activity of MEF2 is low after myocardial infarction. 2) MEF2 activity promotes cardiac hypertrophy. The transition of MEF2 activity from cardioprotective to maladaptive may be regulated by different pathways of  $\beta$ -adrenergic signaling.

MEF2 appears to have two mechanisms of regulation in cardiac hypertrophy: via PKA in acute/short-term activation of  $\beta$ -adrenergic signaling or through CaMK in chronic/long-term activation (**Figure 15**). Short-term activation of  $\beta$ -adrenergic signaling activates PKA activity which phosphorylates MEF2D to repress activity (147). Recently it was shown in neurons and cardiomyocytes that MEF2 has a pro-survival function that is downregulated by PKA activity (231, 232). Supplementing cardiomyocytes with  $\beta$ -blockers, a commonly used drug used to treat heart disease (e.g. Atenolol), enhanced MEF2 activity and prevented isoproterenol-induced cell death (232). HDAC4 is also important in PKA-mediated repression of MEF2. Interestingly the heart expresses a truncated version of HDAC4 which retains the MEF2 interacting domain to selectively repress MEF2 and is able to evade shuttling from the nucleus (194). This mechanism requires PKA interaction with HDAC4 to promote cleavage of HDAC4 by an unknown protease. Zhang et al. (322) observed that the HDAC4 cleavage product was enhanced in response to oxidative stress and proposed that in this case, cleavage was via lysosomal proteases. The resulting truncated HDAC4 protein acts similar to MITR as it contains a MEF2 interacting domain but has lost its histone deacetylase domain. On the other hand, PKA directly phosphorylates HDAC5 and promotes nuclear retention and transgenic mice expressing the catalytic subunit of PKA develop dilated cardiomyopathies (337, 338). To counteract this maladaptive effect, MEF2 target mir-133 is expressed and able to downregulate both PKA and  $\beta$ -I receptor (339).

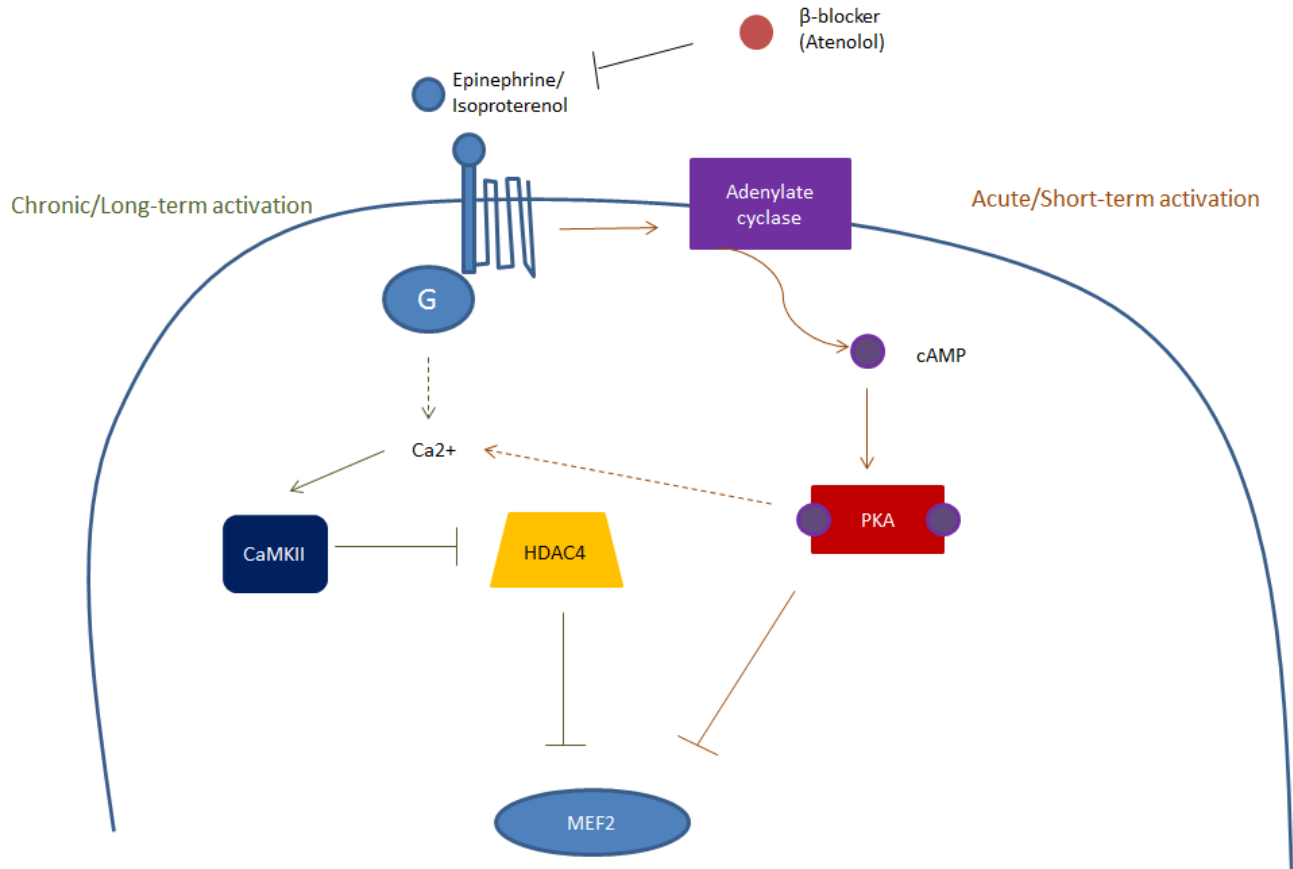


**Figure 15.** MEF2 and  $\beta$ -adrenergic signaling. Acute activation of  $\beta$ -adrenergic signaling (right; orange) results in PKA activation and MEF2 repression. Chronic  $\beta$ -adrenergic signaling (left; green) activates CaMKII, which activates MEF2 via HDAC4 nuclear exclusion. There is evidence that PKA enhances CaMKII activity by increasing intracellular calcium.

Under chronic  $\beta$ -adrenergic signaling, usually modelled by transverse aortic constriction (TAC) in experimental studies, MEF2 activity is enhanced (296). Knockout models of MEF2 co-repressors HDAC5 or HDAC9 results in cardiac hypertrophy (191, 340). Activation of the CaMK pathway results in class II HDAC nuclear exclusion (186) and promotes MEF2 activity as seen in constitutively active CaMKIV mouse mutants that demonstrate cardiac hypertrophy and enhanced MEF2 activity when crossed with a MEF2-lacZ mouse (341). CaMKII is the most highly expressed in the heart and the delta C isoform is induced in TAC models of cardiac hypertrophy while constitutively active mouse models results in cardiac hypertrophy (342). Blocking CaMKII activity prevents pathological remodelling induced by  $\beta$ -adrenergic signaling (343). Mechanistically, CaMKII phosphorylates HDAC4, but not other class II HDACs, resulting in its nuclear exclusion (344). Interestingly it has reported that transgenic dominant

negative MEF2 mice fare worse under TAC conditions compared to TAC alone and this is accompanied with mitochondrial instability and cell death (345), indicating that MEF2 is not strictly maladaptive in chronic pressure overload.

Taking into account both of the effects of PKA and CaMKII on MEF2 activity under  $\beta$ -adrenergic signaling could explain why exogenous activation of MEF2 prevents apoptosis in acute  $\beta$ -adrenergic signaling while loss of MEF2 under models of chronic  $\beta$ -adrenergic signaling, such as pressure overload via TAC, reduced pathological remodeling.

Another potential therapy to treat heart failure is stem cell therapy, either through endogenous stem cell activation or using induced pluripotent stem cells (iPSCs). Reprogramming fibroblasts to cardiac progenitors requires three factors referred to as GMT: Gata4, Mef2c, Tbx5 (346). Using retroviral gene transfer these factors were introduced to immunosuppressed or immunocompetent mouse hearts post-myocardial infarction (347). In MHC-GFP mice this caused cardiac fibroblasts to express GMT and caused 3% of cell to be GFP+. Unfortunately, the best outcomes were in immunosuppressed mice, and even these mice did not sustain expression of these markers however the involvement of MEF2C in reprogramming fibroblasts to cardiomyocytes further demonstrates the importance of MEF2 as a myogenic factor.

#### **4. Summary of Literature Review**

Together these studies demonstrate an important role for MEF2 in development of skeletal and cardiac tissues as well as striated muscle diseases. It is well known that MEF2 regulates the integrity of the sarcomere but more recently MEF2 has been implicated in cell death and survival. During muscle atrophy and hypertrophy the sarcomere is destabilized and/or reorganized which contributes to various pathologies that may activate cell death pathways. Determining how MEF2 may contribute to cell death or survival and whether this is through the disruption of the sarcomere may provide a better understanding of the molecular changes that occur in myopathies and lead to the development of pharmacological treatment strategies.

## **CHAPTER II: Statement of Purpose**

Both skeletal and cardiac muscle require transcription factor MEF2 for development and maintenance of function. Additionally striated muscle diseases including atrophy and hypertrophy have been associated with aberrant MEF2 activity. To date the majority of MEF2 target genes in skeletal and cardiac muscle have been identified at an individual level as opposed to using high throughput techniques such as ChIP-seq, and a thorough comparison of MEF2 target genes across these cell types has not been done. Therefore, the purpose of this work was to identify new MEF2 target genes in skeletal and cardiac muscle and to distinguish MEF2 function in these two cell types with respect to muscle disease.

*Chapter III: Global MEF2 target gene analysis in cardiac and skeletal muscle reveals novel regulation of DUSP6 by p38MAPK-MEF2 signaling.*

The structural similarities of skeletal and cardiac muscle are seen within the sarcomere, the contractile unit of striated muscle. MEF2 has been well documented to regulate critical components related to the actin cytoskeleton and costamere in both cells types yet simultaneously regulate cell specific genes (e.g. MyoG in skeletal muscle or ANF in cardiac muscle). We sought to identify MEF2A target genes in skeletal and cardiac muscle and critically compare recruitment of MEF2A to target genes using ChIP-exo and detailed bioinformatic analysis. Furthermore this work was complemented by transcriptome analysis of MEF2A depleted cells using RNA-seq. DUSP6 was identified as a MEF2A target gene in both cell types and its function was characterized using biochemical analyses.

*Chapter IV: Regulation of Hspb7 by MEF2 and AP-1 in muscle atrophy.*

MEF2 activity often depends on the recruitment of other transcription factors and co-factors such as class II HDACs. Based on the analysis done in Chapter III we observed that AP-1 consensus sequences were enriched in MEF2A-bound DNA. The importance of AP-1 in skeletal muscle regeneration has recently been under investigation in our lab yet the relationship between MEF2 and AP-1 has not been explored. Therefore, using bioinformatic analysis we compared recruitment of MEF2A to publicly available ChIP-seq datasets of two AP-1 components: c-Jun and Fra-1. Hspb7 is a small heat shock protein that contained MEF2A, c-Jun and Fra-1 enrichment and was subsequently chosen for further study and found to have a role in muscle atrophy.

**CHAPTER III: Global MEF2 target gene analysis in cardiac and skeletal muscle reveals novel regulation of DUSP6 by p38MAPK-MEF2 signaling**

Published in “Nucleic Acids Research”

(2015), 42(18): 11349-11362.

Experimental design by

Stephanie Wales and Dr. John C McDermott

Drafting Manuscript by

Stephanie Wales, Dr. Alexandre Blais and Dr. John C McDermott

Conducting experiments

Stephanie Wales (Figure 1, 2, 3, 4A, D, 5)

Sara Hashemi (Figure 4A, B, C)

## Global MEF2 target gene analysis in cardiac and skeletal muscle reveals novel regulation of DUSP6 by p38MAPK-MEF2 signaling.

Wales, S.<sup>1,2,3</sup>, Hashemi, S.<sup>1,2,3</sup>, Blais, A.<sup>4</sup> and J.C. McDermott<sup>1,2,3,5\*</sup>

<sup>1</sup>Department of Biology, York University, 4700 Keele Street Toronto, Ontario, M3J 1P3 Canada

<sup>2</sup>Muscle Health Research Centre (MHRC), York University, 4700 Keele Street, Toronto, Ontario, M3J 1P3 Canada

<sup>3</sup>Centre for Research in Biomolecular Interactions (CRBI), 4700 Keele Street, Toronto, Ontario, M3J 1P3 Canada

<sup>4</sup>Ottawa Institute of Systems Biology, University of Ottawa, Health Sciences Campus, 451 Smyth Road Ottawa, Ontario K1H 8M5 Canada

<sup>5</sup>Centre for Research in Mass Spectrometry (CRMS), York University, 4700 Keele Street, Toronto, Ontario, M3J 1P3 Canada

\*To whom correspondence should be addressed. Tel: +1 416 736 2100; Fax: +1 416 736 5698; E-mail: [jmcderm@yorku.ca](mailto:jmcderm@yorku.ca)

### Abstract

MEF2 plays a profound role in the regulation of transcription in cardiac and skeletal muscle lineages. To define the overlapping and unique MEF2A genomic targets, we utilized ChIP-exo analysis of cardiomyocytes and skeletal myoblasts. Of the 2783 and 1648 MEF2A binding peaks in skeletal myoblasts and cardiomyocytes, respectively, 294 common binding sites were identified. Genomic targets were compared to differentially expressed genes in RNA-seq analysis of MEF2A depleted myogenic cells, revealing two prominent genetic networks. Genes largely associated with muscle development were down-regulated by loss of MEF2A while up-regulated genes reveal a previously unrecognized function of MEF2A in suppressing growth/proliferative genes. Several up-regulated (*Tprg*, *Mctp2*, *Kitl*, *Prrx1*, *Dusp6*) and down-regulated (*Atp1a2*, *Hspb7*, *Tmem182*, *Sorbs2*, *Lmod3*) MEF2A target genes were chosen for further investigation. Interestingly, siRNA targeting of the MEF2A/D heterodimer revealed a somewhat divergent role in the control of *Dusp6*, a MAPK phosphatase, in cardiac and skeletal myogenic lineages. Furthermore, MEF2D functions as a p38MAPK dependent repressor of *Dusp6* in myoblasts. These data illustrate that MEF2 orchestrates both common and non-overlapping programs of signal-dependent gene expression in skeletal and cardiac muscle lineages.

## Introduction

Myocyte Enhancer Factor-2 (MEF2) is a member of the MADS-box super family of transcriptional regulatory proteins originally identified in skeletal muscle but are now an established component in the regulation of a diverse number of tissues including smooth, cardiac and skeletal muscle, neurons and T cells (123, 124, 126, 320). In vertebrates there are four MEF2 isoforms (A-D) which bind to the consensus sequence (C/T TA(A/T)<sub>4</sub>TAG/A) within the promoter/regulatory regions of genes to regulate gene transcription (109, 112). The transcriptional activation properties of MEF2 is regulated by a variety of post-translational mechanisms including regulation by MAPKs such as p38 and ERK5 (217, 219, 226) and PKA (147), and also through interaction with class II HDACs which inhibit MEF2-dependent gene activation (185, 348).

The transcriptional networks underlying both cardiac and skeletal muscle gene expression require MEF2 during embryonic and fetal development and for post-natal control of gene expression for tissue homeostasis in adulthood (78, 140, 191, 349). During embryonic development *Mef2* is expressed in the somite and the presumptive vertebrate heart in successive waves, beginning with *Mef2c* on embryonic day 9.0 (126). This is followed shortly thereafter by *Mef2a* and *Mef2d*. MEF2A and MEF2C are required at different stages of the life cycle. Global deletion of *Mef2c* is embryonic lethal due to impaired heart morphogenesis (78) while *Mef2a* is necessary for post-natal function since gene targeting results in mitochondrial and contractile defects in the heart (134). *Mef2d* homozygous null mice have no phenotypic abnormalities unless exposed to cardiac stress (135). Due to the impaired development and embryonic lethality associated with *Mef2* null mice, tissue specific conditional mutant mice have been useful in fully dissecting the role of MEF2 in a plethora of tissues. Interestingly, individual skeletal muscle deletion of *Mef2c*, but not *Mef2a* or *Mef2d* impairs proper muscle development in mice (145, 298). However, the MEF2 complex collectively has an important role in response to post-natal injury as a compound conditional deletion of *Mef2a*, *-c* and *-d* results in an inability to repair muscle after myotrauma (140). Additionally, MEF2 has been implicated in pathological heart hypertrophy in the adult by provoking the induction of fetal gene expression which is a hallmark of cardiomyocyte hypertrophy in the failing heart (191, 341, 350).

Functionally, cardiac and skeletal muscles share many properties and are similar in their reliance on a highly ordered sarcomeric structure. However, there are also important differences



between the two lineages that are subserved by interrelated but also subtly different programs of gene expression. Since MEF2 is expressed in both cell types it represents a useful paradigm for studying common and non-overlapping patterns of gene expression targeted by a transcriptional regulatory complex. A number of very well characterized MEF2 target genes that encode a network of structural proteins in cardiac and skeletal muscle such as Acta1, cTnT, MCK, MyHC, and MyLC, are already known (reviewed in (351)), and various large scale surveys to identify MEF2 targets has been completed independently in skeletal and cardiac muscle (214, 148, 352) however a detailed global inventory of MEF2 target genes in both tissues has not been done. A systematic comparison would provide a more complete picture of common and non-overlapping programs of MEF2-dependent gene expression. Moreover, an unbiased identification of MEF2 target genes may also reveal other properties of these lineages that are controlled by MEF2 dependent gene expression. It has been reported that MEF2 fulfills divergent roles in other cell types such as neurons, B cells and T cells regulating processes such as apoptosis and survival (125, 231, 293, 353). Clearly, MEF2 targets a more diverse set of genes than previously thought, warranting an unbiased comparison of genomic targets in skeletal and cardiac muscle.

Thus, the primary goal of this study was to identify a complete set of MEF2 target loci in skeletal and cardiac muscle using chromatin immunoprecipitation coupled with high throughput sequencing. The methodology used was ChIP-exo which utilizes exonuclease activity to digest unprotected DNA, and thereby provides refined sequencing data with high resolution identification of bound sequences (354). Here we report ChIP-exo identified global genomic MEF2A target genes in differentiating myoblast cells and cardiomyocytes. These studies characterize common and non-overlapping programs of MEF2-dependent gene expression and also reveal previously unanticipated functions of MEF2 in striated muscle.

## Methods

**Cell Culture.** C2C12 myoblasts and COS7 fibroblasts were obtained from American Tissue Culture Collection (ATCC). Cells were maintained in Dulbecco's Modified Eagle Medium (DMEM) with High Glucose and L-Glutamine (Hyclone) supplemented with 10% fetal bovine serum (HyClone) and 1% Penicillin/Streptomycin (Invitrogen). C2C12 were induced to differentiate in differentiation medium (DM) containing DMEM/High Glucose/L-Glutamine supplemented with 2% Horse Serum (Hyclone) and 1% Penicillin/Streptomycin for the indicated time. Primary neonatal cardiomyocytes were prepared from 1 to 3 day old rats using the Neonatal Cardiomyocyte Isolation System (Worthington Biochemical Corp). Briefly, whole hearts were dissociated with trypsin (Promega) and collagenase (Worthington Biochemical Corp). The cells were re-suspended in F12 DMEM (Gibco) supplemented with 10% FBS, 1% Penicillin/Streptomycin and 50 mg/L gentamycin sulfate (Invitrogen). The isolated cells were plated for 60 minutes at 37°C, allowing differential attachment of non-myocardial cells. Cardiomyocytes were counted and transferred to pre-gelatin coated 60-mm plates. The day after, medium was removed and replaced with fresh medium. All cells were maintained in an humidified, 37°C incubator at 5% CO<sub>2</sub>. Pharmacological drug treatments were completed for the indicated times and replenished with fresh medium every 24 hr.

**Transfections.** COS7 were transfected using the calcium phosphate precipitation method. Cells were then harvested 48 hr post transfection. For siRNA experiments in C2C12 Lipofectamine (Invitrogen) was used according to the manufacturer's instructions. Cells were then harvested 24 hr later or the media was changed to DM. Neonatal cardiomyocytes were transiently transfected with siRNA using Lipofectamine RNAiMax (Invitrogen) according to the manufacturer's instructions.

**Plasmids.** Expression plasmids for pcDNA3-MEF2D, pCMV-dsRed2, pMT3-p38 and pcDNA3-MKK6ee have been described (218, 147)(10, 32). The following reporter constructs were used: pRL-Renilla (Promega) and pGL3Basic-*Dusp6*-Luciferase (1010 bp; (355)).

**Antibodies and reagents.** Rabbit polyclonal MEF2A antibody has been previously described (38). The following antibodies were purchased from Santa Cruz: actin (sc-1616), dsRed (sc-33354), MEF2A (sc-313X; used in CHIP), donkey anti-goat IgG-HRP (sc-2020), ERK-1 (sc-93). The following antibodies were obtained from Cell Signaling: p38 (9212), phospho-p38 (9211), phospho-ERK1/2 (4370). Myogenin (clone F5D) monoclonal antibodies were provided by the

Developmental Studies Hybridoma Bank. Goat anti-rabbit IgG-HRP (170-6515) and goat anti-mouse IgG-HRP (170-6516) were from Bio-Rad Laboratories. The remaining antibodies are as follows: MEF2D (BD Biosciences, 610775), DUSP6 (Abcam, ab76310), Rabbit IgG (Millipore, 12-370), IRDye 680RD goat anti-rabbit (LiCOR) and IRDye 680RD goat anti-mouse (LiCOR). SB 202474 (Santa Cruz) and SB 203580 (Cell Signaling) was used at a concentration of 5  $\mu$ M. **siRNA.** Knockdown of target genes was done using siRNA obtained from Sigma-Aldrich and are listed in Supplementary Figure S4. In C2C12 siRNA was transfected at the following concentration: *Mef2a* (30 nM), *Mef2d* (70 nM), *Atp1a2*, *Dusp6*, *Hspb7*, *Kitl*, *Lmod3*, *Mctp2*, *Prrx1*, *Sorbs2*, *Tmem182*, and *Tprg* at 50 nM. In cardiomyocytes siRNA were transfected at a final concentration of 200 nM.

**Immunoblots.** Cells were washed with 1XPBS and lysed in NP-40 lysis buffer (50 mM Tris, 150 mM NaCl, 0.5% NP-40, 2 mM EDTA, 100 mM NaF and 10 mM Na pyrophosphate) containing protease inhibitor cocktail (Sigma-Aldrich), 1 mM phenylmethylsulfonyl fluoride (Sigma-Aldrich), and 1 mM sodium orthovanadate (Bioshop). Protein concentrations were determined by Bradford assay (Bio-Rad). Twenty  $\mu$ g of total protein were resolved on 10% SDS-PAGE and then transferred onto Immobilon-FL PVDF membrane (Millipore) for 1 hr or overnight. Non-specific binding sites were blocked using 5% milk in PBS or TBST. Membranes were incubated with primary antibodies overnight at 4°C in 5% milk in PBS or 5% BSA in TBST. HRP-conjugated secondary antibody was added for 1 hr at RT. Protein was detected with ECL Chemiluminescence reagent (Pierce). In cardiomyocytes, immunoblots were performed as described above except antibodies were incubated with Odyssey Blocking Buffer (LiCOR) and membranes were imaged using the LiCOR Odyssey System.

**Luciferase Analysis.** Cells were washed with 1XPBS and then lysed in Luciferase Lysis Buffer (20 mM Tris pH 7.4 0.1% Triton X-100). Lysate was briefly vortexed and centrifuged at maximum speed for 15 minutes at 4°C. Enzymatic activity was measured in each sample on a luminometer using Luciferase assay substrate (E1501, Promega) or Renilla assay substrate (E2829, Promega). Western blots of luciferase extracts contained equal volumes from each triplicate.

**Chromatin Immunoprecipitation.** Methods were carried out as described previously described (356) however a third IP Wash Buffer was added (IP Wash Buffer III; 20 mM Tris pH 8.1, 250 mM LiCl, 1% NP-40, 1% deoxycholate, 1 mM EDTA).

**RNA extraction.** Total RNA was extracted from cells using the RNeasy Plus kit (Qiagen) and Qiashredder (Qiagen). RNA was converted to cDNA using Superscript III (Invitrogen) according to the manufacturer's instructions.

**Quantitative PCR.** 2.5  $\mu$ l gDNA or cDNA was combined with SybrGreen (BioRad) and 500 nM primers in a final volume of 20  $\mu$ l. cDNA was diluted 1:10 prior to use. Each sample was prepared in triplicate and analyzed using Rotor-Gene Q (Qiagen). Parameters for qRT-PCR: 30s 95°C, [5s 95°C, 30s 60°C] x 40 cycles. Parameters for ChIP-qPCR: 5min 95°C, [5s 95°C, 15s 60°C] x 40 cycles. Fold enrichment (ChIP-qPCR) and Fold change (qRT-PCR) was quantified using the  $\Delta\Delta$ Ct method. Primers used in ChIP-qPCR and qRT-PCR are listed in Supplementary Figure S5 and S6, respectively.

**ChIP-exo.**  $15 \times 10^6$  C2C12 (48 hr DM) and  $8 \times 10^6$  primary rat cardiomyocytes were prepared for ChIP-exo as follows: Cells were washed with 1XPBS and treated with 37% formaldehyde (Sigma) for 15 minutes at 37°C. The cell pellet was isolated similar to ChIP-qPCR as previously described (356). DNA was sonicated to approximately 250 bp in length. Crosslinked chromatin was sent to Peconic Genomics with 5  $\mu$ g anti-MEF2A (Santa Cruz) and Rabbit IgG (Millipore). Peconic Genomics completed ChIP-exo, sequencing, and sequence alignment as previously described (31). Sequencing reads were aligned to the mm10 (C2C12) or rn5 (cardiomyocytes) genome assembly. Raw data was filtered for a quality score of 37, and duplicates were removed using Picard (<http://picard.sourceforge.net/>). MACS 1.4.2 was used to do peak calling analysis (357). To identify MEF2A target genes in skeletal and cardiac muscle corresponding to peak location, MEF2A enrichment peaks identified in MACS were converted to mm9 using UCSC LiftOver (358).

**RNA-seq.** 30 nM of *Mef2a* siRNA2 or scrambled control was transfected into C2C12 as described above. Five  $\mu$ g of total RNA was isolated from C2C12 at 48 hr DM, as described above, in duplicate. Purified RNA was delivered to McGill University and Genome Quebec Innovation Centre (MUGQIC) for cDNA library preparation (Illumina TruSeq stranded cDNA library), RNA-sequencing (Illumina HiSeq2000, 100 bp paired-end reads; 4 samples per lane), and bioinformatic analysis. Sequencing reads were aligned to the mm10 genome assembly.

## Results

### ChIP-exo analysis of MEF2A target genes in skeletal and cardiac muscle identifies overlapping regulatory domains with divergent gene function

To identify novel MEF2A target genes in skeletal and cardiac muscle, ChIP-exo was performed in differentiating cultured C2C12 myoblasts (MB; 48 hr Differentiation Media (DM)) and primary cardiomyocytes (CM) using a MEF2A specific antibody or a rabbit IgG control (Figure 1A). C2C12 myoblasts fuse into multinucleated myotubes when grown in low serum DM. During the initial phase of myogenesis MEF2A and MEF2D expression increases (Supplementary Figure S1); therefore ChIP-exo was performed at 48 hr DM, a time at which MEF2 transcriptional activity has been documented to be high.

Of the 2783 and 1648 MEF2A peaks discovered in MBs and CMs, respectively, 294 common enrichment peaks were identified (Figure 1B; Supplementary Table S1-S3). Nearby genes were identified using Genomic Regions Enrichment of Annotations Tool (GREAT; (359)) using the 5+1 kb basal promoter with 1 Mb extension rule. Based on this analysis it was possible for some MEF2A peaks to be associated with more than one gene. The 294 common MEF2A binding peaks corresponded to 473 putative MEF2A target gene associations in skeletal and cardiac muscle. Region-gene associations of MEF2A peaks were then compared using five different parameters relative to the transcription start site (TSS): proximal promoter ( $\pm 5$  kb), upstream (-5 kb to -50 kb), downstream (+5 to +50 kb), intergenic (>50 kb from any Gene), or no gene association (Figure 1C). The pattern of MEF2A recruitment to different regions of the genome in skeletal and cardiac muscle was relatively similar. Approximately only 7% of MEF2A peaks in both cell types were associated with the proximal promoter while nearly 63% of all MEF2A peaks were found in the intergenic region.

Further analysis using CENTDIST (360) revealed common transcription factor motifs within MEF2A enrichment peaks ( $p$ -value<0.05; Figure 1D). The top two motifs within skeletal and cardiac peaks were MEF2 and AP-1. CREB and BACH motifs were also prevalent in both datasets, however it is noted that the BACH motif is quite similar to AP-1. Interestingly, AP-1 motifs were also found to be enriched in a genome-wide screen of MyoD binding sites in skeletal muscle (216). E-box motifs were also enriched in skeletal muscle but ranked position 13.

Lastly, the functional role of MEF2A target genes was assessed using Gene Ontology (GO) analysis to identify terms enriched in either Biological Processes or Cellular Component

annotations determined in GREAT (Figure 1E; Supplementary Table S1 and S2). Enriched Cellular Component GO terms were similar in skeletal muscle and cardiomyocytes with annotations such as Contractile Fiber and Myofibril. GO terms associated with Biological Processes was the first analysis that suggested MEF2A had a different role in skeletal and cardiac tissue, targeting genes that affected MAP kinase activity or apoptosis, respectively. Both cell types, however, were associated with actin movement.



**Figure 1.**

**Figure 1. Identification of MEF2A target genes in myoblasts and cardiomyocytes using ChIP-exo.** (A) Workflow of ChIP-exo analysis. C2C12 (48 hr DM; MB) and primary cardiomyocytes (CM) were collected to identify MEF2A target genes using ChIP-exo. A non-specific IgG antibody was used as a control. (B) The number of common MEF2A enriched peaks in MB and CM identified in ChIP-exo are indicated in a Venn diagram. (C) The percentage of peaks within the Proximal Promoter ( $\pm 5$  kb), Upstream (-5 to -50 kb), Downstream (+5 to +50 kb), or Intergenic region ( $>50$  kb from any annotated gene) identified in ChIP-exo using GREAT. Location is relative to the transcription start site. (D) The five most dominant transcription factor binding motifs found within MEF2A-enriched peaks as determined by CENTDIST (p-value $<0.05$ ). (E) Biological Processes and Cellular Component GO terms of MEF2A enriched peaks from MB and CM.



## **RNA-seq analysis of MEF2A depleted myoblasts reveals multiple MEF2 gene networks in regulating cell processes**

To further interrogate the identification of MEF2A target genes, RNA-seq analysis was performed in C2C12 (48 hr DM) depleted of MEF2A using siRNA mediated gene silencing and compared to a scrambled siRNA control (Figure 2A). Efficiency of MEF2A knockdown at this time point was assessed using western blotting comparing two independent siRNAs programmed to target MEF2A (Figure 2B). siMEF2A-2 was subsequently used in RNA-seq analysis which resulted in 828 downregulated and 452 upregulated genes (edgeR p-value<0.05; Supplementary Table S4). The functional role of MEF2A was assessed using GO::TermFinder (361) to identify enriched GO Biological Processes, however, the up- and down-regulated genes were assessed separately. Figure 2C shows the top five GO Biological Processes enriched in each group. This segregation revealed two different roles of MEF2A: Not only does loss of MEF2A lead to a downregulation of muscle function, as has been previously shown, but also results in the unanticipated upregulation of genes associated with cellular migration and locomotion, a cellular process previously not associated with MEF2 function.

The differentially expressed genes identified in RNA-seq were compared with those enriched in ChIP-exo analysis in MB (Figure 2D). Up- and down-regulated genes were separated and then grouped as either ChIP (-) or ChIP (+). As expected, a number of MEF2A target genes identified in ChIP-exo were also found to be differentially regulated in MEF2A depleted myoblasts. 190/828 downregulated genes and 121/452 upregulated genes were found to be MEF2A targets in ChIP-exo. The location of each MEF2A enrichment peak of these differentially expressed genes was then assessed (Figure 2E). Genes were grouped into four bins based on the location of the MEF2A enrichment peak relative to the TSS:  $\pm 5$  kb, -5 to -50 kb, +5 to +50 kb, and >50 kb. This classification revealed that the majority of MEF2A recruitment to downregulated genes occurs equally within the  $\pm 5$  kb, -5 to -50 kb, and +5 to +50 kb regions. In contrast approximately 65% of genes that were upregulated in response to MEF2A knockdown were associated with MEF2A enrichment peaks >50 kb from the TSS. MEF2A recruitment to the proximal promoter ( $\pm 5$  kb) of upregulated genes was less than 5%.

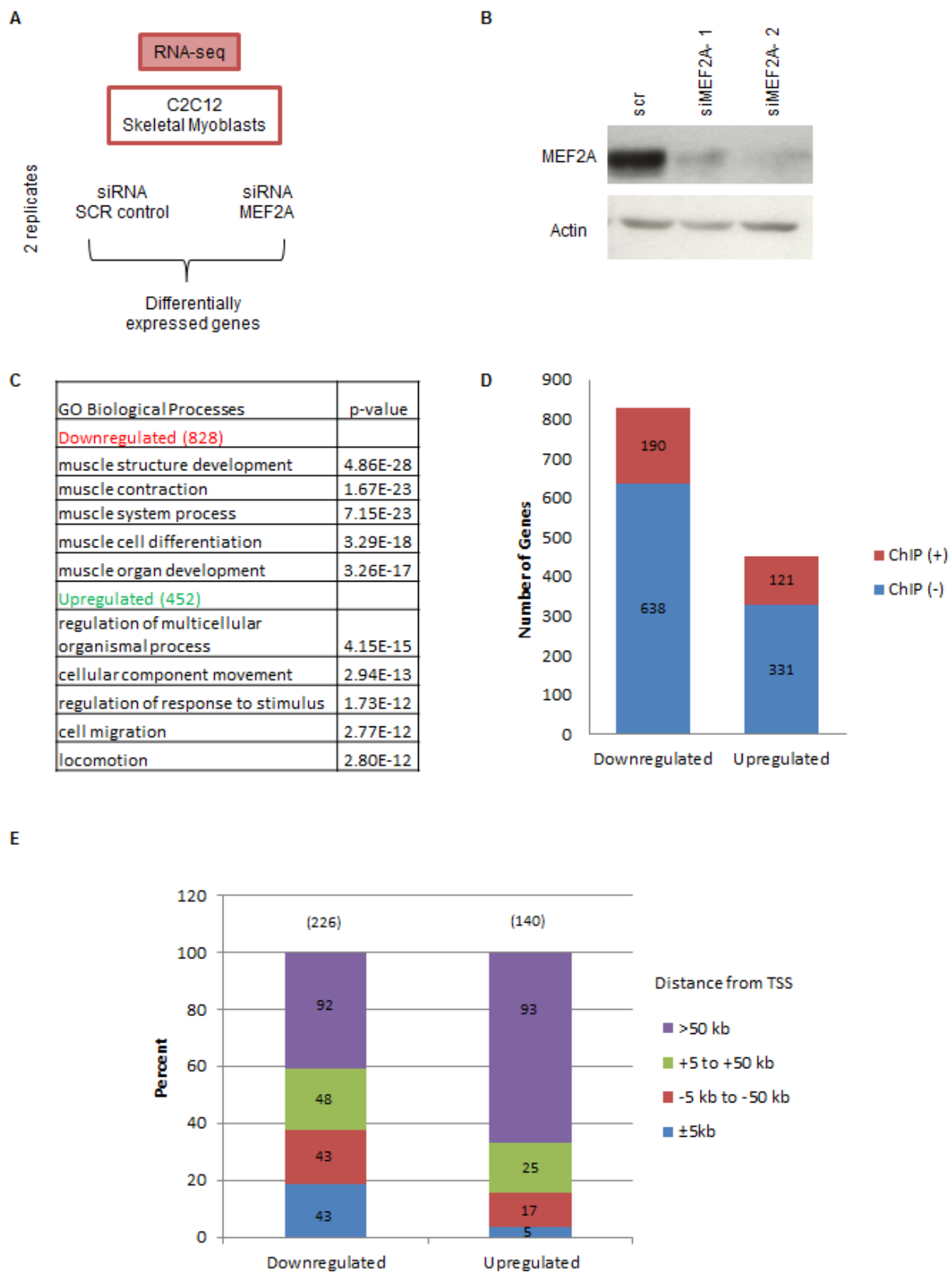


**Figure 2.**

**Figure 2. RNA-seq analysis of MEF2A depleted skeletal myoblasts.** (A) RNA-seq analysis workflow. MB were transfected with 30 nM of siMEF2A-2 or a scrambled siRNA control. 5 µg of RNA was prepared for RNA-seq analysis in duplicate. Differentially expressed genes were assessed using edgeR p-value<0.05. (B) Two different siRNA targeting *Mef2a* were transfected into myoblasts at 30 nM and allowed to differentiate for 48 hr in DM. Cells were harvested and protein was extracted to assess changes in MEF2A using western blotting. (C) Distinguished roles for MEF2A in skeletal myogenesis were revealed when up- and down-regulated genes were grouped separately prior to GO (Biological Processes) term analysis. (D) The differentially expressed genes that were also identified as MEF2A target genes in MB were determined (ChIP (+)). Differentially expressed genes that were not identified as MEF2A targets are labelled ChIP (-). (E) Binding profiles of MEF2A recruitment to associated genes in MB based on their differential expression in RNA-seq analysis.

## Functional analysis of MEF2A target genes

To investigate whether MEF2A shared novel target genes in cardiac and skeletal muscle, the differentially expressed genes identified in RNA-seq were grouped in a similar classification to Fig 2D, however MEF2A target genes in CM were included. Three divisions of differentially expressed genes were established: ChIP (-), ChIP (+) MB, and ChIP (+) MB and CM. Only 4% of differentially expressed genes were identified as MEF2A target genes in MB and CM (Figure 3A). This corresponded to 38 downregulated and 20 upregulated genes (Supplementary Table S4). From this list, ten putative MEF2A target genes were selected for further study. The location of MEF2A recruitment is indicated based on the peak location relative to the TSS of each gene (Figure 3B). The presence of a MEF2 consensus sequence within 1 kb of the enrichment peak is also indicated.

To validate that the identified genes from ChIP-exo and RNA-seq were true MEF2A target genes, *Dusp6* (Dual specificity phosphatase 6), *Hspb7* (Heat shock protein family, member 7), *Kitl* (Kit ligand), *Lmod3* (Leiomodin 3) and *Prrx1* (Paired related homeobox 1) were chosen for further study. Only *Kitl*, *Lmod3* and *Hspb7* contain nearby MEF2 consensus sequences. We confirmed MEF2A recruitment to these genes using gene targeted ChIP-qPCR in C2C12 at 48 hr DM (Figure 3C). Primers were designed to flank the MEF2A enrichment peak or the nearby MEF2 consensus sequence (if present). Figure 3D represents, for each gene, the ChIP-exo sequencing read density in C2C12 as well as MACS peak calls, and was prepared using the Integrative Genome Viewer (IGV; (362)). In some cases, genes had more than one enrichment peak. For example, MEF2A was recruited to two locations upstream of *Dusp6* at  $\pm 5$  kb and -5 to 50 kb in both CM and MB. In this case we focused on the more proximal binding event 150 bp upstream from the TSS in ChIP-qPCR analysis. *Prrx1*, however, had three MEF2 binding events in MB but only one (+91 kb; MACS\_peak\_212) had a common binding event in CM. Using ChIP-qPCR we detected variable MEF2A recruitment at all genes compared to *Acta2*. Interestingly the level of MEF2A recruitment to target genes in Figure 3C corresponded to similar enrichment patterns detected in ChIP-exo.

Two independent *Mef2a* siRNAs were individually transfected into MB. At 48 hr DM the expression of three up (*Kitl*, *Prrx1* and *Dusp6*) and two downregulated (*Hspb7* and *Lmod3*) genes were then assessed (Figure 3E). Similar to RNA-seq results, loss of MEF2A resulted in the downregulation of *Lmod3* and *Hspb7*. Conversely *Dusp6*, *Prrx1* and *Kitl* were upregulated in

response to MEF2A knockdown. Interestingly MEF2D was also shown to be recruited to *Prrx1*, *Lmod3*, and *Hspb7* in myoblasts and these genes were differentially expressed in response to MEF2D overexpression (148).

To begin to understand the functional role of these putative MEF2 target genes we used siRNA gene silencing to suppress the expression of *Atp1a2* (ATPase, Na<sup>+</sup>/K<sup>+</sup> transporting, alpha 2 polypeptide), *Dusp6*, *Hspb7*, *Kitl*, *Lmod3*, *Mctp2* (Multiple C2 domains transmembrane 2), *Prrx1*, *Tmem182* (Transmembrane protein 182), *Sorbs2* (Sorbin and SH3 domain containing 2), and *Tprg* (Transformation related protein 63 regulated), and determined their role in myogenesis by assessing changes in *Myogenin* expression in myoblasts as a readout of the irreversible commitment to myogenic induction (Figure 3F). Prior to this, the efficiency of knockdown of each target gene was determined using three siRNAs labelled A-C (Supplementary Figure S2). The two with the most efficient knockdown of the targeted gene product were selected to assess *Myogenin* expression. The knockdown of a number of these genes resulted in downregulation of *Myogenin* expression in myoblasts in GM. In particular, loss of *Hspb7* and *Kitl* reduced *Myogenin* by 50% indicating that a number of the identified MEF2 target genes are crucial for efficient myogenic differentiation and their precise role in the myogenic program remains to be characterized.

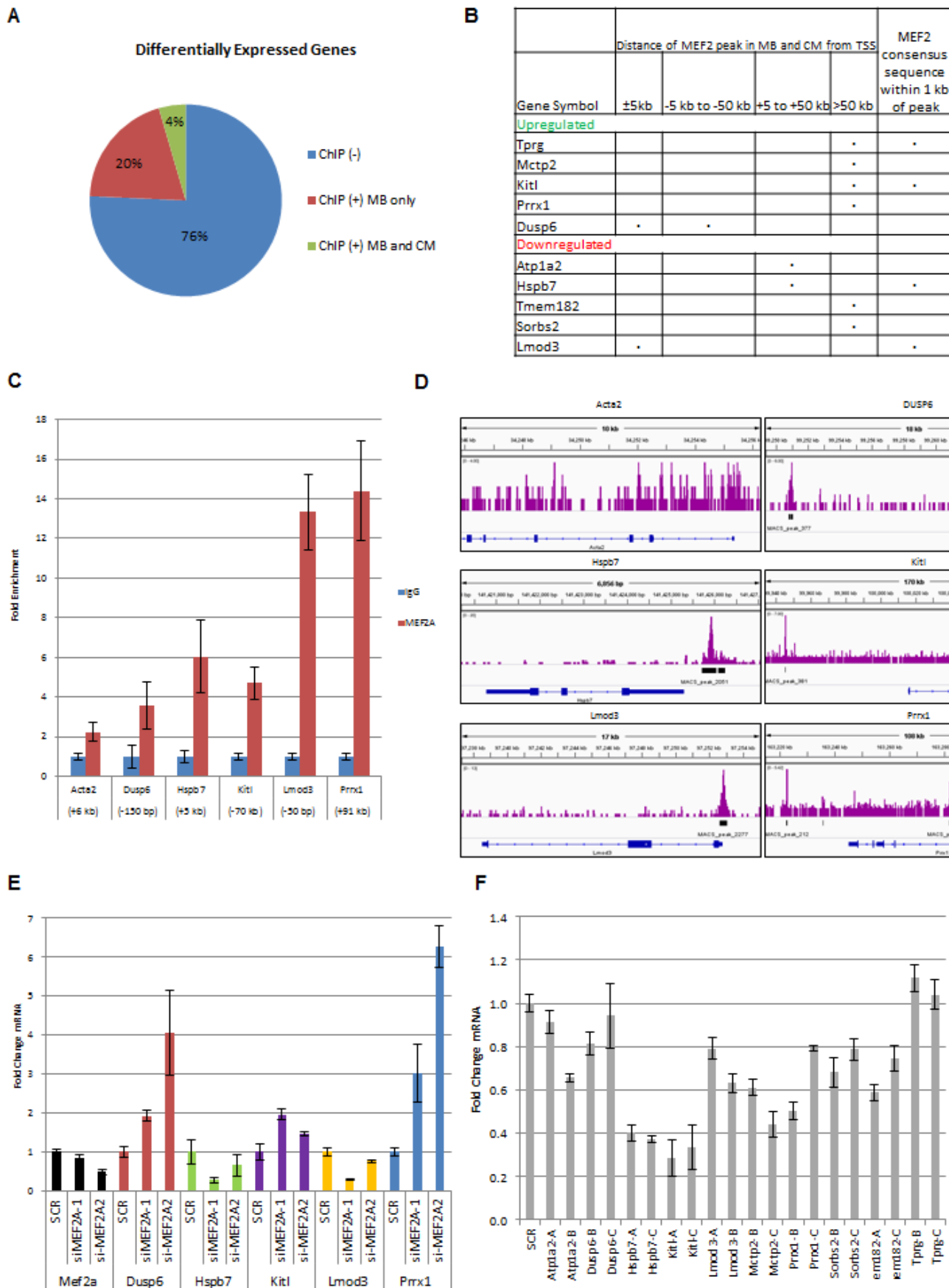


Figure 3. 88

**Figure 3. Functional analysis of MEF2A target genes.** (A) The percentage of differentially expressed genes in MB that were also identified as MEF2A target genes (ChIP (+)) in MB alone or MB and CM. (B) Comparative analysis of ten putative MEF2A target genes. Selected genes were differentially expressed in RNA-seq analysis in MB and shared overlapping MEF2A enrichment peaks in MB and CM. The locations of common MEF2A recruitment peaks relative to the TSS and nearby MEF2 consensus sequences are indicated. (C) MEF2A recruitment was assessed in C2C12 (48 hr DM) using ChIP-qPCR. *Acta2* was used as a negative control locus. Error bars represent  $\pm$  SD, n=3. (D) Screenshot from IGV depicting C2C12 ChIP-exo read density and MACS peak calls. Read densities are in purple, MACS peak calls are in black and Refseq genes are in blue. (E) Two different siRNA targeting *Mef2a* were transfected into C2C12 at 30 nM and allowed to differentiate for 48 hr in DM. Cells were harvested and RNA was extracted to assess changes gene expression using qRT-PCR. Samples were normalized to  $\beta$ -*actin*. Error bars represent  $\pm$  SD, n=3. (F) Knockdown of individual target genes in MB. C2C12 were transfected with 50 nM siRNA and harvested 24 hr later. mRNA was assessed similar to that in (E).

## **DUSP6 is a novel MEF2 target gene in cardiac and skeletal muscle**

We were particularly interested in the identification of *Dusp6* as a MEF2A target since it was shown to be necessary in regulating the skeletal muscle satellite cell population and has also been implicated in cardiac hypertrophy (363, 364). Based on the overlap of MEF2 recruitment to the *Dusp6* promoter in MBs and CMs and its relative location in relation to other transcriptional regulatory domains of the *Dusp6* gene locus (355), *Dusp6* was selected for further mechanistic analysis in terms of how it is regulated by MEF2.

To confirm that *Dusp6* is also a MEF2A target gene in cardiomyocytes ChIP-qPCR was done in primary cardiomyocytes (Figure 4A). This analysis confirmed that MEF2A is recruited to a shared location within the *Dusp6* promoter in both myoblasts and cardiomyocytes. Furthermore, MEF2A or MEF2D depletion from cardiomyocytes (Figure 4B, C) or myoblasts (Figure 4D) and corresponding DUSP6 expression was assessed in western blot analysis. Knockdown of either MEF2 subunit in cardiomyocytes dramatically increased DUSP6 expression (Figure 4B, C). Although loss of MEF2A at 48 hr DM upregulated *Dusp6* transcription in myoblasts (Figure 3B), at the protein level, DUSP6 was unaffected by knockdown of MEF2A in C2C12 (24 hr DM; Figure 4D) and we suspect this is a temporal lag in response to the knockdown. In contrast, loss of MEF2D (the heterodimeric partner of MEF2A in MBs (146)) increased DUSP6 expression.



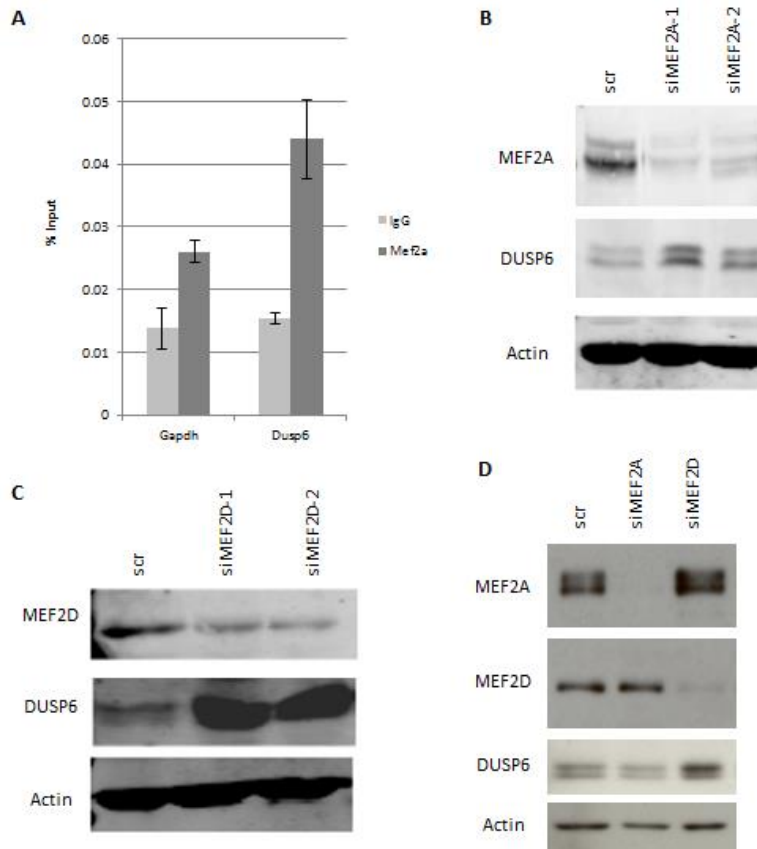


**Figure 4. siRNA mediated gene silencing of MEF2 in cardiomyocytes or myoblasts induces DUSP6 expression.** (A) MEF2A is recruited to the *Dusp6* promoter in primary cardiomyocytes. *Gapdh* was used as a negative control locus. Error bars represent  $\pm$  SD, n=3. (B) Knockdown of MEF2A or MEF2D (C) in primary cardiomyocytes upregulates *Dusp6* expression. siRNA was added at a final concentration of 200 nM. Protein was harvested and analyzed by immunoblotting with the indicated antibodies. (D) Knockdown of MEF2D upregulates DUSP6 expression in MB. *Mef2a* or *Mef2d* were targeted using 30-70 nM siRNA. C2C12 were harvested at 24 hr DM for immunoblot analysis.

### Regulation of DUSP6 by MEF2 is p38MAPK dependent in myoblasts

DUSP6 is a dual specificity protein phosphatase, predominately targeting ERK1/2 activity (365, 366). Interestingly, *Dusp6* expression is mediated by growth factors and ERK1/2 activation in a negative feedback loop (355, 367). Upon serum withdrawal in C2C12 myoblasts we observed a decrease in DUSP6 expression during the initial phase of myogenesis (Figure 5A) under conditions when we have previously documented that MEF2 protein levels and DNA binding activity are increasing (138). In addition there was a corresponding decrease in ERK1/2 activity and activation of p38MAPK. Since MEF2 becomes activated in part due to

phosphorylation by p38MAPK (217) and there is an inverse relationship between DUSP6 expression and p38MAPK activity we sought to determine whether p38MAPK also has a role in regulating *Dusp6*. C2C12 were treated with a well characterized p38MAPK inhibitor SB 203580 (5  $\mu$ M) or its inactive analogue SB 202474 as a control. A time course treatment of MBs with or without SB 203580 treatment revealed that while p38MAPK inhibition blocked myogenesis, as shown by a decrease in Myogenin expression, this was accompanied by an upregulation of DUSP6 (Figure 5B). MEF2A and MEF2D are downregulated in response to SB 203580 treatment, probably as a result of an overall delay in myogenesis (Supplementary Figure S3). To determine whether p38MAPK was acting directly through MEF2 to modulate DUSP6 expression, C2C12 were transfected with two sets of siRNA targeting *Mef2a* or *Mef2d* and then treated with SB 203580 for 24 hr in DM (Figure 5C). p38MAPK inhibitor treatment consistently upregulated DUSP6, with or without MEF2A. In MEF2D depleted cells, however, SB 203580 treatment did not have any effect on DUSP6 induction. Our interpretation of these data, in contrast to the usual potentiating effect of p38MAPK on MEF2 activity, is that MEF2D is required for the p38MAPK-dependent repression of DUSP6.

To test this novel observation further in a carefully controlled reconstruction assay we transfected COS cells (as a neutral cell type to circumvent endogenous regulation by factors in MBs) with a *Dusp6* promoter construct, *Dusp6*-luc (1010 bp; (355)), with or without a constitutively active MKK6 (MKK6<sup>ee</sup> to activate p38MAPK), p38MAPK, or MEF2D. The results of this assay were unequivocal in that individually, MEF2D and activated p38MAPK activate expression of the *Dusp6* reporter gene but when transfected in combination, MEF2D and activated p38MAPK cannot induce expression of *Dusp6*-luc (Figure 5D). Also, SB 203580 treatment reverses this effect by enhancing *Dusp6* reporter gene activation, further supporting the direct involvement of p38MAPK in this negative regulation. Simultaneous western blot analysis of this experiment shows that MKK6<sup>ee</sup>/p38MAPK induce the previously well characterized post-translational modifications of MEF2 (368) and SB 203580 treatment reverses these PTMs as expected (Figure 5D). Collectively, these data lead us to the novel conclusion that p38MAPK signaling to MEF2D leads to transcriptional repression of the *Dusp6* promoter (Figure 5E).

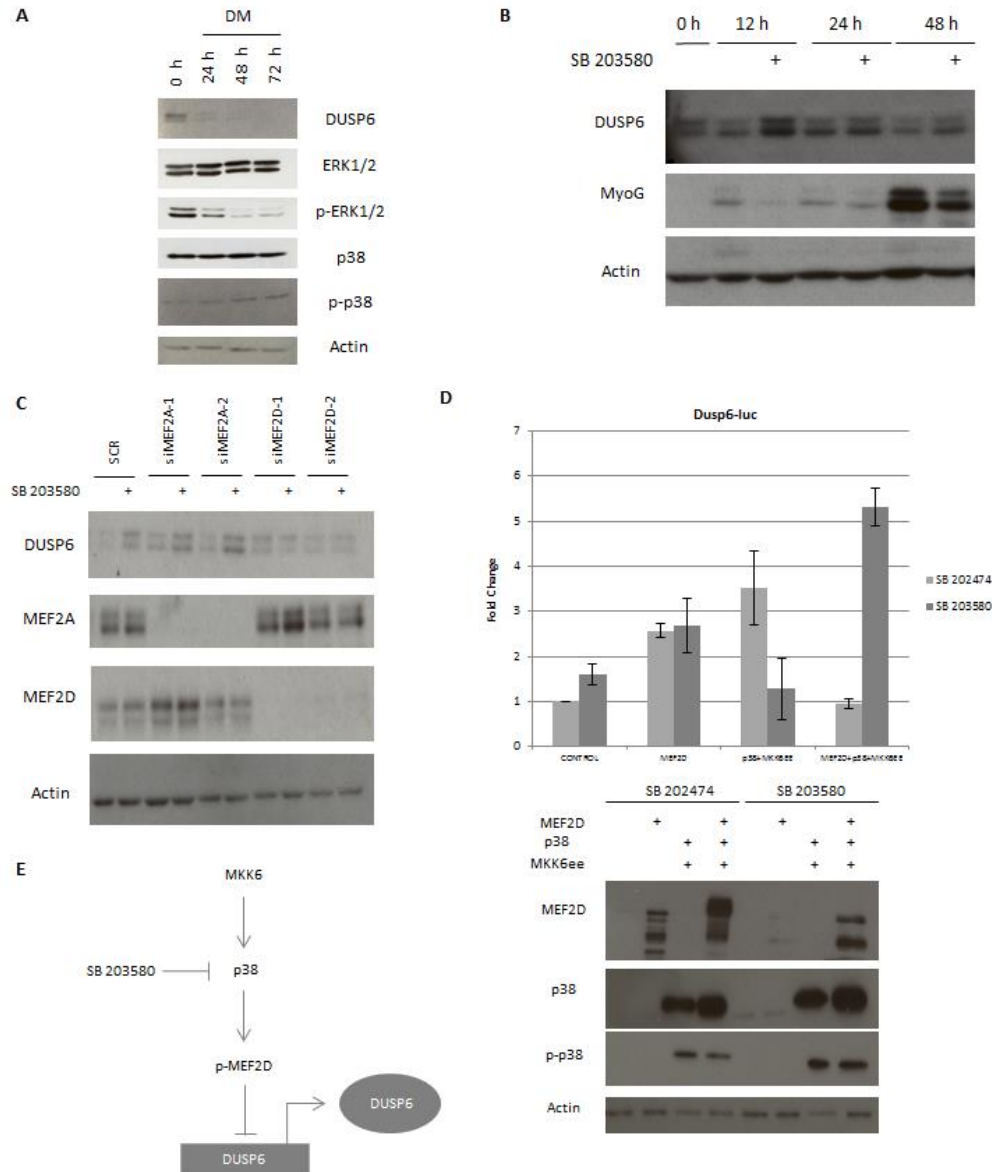


**Figure 5. MEF2D inhibits DUSP6 in a p38MAPK dependent manner in myoblasts.** (A) C2C12 were allowed to differentiate, harvested at the times specified and analyzed by immunoblotting with the indicated antibodies. (B) Myogenesis is inhibited when C2C12 are treated with p38MAPK inhibitor SB 203580 (5  $\mu$ M). Media was changed to DM for the indicated time and protein was assessed by immunoblotting. Control cells were treated with an inactive analogue, SB 202474. (C) C2C12 were transfected with 30nM siMEF2A or 70 nM siMEF2D and treated with SB 203580 (5  $\mu$ M) for 24 hr in DM. Cells were harvested as described above. (D) COS7 were transfected with *Dusp6*-luc and the indicated plasmids. One day after transfection cells were treated with 5  $\mu$ M SB 203580 or inactive analogue for 24 hr. Luciferase values were normalized to Renilla. Error bars represent  $\pm$  SEM, n=3. Corresponding western blots are shown. (E) *Dusp6* is negatively regulated by MEF2D in a p38MAPK dependent manner.

## Discussion

Using forefront methods in genomic analysis we have characterized the panoply of MEF2A genomic targets in striated muscle. Moreover, by coupling this chromatin based genome wide analysis of MEF2A DNA binding to MEF2A gene silencing and RNA-seq we have been able to comprehensively catalog both direct and indirect genomic targets of MEF2. These data identify some novel aspects of MEF2 function that have, thus far, not been appreciated. Particularly, this comparative analysis will lead to new directions in understanding the function of MEF2 in a variety of contexts in its role as an important regulator of gene expression in all muscle types, neurons and immune system cells, both during development and in a variety of post-natal physiological and pathological circumstances. In addition, more detailed analysis by gene silencing of some of the identified MEF2A target genes led us to identify a number of downstream targets that fulfill a potentially important role in the myogenic program. Finally, mechanistic studies concerning the regulation of the *Dusp6* locus by MEF2 has led us to the novel conclusion that p38MAPK-MEF2 signaling leads to repression of DUSP6 expression during the myogenic cascade.

ERK1/2 inactivation through DUSP6 expression has been linked to pluripotency in embryonic stem cells (369), cardiac hypertrophy (363, 370) and the satellite stem cell pool in muscle (364). Therefore there is an evident requirement of DUSP6 to downregulate ERK1/2 signaling in the very early phases of differentiation. In skeletal muscle cells p38MAPK and ERK1/2 exhibit inverse activity: in growth conditions, p38MAPK is inactive and ERK1/2 is active (371), however upon the withdrawal of growth factors, p38MAPK becomes active, ERK1/2 is inhibited, and the myogenic cascade proceeds. The results presented here may be linked to a previously reported biphasic role for ERK1/2 in muscle in which ERK1/2 is implicated in proliferation of myoblasts under growth conditions but also in differentiation conditions in myotube fusion (372, 373). In this model DUSP6 expression itself has to be extinguished for the myogenic program to proceed and for ERK1/2 involvement in myoblast fusion later in the program. Our contention is therefore that the induction of MEF2 and p38MAPK activity at the onset of differentiation is required for the transcriptional suppression of *Dusp6* which then allows myogenesis to proceed.

The canonical interpretation of the p38MAPK-MEF2 signaling pathway has, so far, been that when covalently modified by p38MAPK mediated phosphorylation, MEF2 transcriptional

activation properties are enhanced (217) however, as alluded to above, our data illustrate that MEF2D represses *Dusp6* expression in a p38MAPK dependent manner. Interestingly, this potentially repressive role of MEF2 at some genes may also clarify the previously unexplained observation that in a compound transgenic in which the MEF2 sensor mice were bred with *Mef2a* homozygous nulls, an unexpectedly high  $\beta$ -Galactosidase staining was observed in some tissues in the mice (134). This observation is consistent with a potent repressive effect of MEF2 in certain cellular contexts. Indeed there have been several negative regulators of MEF2 identified including HDAC4 (348), Cabin1 (374), MITR (193), HIPK2 (220) and PKA (147, 230), however it is unclear at this point how p38MAPK can lead to MEF2-mediated transcriptional repression. Indeed, primary limb mesenchymal cultures treated with p38MAPK inhibitor also exhibited enhanced MEF2 activity which implies that the regulation of MEF2 activity by p38MAPK activity is not as straightforward as previously thought (375).

*Dusp6* provides not only an example of a common MEF2 target gene in skeletal and cardiac muscle but also demonstrates the complex role of MEF2 as a heterodimer. Characterization of binding sites of the single *Mef2* gene in *Drosophila* using CHIP-chip and mutagenesis first revealed that MEF2 has a more significant role in muscle development than originally thought and further showed that MEF2 activity is regulated in a complex manner to function differently at certain developmental timepoints (213). In vertebrate development, it is not surprising that with four *Mef2* genes, the complexity of MEF2-dependent gene expression increases. With respect to the role of MEF2A/D heterodimers in skeletal muscle, MEF2A and MEF2D are subject to differential regulation by PKA (147), among other kinases, and MEF2D is differentially spliced in a skeletal muscle specific manner (148), which together may explain the seemingly more dominant role of MEF2D in regulating *Dusp6* in MB. It is also critical to recognize that the majority of MEF2A target genes identified in CM and MB are not shared. This could be explained by differential upstream signaling, different co-factor interactions, and chromatin accessibility. Although the majority of target genes between CM and MB were different, the predominant transcription factor motifs and GO processes were largely similar indicating conservation of MEF2 function at the level of cellular processes. However, one exception to this is that MEF2A target genes in CM were associated with GO Biological Processes involving apoptosis and cell death. Currently there is no direct evidence that MEF2 regulates apoptosis in cardiomyocytes.

In terms of the global target gene network that we have identified, there are some results that surprised us. The first was that some distal MEF2 binding events were observed greater than 50 kb from the TSS. Similar to our findings, MEF2 binds to intra- and intergenic enhancer regions during cardiac hypertrophy (376). Together this indicates that MEF2 has an emerging role as a transcription factor that is able to regulate gene expression globally. Furthermore, MEF2A was recruited to different genomic regions in up- and down-regulated genes. An interesting possibility would be that the position of MEF2 recruitment relative to the TSS dictates its function as a positive or negative regulator of transcription. The second observation is that there are a number of genes that were upregulated in response to MEF2A knockdown in myoblasts including *Tprg*, *Mctp2*, *Kitl*, *Prrx1* and *Dusp6*. Repression of these genes may not be solely regulated by MEF2 as AP-1 binding sites, which are associated with proliferation, are frequently found not only in MEF2 enriched binding sites (as reported here in both CM and MB) but also in MyoD target genes (216). AP-1 and MyoD are known to antagonize each other's function through direct protein-protein interactions (377, 378), and yet together, can also form MyoD-directed enhancers (379). Based on data presented here it is likely that MEF2 may either have a role in AP-1-MyoD dependent gene expression, or AP-1 and MEF2 may function in combination and independently of MyoD to regulate developmental processes.

Using high throughput genomic approaches we have identified a comprehensive list of MEF2 target genes in skeletal and cardiac muscle that will be further investigated in a variety of cellular contexts. Mechanistic smaller scale follow up studies based on the high throughput data have so far revealed the novel observation that MEF2 represses *Dusp6* in skeletal and cardiac muscle and this is p38MAPK dependent in myoblasts. Understanding the global role of MEF2 in striated muscle gene expression has implications not only for our understanding of development, but also in contexts where the expression of developmental genes is recapitulated such as in post-natal skeletal muscle regeneration and cardiac hypertrophy.

### **Accession Numbers**

Gene Expression Omnibus (GEO) accession number: GSE61207.

### **Supplementary Data**

Supplementary data are available at NAR Online.

## Funding

This work was supported by the Canadian Institutes of Health Research [102688 to J.C.M., 120349 to A.B.]

## Acknowledgements

The authors would like to thank Stephen M. Keyse (Ninewells Hospital and Medical School, Dundee, UK) for the *Dusp6*-luciferase construct.

## Supplementary Data

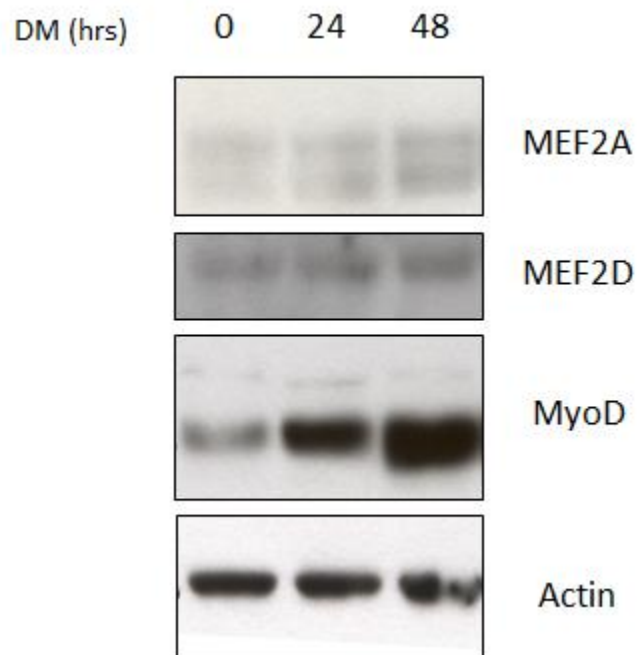


**Figure S1. MEF2A and MEF2D protein expression during C2C12 differentiation.** Protein was harvested at the indicated timepoints and analyzed by immunoblotting.

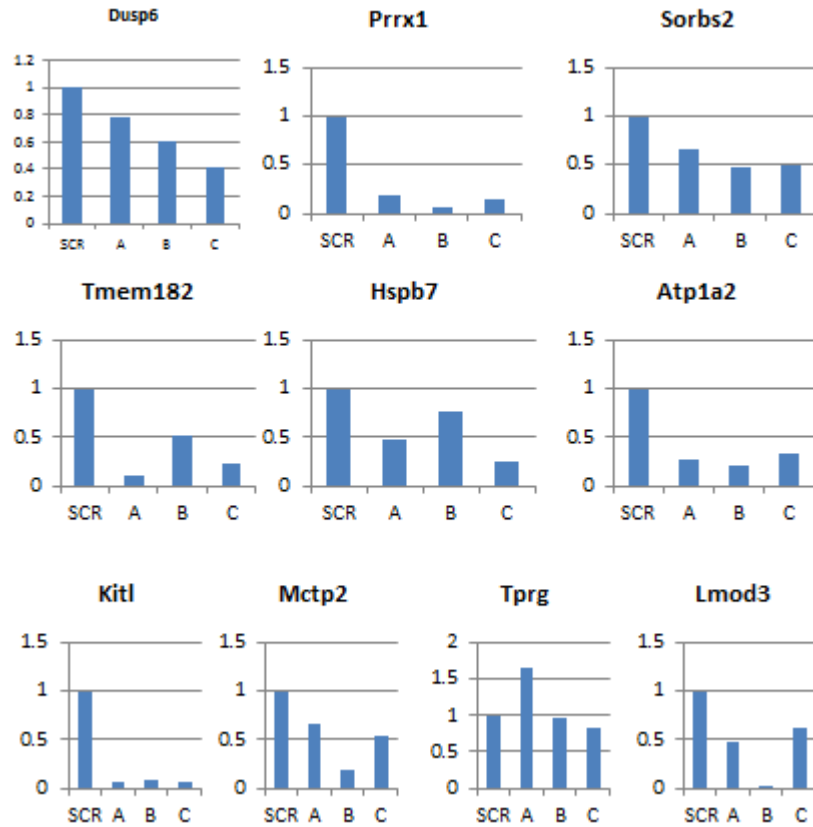


**Figure S2. Efficiency of siRNA mediated gene silencing.** C2C12s were transfected with 50 nM siRNA and harvested 24 hr later. RNA was extracted to assess changes in expression of each target gene using qRT-PCR. Samples are presented as fold change and were normalized to  $\beta$ -actin.



**Figure S3. Effect of p38MAPK inhibition on MEF2 expression.** C2C12s were treated with 5  $\mu$ M SB 203580 or control (SB 202474) for 48 hr in DM. Protein was harvested and analyzed by immunoblotting with the indicated antibodies.



**Figure S4. siRNA catalog numbers (Sigma-Aldrich).**

	siRNA-1 (A)	siRNA-2 (B)	siRNA-3 (C)
scrambled	SIC001		
Mef2a	SASI_Mm01_00120787	SASI_Mm01_00120788	
Mef2d	SASI_Rn01_00057714	SASI_Rn01_00057717	
Atp1a2	SASI_Mm01_00139387	SASI_Mm01_00139389	SASI_Mm01_00139390
Dusp6	SASI_Mm01_00051559	SASI_Mm01_00051560	SASI_Mm01_00051561
Hspb7	SASI_Mm01_00161042	SASI_Mm01_00161043	SASI_Mm01_00161044
Kitl	SASI_Mm01_00090429	SASI_Mm01_00090430	SASI_Mm02_00322344
Lmod3	SASI_Mm02_00295741	SASI_Mm02_00295742	SASI_Mm02_00295743
Mctp2	SASI_Mm01_00067344	SASI_Mm01_00067345	SASI_Mm01_00067346
Prrx1	SASI_Mm01_00148745	SASI_Mm01_00148746	SASI_Mm01_00148747
Sorbs2	SASI_Mm02_00344595	SASI_Mm02_00344596	SASI_Mm02_00344597
Tmem182	SASI_Mm02_00296151	SASI_Mm02_00296152	SASI_Mm02_00296153
Tprg	SASI_Mm02_00345802	SASI_Mm01_00147001	SASI_Mm01_00147002

**Figure S5. Primers used in ChIP-qPCR.**

ChIP-qPCR	
Dusp6	F 5' AATTCATCAACACAACCTGTTCC 3' R 5' AGCTCCTCAATGGATACAAACAG 3'
Acta2	F 5' TTCCAGGACCTTTTGCATCC 3' R 5' CCGGTTAGGGTTCAGTGGTG 3'
Gapdh	F 5' GCACAGTCAAGGCCGAGAAT 3' R 5' GCCTTCTCCATGGTGGTGAA 3'
Hspb7	F 5' GGTTGGCCCACCCTTTGTAG 3' R 5' TCAGGATTGCCAGGGTGTCT3'
Kitl	F 5' TACGAAAACTAGCCTTGCTACCT 3' R 5' ACATAAGCACTAATGTCTGGCA3'
Lmod3	F 5' TGA CTCTGCC CAGAAAACCT 3' R 5' GTTGAGCTGCTGGGAGTGAC 3'
Prrx1	F 5' GATGAGCAGCAACTCAGACC 3' F 5' GGGACGTTTGAGGTGGCATAA 3'

**Figure S6. Primers used in qRT-PCR.**

qRT-PCR	
	KiCqStart <sup>®</sup> SYBR <sup>®</sup> Green Primers
Dusp6	M_Dusp6_1
Hspb7	M_Hspb7_1
Kitl	M_Kitl_1
Lmod3	M_Lmod3_1
Prrx1	M_Prrx1_1
	Other
Mef2a	F 5' ATGGTTGTGAGAGCCTGATG 3' R 5' AGAAGTTCTGAGGTGGCAAGC 3'
β-actin	F 5' AAGTGTGACGTTGACATCCGTAA 3' R 5' TGCCTGGGTACATGGTGGTA 3'
Myogenin	F 5' CAGCTCCCTCAACCAGGAG 3' R 5' GACTGCAGGAGGCGCTGT 3'

## **CHAPTER IV: Regulation of Hspb7 by MEF2 and AP-1 in muscle atrophy**

Manuscript prepared for submission to the Journal of Biological Chemistry.

Experimental design and drafting manuscript by

Stephanie Wales, Dr. Alexandre Blais and Dr. John C McDermott

Experiments conducted by

Stephanie Wales (Figure 1-8)

Dabo Yang and John Girgis (Figure 7-8)

## Regulation of Hspb7 by MEF2 and AP-1 in muscle atrophy.

Wales, S.<sup>1,2,3</sup>, Yang, D.<sup>4</sup>, Girgis, J.<sup>4</sup>, Blais, A.<sup>4</sup> and J. C. McDermott<sup>1,2,3,5</sup>

<sup>1</sup>Department of Biology, York University, 4700 Keele Street Toronto, Ontario, M3J 1P3 Canada

<sup>2</sup>Muscle Health Research Centre (MHRC), York University, 4700 Keele Street, Toronto, Ontario, M3J 1P3 Canada

<sup>3</sup>Centre for Research in Biomolecular Interactions (CRBI), 4700 Keele Street, Toronto, Ontario, M3J 1P3 Canada

<sup>4</sup>Ottawa Institute of Systems Biology, University of Ottawa, Health Sciences Campus, 451 Smyth Road Ottawa, Ontario K1H 8M5 Canada

<sup>5</sup>Centre for Research in Mass Spectrometry (CRMS), York University, 4700 Keele Street, Toronto, Ontario, M3J 1P3 Canada

### Abstract

The individual roles of MEF2 and AP-1 in myogenesis have been explored yet the relationship between these proteins in muscle development, disease and aging has not been clearly defined. Using MEF2A ChIP-exo, c-Jun and Fra-1 ChIP-seq data and predicted AP-1 consensus motifs, we identified common MEF2 and AP-1 target genes, several of which have a function in regulating the actin cytoskeleton. Since muscle atrophy results in remodelling or degradation of the actin cytoskeleton, we characterized the expression of five putative MEF2/AP-1 target genes (Dstn, Flnc, Hspb7, Lmod3 and Plekhh2) under atrophic conditions using Dexamethasone (Dex) in C2C12 myoblasts or in aging (8wk vs 63wk old mice). Hspb7, a small heat shock protein, showed upregulation in Dex treated cells and with age. Further biochemical analyses revealed that loss of MEF2A using siRNA-mediated gene silencing prevented Dex-regulated induction of Hspb7 and MEF2A could co-operate with Dex to induce Hspb7 expression in myoblasts. Fra-2 or c-Jun expression prevented GR-mediated upregulation of Hspb7, but loss of Fra-2 or c-Jun enhanced Hspb7 expression. A role for Hspb7 in skeletal muscle has not been identified but it has been associated with autophagy in other tissues. Using a combination of fasting and colchicine to monitor autophagic flux *in vivo*, we observed that Hspb7 expression was upregulated along with other autophagy-related genes. Furthermore, electroporation of Hspb7 into the TA muscle reduced induction of autophagy related genes after fasting. Together these data indicate that MEF2 and AP-1 have opposite roles in the regulation of Hspb7, and may rely on additional co-operatively with the glucocorticoid receptor. Additionally, we provide evidence of a role for Hspb7 in autophagy in muscle which has implications for muscle atrophy and aging.

## Introduction

Muscle atrophy is a phenomenon associated with reduced muscle fiber number and size caused by increased proteolysis and decreased protein synthesis (380). In the elderly, muscle wasting is referred to as sarcopenia (381), and in patients with cancer, AIDS and other chronic disease, muscle atrophy is referred to as cachexia (382). Improving or maintaining muscle mass in these conditions has immediate effects on the overall quality of life, and there is evidence that sarcopenia in cancer patients directly affects the time to tumour progression and disease recurrence (383, 384). In the ubiquitin proteasome pathway, the FoxO family of transcription factors activates muscle atrophy through induction of two E3 ubiquitin ligases MAFbx/Atrogin-1 and MuRF1 (385). Current treatment programs for muscle atrophy include activating the Akt pathway, which induces muscle hypertrophy by inactivating FoxO proteins (386), however, Akt can be inhibited by Myostatin, a member of the TGF- $\beta$  superfamily (167), superseding Akt activation as a treatment option. A new antibody recently characterized to bind to both members (A and B) of the Myostatin/Activin type II receptor (ActRII) induces hypertrophy in a muscle wasting model *in vivo* (387). Additionally, targeting ActRIIB in cancer cachexia models can prevent atrophy which resulted in prolonged survival without tumour manipulation (388).

The autophagy pathway is another mechanism of protein degradation that has also been implicated in muscle wasting. Foxo3, unlike other members of the FoxO family is able to also regulate autophagy in addition to the ubiquitin-proteasome pathway (284, 285). Several possible autophagy pathways have been identified in muscle, two of which are macroautophagy and chaperone mediated autophagy (CMA). Although both ultimately lead to protein degradation in the lysosome, they achieve this through different mechanisms. In CMA, Hsc70 targets proteins directly to the lysosome (278). Macroautophagy requires de novo synthesis of autophagosomes in a multi-step process that involves Atg protein family members. Autophagy is required for muscle homeostasis as mouse knockout models, which lack proteins involved in autophagosome formation such as Atg5 and Atg7, result in muscle atrophy (389, 390). Aged muscle shows decreased autophagy and therefore buildup of protein aggregates (391). LC3B (Map1lc3b) is an Atg protein that is a good readout for autophagy as it is post-translationally modified before it becomes part of the autophagosome (274). First, pro-LC3B is cleaved by Atg4 to form cytosolic LC3B-I. Atg7 then lipidates LC3B-I to form LC3B-II which can form part of the autophagosome. Using samples from various atrophic mouse models, LC3B was shown to be

strongly upregulated (264) and furthermore Foxo3 can directly regulate several autophagy related genes including LC3B (284, 285). A form of autophagy termed chaperone-assisted selective autophagy (CASA) merges the chaperone mediated and macroautophagy pathways. In CASA, Hsc70 forms a complex with Bag3, Hspb8 and E3 ubiquitin ligase CHIP, to identify protein aggregates and target them to the autophagosome (282).

Myocyte Enhancer Factor 2 (MEF2) is a member of the MADS-box family of transcription factors found in many tissues including skeletal and cardiac muscle (78, 126). MEF2 functions in a homo- or hetero-dimer complex with four different MEF2 isoforms in vertebrates (MEF2A-D) which bind to the consensus sequence (C/TTA(A/T)<sub>4</sub>TAG/A). Previously we had shown that MEF2A can target a shared subset of genes in C2C12, an *in vitro* model of skeletal myogenesis, and primary cardiomyocytes (225). Gene Ontology (GO) analysis contained terms enriched for actin cytoskeleton organization and actin filament-based processes. In addition these common binding sites shared similar neighbouring consensus sequences for AP-1, a serum responsive transcription factor that may be composed of a Jun homodimer or a Jun-Fos heterodimer. AP-1 recognizes the consensus sequence TGAG/CTCA (392). Global analysis of MyoD target genes in skeletal myoblasts also showed that AP-1 motifs are prominent in neighbouring sequences (214, 216). Neighbouring MEF2 and AP-1 sequences were also enriched in macrophages and neurons (393, 394). Several AP-1 subunits have been shown to regulate myogenesis. c-Jun can antagonize MyoD transcriptional activity *in vitro* (377, 378). Using high throughput data, Blum et al. (2012) showed that c-Jun and MyoD co-ordinate muscle enhancers, indicating a more complex role for AP-1 in muscle (379). Additionally, Fos family member, Fra-2, likely has a role in maintenance of the satellite cell pool (395).

While MEF2 and AP-1 have individually been shown to have a role in myogenesis, their potential interaction has not been documented. Additionally, although loss of MEF2 and AP-1 have been implicated in loss of sarcomere integrity during development and satellite cell-mediated muscle regeneration (137, 298, 396), the combined role of these factors in muscle atrophy has not been investigated. Here, we document that MEF2 and AP-1 regulate several genes associated with the actin cytoskeleton. Amongst them, the small heat shock protein, Hspb7 is implicated in muscle atrophy.

## Methods

**Cell Culture.** C2C12 myoblasts were obtained from American Tissue Culture Collection (ATCC). Cells were maintained in Dulbecco's Modified Eagle Medium (DMEM) with High Glucose and L-Glutamine (Hyclone) supplemented with 10% fetal bovine serum (HyClone) and 1% Penicillin/Streptomycin (Invitrogen). C2C12 were induced to differentiate in differentiation medium (DM) containing DMEM/High Glucose/L-Glutamine supplemented with 2% Horse Serum (Hyclone) and 1% Penicillin/Streptomycin for the indicated time. Cells were maintained in an humidified, 37°C incubator at 5% CO<sub>2</sub>. Pharmacological drug treatments were completed for the indicated times and replenished with fresh medium every 24 hr.

**Transfections.** C2C12 were transfected using the calcium phosphate precipitation method. Cells were then harvested 48 hr post transfection or the media was changed to DM. For siRNA experiments in C2C12 proliferating myoblasts Lipofectamine (Invitrogen) was used according to the manufacturer's instructions. Cells were then harvested 24 hr later or the media was changed to DM.

**Plasmids.** Expression plasmids for pMT2-MEF2A, pCMV-c-Jun, pcDNA3.1-Fra-2, pCMV-dsRed2, pcDNA-GFP have been described previously (223, 395). pCAGGSnHC-HSPB7-HA was generously donated by Lin et al. (397).

**Antibodies and reagents.** Rabbit polyclonal MEF2A antibody has been previously described (368). The following antibodies were purchased from Santa Cruz: actin (sc-1616), dsRed (sc-33354), MEF2A (sc-313X; used in ChIP), donkey anti-goat IgG-HRP (sc-2020), Fra-2 (sc-604), c-Jun (sc-1694), GFP (sc-9996), MCK (sc-365046), MyoD (sc-304). anti-LC3B (Cell Signalling, 2775). Myogenin and HA monoclonal antibodies were obtained from the Developmental Studies Hybridoma Bank. The remaining antibodies are as follows: Hspb7 (Abcam, ab150390), Rabbit IgG (Millipore, 12-370). Dexamethasone (sc-29059) was used at a concentration of 10 μM, unless otherwise indicated. DMSO was used as a volume control. Rapamycin (10 μg/ml) was used purchased from Santa Cruz (sc-3504).

**siRNA.** Knockdown of target genes was done using siRNA obtained from Sigma-Aldrich and are listed in Supplementary Table S2. In C2C12 siRNA was transfected at the following concentration: *Mef2a* (30 nM), *c-Jun* (50 nM), *Fra-2* (50 nm)

**Immunoblots.** Cells were washed with 1XPBS and lysed in NP-40 lysis buffer (50 mM Tris, 150 mM NaCl, 0.5% NP-40, 2 mM EDTA, 100 mM NaF and 10 mM Na pyrophosphate)

containing protease inhibitor cocktail (Sigma-Aldrich), 1 mM phenylmethylsulfonyl fluoride (Sigma-Aldrich), and 1 mM sodium orthovanadate (Bioshop). Protein concentrations were determined by Bradford assay (Bio-Rad). Twenty µg of total protein were resolved on 10% SDS-PAGE and then transferred onto Immobilon-FL PVDF membrane (Millipore) for 1 hr or overnight. Non-specific binding sites were blocked using 5% milk in PBS or TBST. Membranes were incubated with primary antibodies overnight at 4°C in 5% milk in PBS or 5% BSA in TBST. HRP-conjugated secondary antibody was added for 1 hr at RT. Protein was detected with ECL Chemiluminescence reagent (Pierce).

**Chromatin Immunoprecipitation.** Methods were carried out as described previously described (34) however a third IP Wash Buffer was added (IP Wash Buffer III; 20 mM Tris pH 8.1, 250 mM LiCl, 1% NP-40, 1% deoxycholate, 1 mM EDTA).

**RNA extraction.** Total RNA was extracted from C2C12 using the RNeasy Plus kit (Qiagen) and Qiashredder (Qiagen). RNA isolated from tissue was extracted using Trizol (Invitrogen). RNA was converted to cDNA using Superscript III (Invitrogen) according to the manufacturer's instructions.

**Quantitative PCR.** SybrGreen (BioRad or ABM) was combined with 2.5 µl gDNA or cDNA and 500 nM primers in a final volume of 20 µl. cDNA was diluted 1:10 prior to use. Each sample was prepared in triplicate and analyzed using Rotor-Gene Q (Qiagen). Parameters for qRT-PCR using BioRad: 30s 95°C, [5s 95°C, 30s 60°C] x 40 cycles. Parameters for qRT-PCR using ABM: 10m 95°C, [3s 95°C, 30s 60°C] x 35 cycles. Parameters for ChIP-qPCR: 5min 95°C, [5s 95°C, 15s 60°C] x 40 cycles. Fold enrichment (ChIP-qPCR) and Fold change (qRT-PCR) was quantified using the  $\Delta\Delta C_t$  method. Primers used in ChIP-qPCR and qRT-PCR are listed in Supplementary Figure Table S3.

**Bioinformatics.** AP-1 consensus sequences were mapped using cisGenome. GREAT (default settings) identified GO terms based on DNA sequences obtained from available datasets.

MEF2A: GSE61207; Fra-1: ENCSR000AIK c-Jun: GSE37525.

**Animal Care.** For aging experiments, 63 and 8 week old C57BL/6 male mice were obtained from Jackson Lab or Charles River, respectively. Mice were sacrificed using cervical dislocation in accordance with the Institutional Animal Care and Use Committee of York University. For autophagy experiments 6-8 week old C57BL/6 male mice were sacrificed in accordance with University of Ottawa Animal Care and Use Committee. Autophagic flux was monitored as



described by Ju et al. (398) with the following changes: 1) Mice were placed on a 24 hr fast. 2) After ptfLC3, Hspb7-HA or pCAGGSnHC electroporation, two days of recovery was allowed.

**Statistics.** Data are presented as mean  $\pm$ SEM. Statistical analysis was done using one-tailed paired student t-test.

## Results

### Common MEF2 and AP-1 target genes in muscle affect components of the cytoskeleton

MEF2 and AP-1 are transcription factors involved in myoblast proliferation and differentiation, yet whether they regulate common target genes during differentiation has not been thoroughly explored. To determine whether MEF2 and AP-1 have similar target genes we utilized MEF2A ChIP-exo data previously obtained from differentiating C2C12 (48 hr DM) (225) and compared these binding events to c-Jun (379) and Fra-1 (Wold group, ENCODE) ChIP-seq data, the only muscle specific ChIP-seq datasets currently available of any AP-1 component that we are aware of. Fra-1 is primarily associated with bone development (399, 400) and c-Jun has been implicated in many tissues including muscle (377–379). Both the c-Jun and Fra-1 ChIP-seq data was completed in C2C12 myoblasts in growth medium (GM). c-Jun yielded 9778 binding events while Fra-1 had 6507. To determine the percentage of shared binding sites across these datasets we first used three transcription factor-centric viewpoints from MEF2A, c-Jun and Fra-1 (Figure 1A). From a MEF2A-centric analysis, the majority of MEF2A binding sites (69%) bound to DNA independent of c-Jun or Fra-1 recruitment, yet 17% of MEF2A bound DNA also contained c-Jun recruitment and 12% contained both c-Jun and Fra-1. Fra-1 and MEF2A alone shared few binding sites (2%). From the 9778 c-Jun ChIP-seq peaks, over 30% also has Fra-1 recruitment, but the majority of c-Jun targets did not show enrichment for MEF2A or Fra-1. Conversely, over half of all Fra-1 binding events were associated with c-Jun recruitment (56%).

Functional roles for common MEF2A and AP-1 binding sites were identified using Genomics Regions Enrichment of Analysis Tool (GREAT), which revealed enriched GO terms for Biological Processes, the top ten of which are in Figure 1B. The GO terms were ranked by Binomial raw p-value and the number of genes within each GO term is indicated. DNA enriched for MEF2A-alone was associated with traditional functions such as actin-filament based processes and skeletal muscle tissue development but also myeloid cell development (blue). There were no GO terms identified for MEF2A and Fra-1, however, MEF2A and c-Jun had GO terms for striated muscle development, vascular development and heart morphogenesis (purple). Common terms across all three groups were related to the actin cytoskeleton and negative regulation of smooth muscle cell proliferation (black). c-Jun and Fra-1 targets had GO terms related to infection such as response to bacterium (pink).

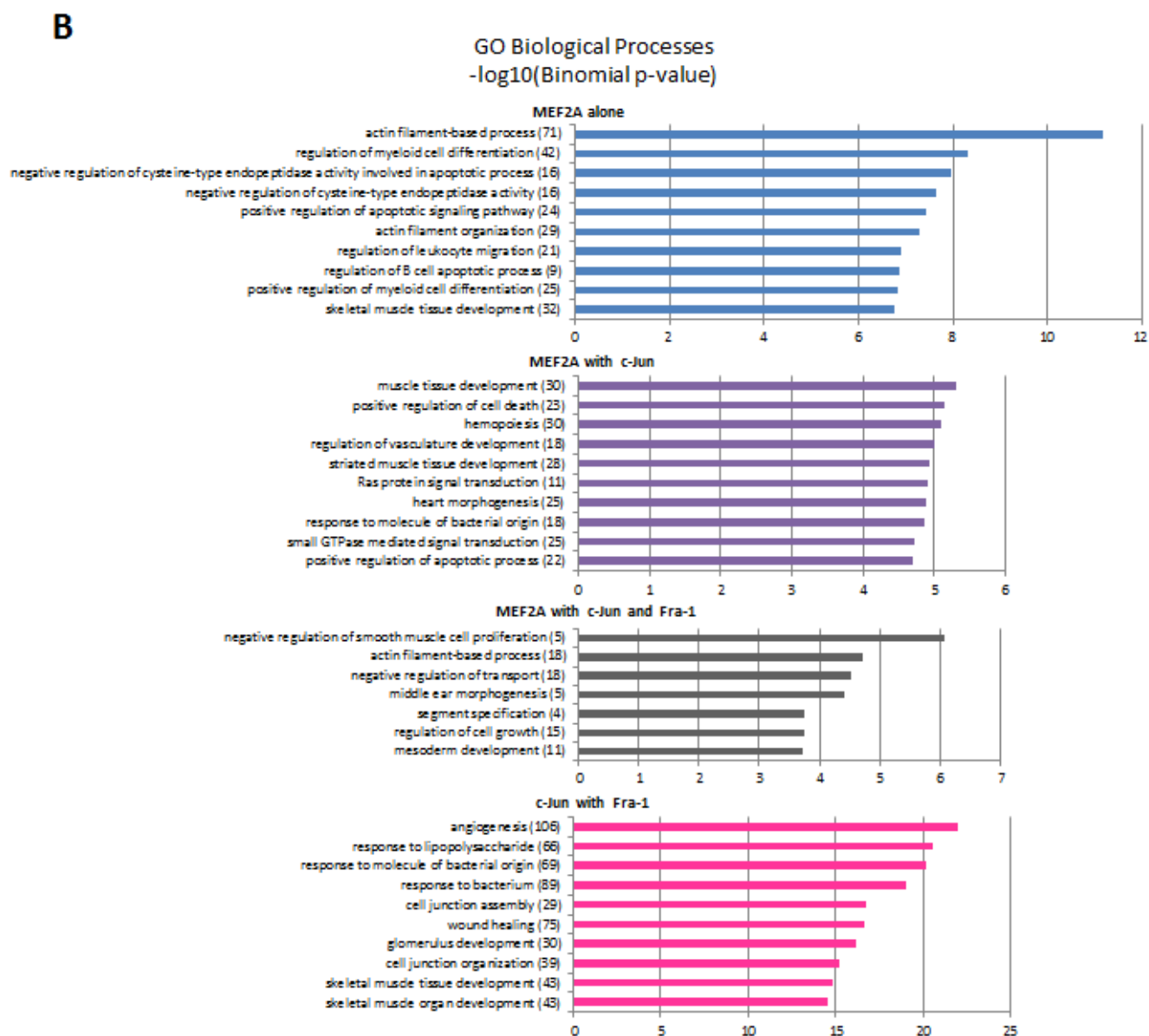
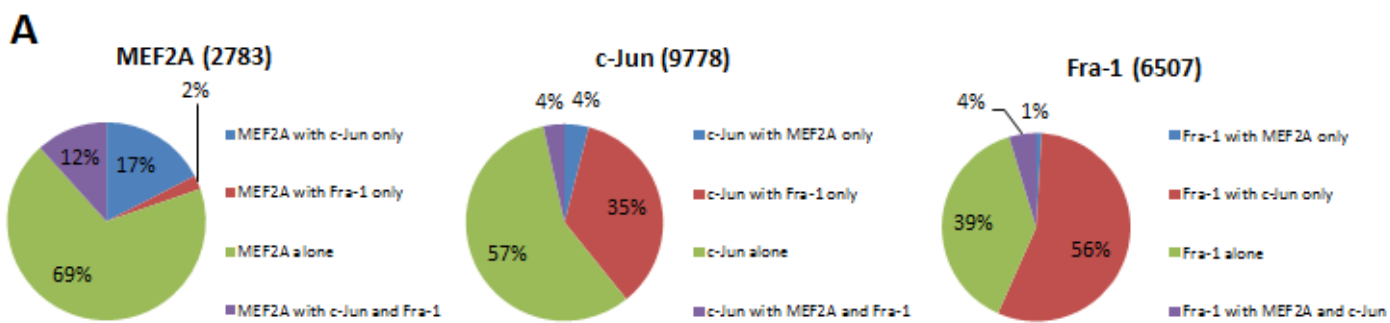


Figure 1.

**Figure 1. A comparison of MEF2A and AP-1 target genes in skeletal muscle.** A) Percent overlap between MEF2A, c-Jun, and Fra-1. Within each pie graph is the percentage of binding events corresponding to a MEF2A, c-Jun, or Fra-1 centric view. The total number of ChIP-seq binding events for each category is indicated in parentheses. B) Functional roles for MEF2A alone, MEF2A/c-Jun, MEF2A/c-Jun/Fra-1 and c-Jun/Fra-1. Using the datasets from 1A, GREAT analysis revealed GO terms for Biological Processes. The total number of genes per GO term are indicated to the right of each GO term.

Since the MEF2A dataset was obtained from differentiating myoblasts and given that several other AP-1 components aside from c-Jun and Fra-1 could also be targeting MEF2 target genes we determined the location of AP-1 consensus sequences containing the sequence TGAGTCA using cisGenome allowing zero mismatches. From the mm9 genome, this search identified 264, 537 AP-1 consensus sites. We decided to focus on the MEF2A/AP-1 common genes within  $\pm 10$ kb of the transcription start site (TSS) and observed that 13 out of these 76 genes are associated with the molecular function *cytoskeleton protein binding* (Supplementary Table S1). We assessed the expression of five of these genes during C2C12 myogenesis: Destrin (Dstn), Filamin C (Flnc), Heat shock protein family, member 7 (Hspb7), Leiomodulin 3 (Lmod3) and Pleckstrin homology domain containing family H, member 2 (Plekhh2). The recruitment pattern of MEF2A, c-Jun, Fra-1 and any AP-1 consensus sequences is indicated in an image from UCSC (Figure 2). The overall trends demonstrate several points. First, as MEF2A was done using ChIP-exo, which involves exonuclease digestion prior to sequencing, MEF2A peaks are more defined indicating one of the advantages of ChIP-exo over conventional ChIP-seq. Second the scale of c-Jun and Fra-1 recruitment differ dramatically which could indicate differential DNA binding affinity of AP-1 family members. From these five MEF2A target genes, c-Jun (ChIP-seq) was recruited to an overlapping or neighbouring binding event near Flnc, Hspb7 and Plekhh2. Fra-1 and MEF2A recruitment only overlapped at the promoter of Flnc, and Fra-1 was detected within the second intron of Hspb7. Dstn is an actin-depolymerizing protein (401) while Flnc, a muscle specific filamin (402), promotes the cross-linking of actin. We had previously identified Hspb7 (small heat shock protein) and Lmod3 (tropomodulin family member) as MEF2 target genes in cardiac muscle as well (225). Recently a human nemaline myopathy has been associated with mutations in Lmod3 (301, 315, 318). Hspb7 expression is higher in mdx mice, a genetic model of muscular dystrophy, but no functional role has been established in muscle (403). The role of Plekhh2 appears to be to stabilize the cortical actin cytoskeleton (404). All of these proteins are primarily found in the cytoplasm except for Hspb7 which has been shown to also reside in sub-nuclear speckles (405).

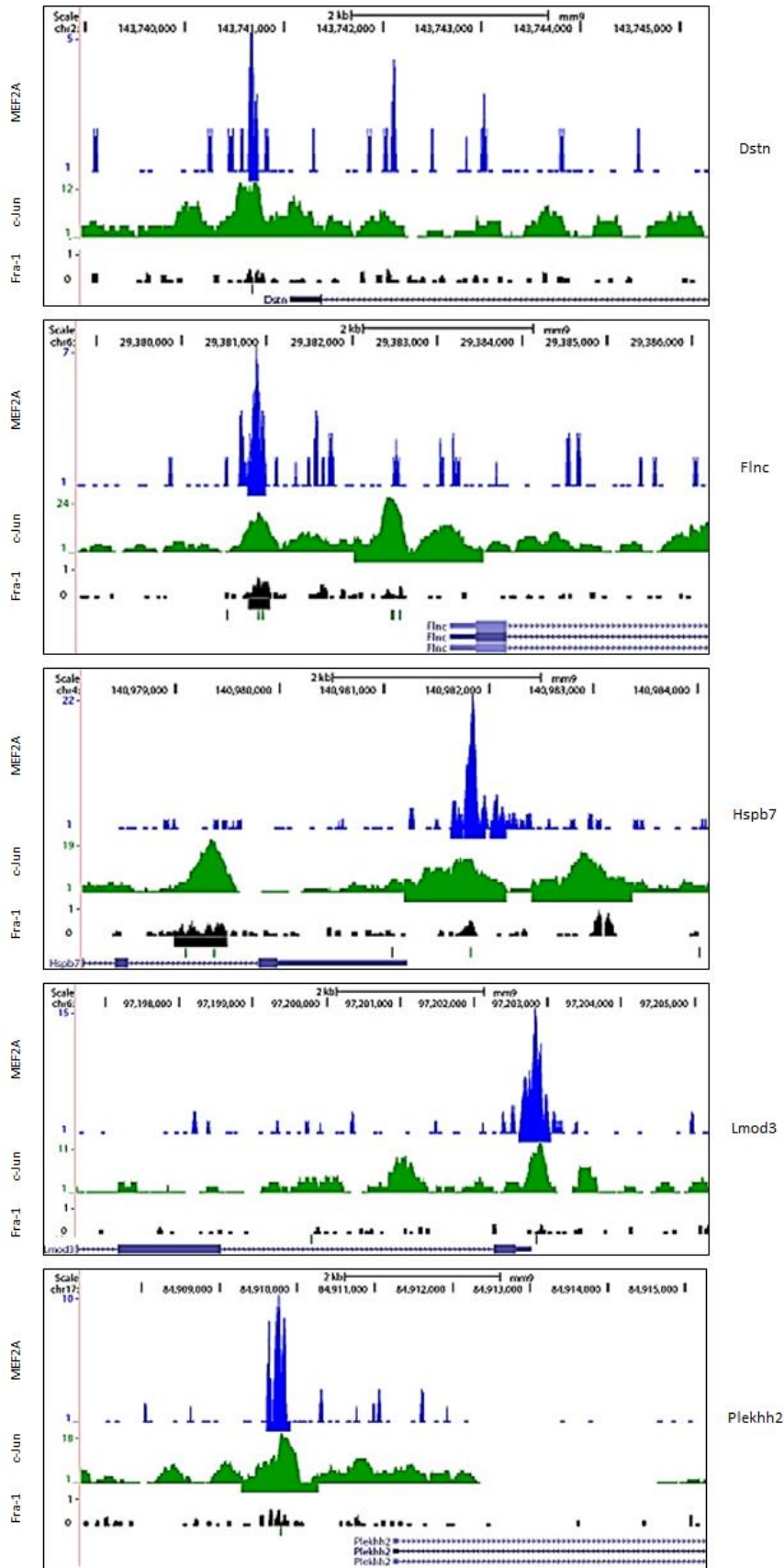


Figure 2.

***Figure 2. Differential recruitment of MEF2A and AP-1 to actin cytoskeletal target genes.***

UCSC Genome Browser image depicting the location of MEF2A (blue), c-Jun (Green) and Fra-1 (Black) recruitment to *Dstn*, *Flnc*, *Hspb7*, *Lmod3* and *Plekhh2*. Horizontal bars below read densities indicate an enrichment peak (if present). AP-1 consensus sequences are also indicated as vertical green dashes below Fra-1 data.

### **Actin cytoskeletal genes are directly regulated by MEF2A and AP-1**

Aside from c-Jun and Fra-1, AP-1 has many family members including Fra-2, Junb, c-Fos, and several others. We assessed the expression pattern of MEF2A and AP-1 family members during C2C12 differentiation (Figure 3A). As Myogenin and MEF2A levels increase with myogenesis, only one AP-1 subunit, Fra-2, also increased. c-Jun, Junb and most dramatically, Fra-1 are reduced after serum withdrawal. To move forward in determining a role for MEF2 and AP-1 in myogenesis we decided to focus on Fra-2 and c-Jun since they are expressed in myoblasts and have been shown to have a role in myogenesis (377–379, 395). Additionally the Fra-2:c-Jun heterodimer is one of the main AP-1 complexes present in C2C12 differentiation (406). Fra-2 is present in different isoforms and subject to post-translational modifications by ERK (395, 406). Unfortunately no Fra-2 ChIP-seq dataset is currently available.

The expression of these genes during myogenesis was determined using qRT-PCR at GM (myoblasts) and 48 hr DM (myocytes) (Figure 3B). During C2C12 differentiation, the expression of each gene except for *Dstn* increased. To confirm MEF2A recruitment to *Dstn*, *Flnc*, *Hspb7*, *Lmod3* and *Plekhh2*, ChIP-qPCR was done in growth conditions GM and at 48 hr DM. During differentiation, MEF2A was recruited to each gene compared to recruitment to SMA (Figure 3C). MEF2A recruitment to *Lmod3* and *Hspb7* were the most significant and reflect ChIP-seq data (Figure 2). We could not successfully ChIP c-Jun or Fra-2 using available antibodies.

To determine whether actin cytoskeletal genes are sensitive to the loss of AP-1 and MEF2 we utilized siRNA mediated gene silencing. Our previous ChIP-exo data was completed using a MEF2A antibody, therefore, we used siRNA targeting MEF2A. Since AP-1 may function in a Jun-Fos or Jun-Jun homodimer and because in muscle c-Jun and Fra-2 have been documented to be critical factors in regulating myoblast proliferation (377, 395) we used siRNA targeting c-Jun and Fra-2 (Figure 3D). Knock-down of MEF2A resulted in significant downregulation of *Hspb7* (Figure 3E) but other genes were not significantly affected.



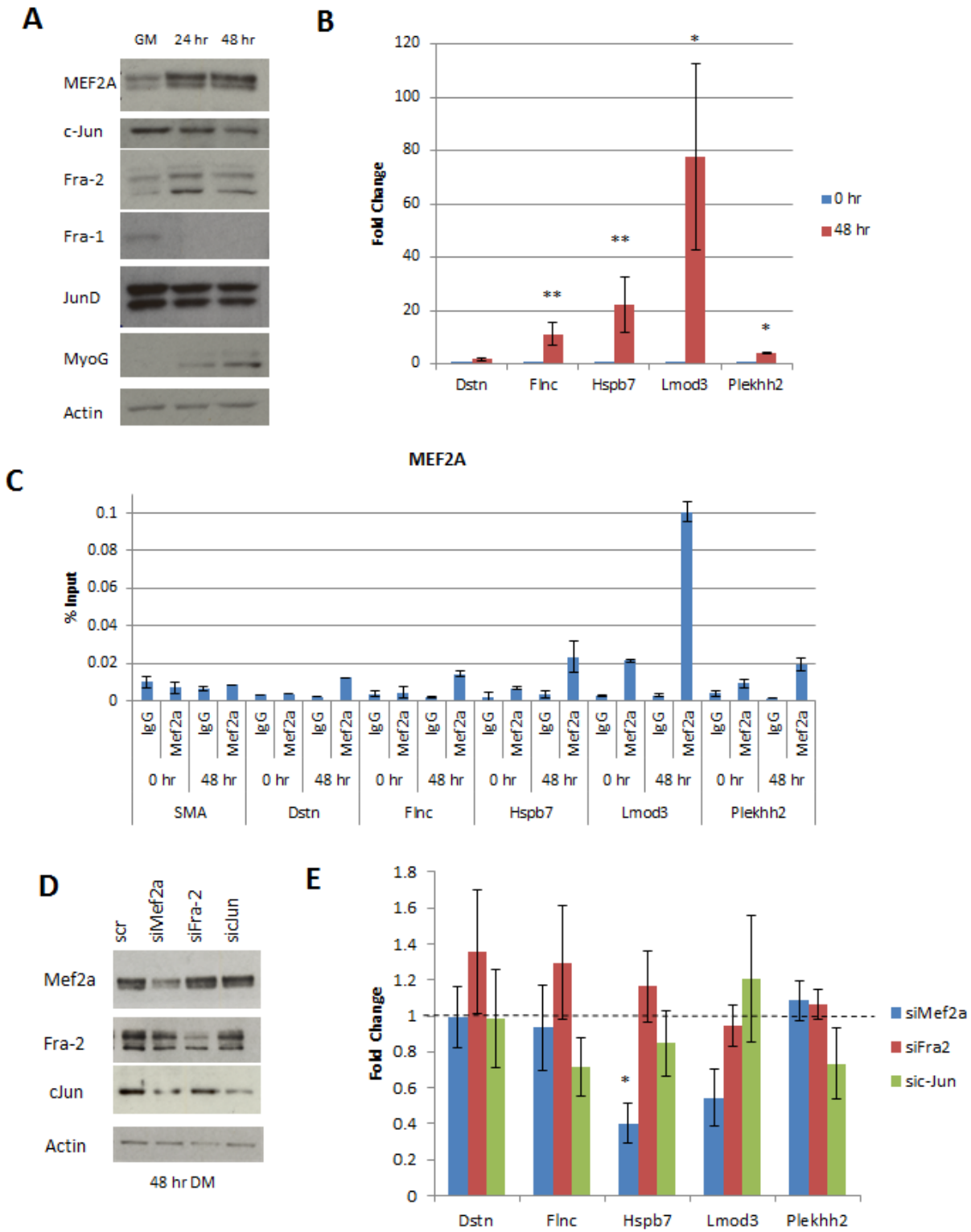


**Figure 3.**

**Figure 3. MEF2A and AP-1 regulation of actin cytoskeletal genes.** A) MEF2A and AP-1 protein expression during myogenesis. C2C12 were allowed to differentiate from myoblasts (GM) to 48 hr DM. B) Expression pattern of MyoG, Dstn, Flnc, Hspb7, Lmod3 and Plekhh2 during C2C12 differentiation in GM and 48 hr DM. Values were calculated using the  $\Delta\Delta Ct$  method and normalized to  $\beta$ -actin (n=3, \*P<0.05, \*\*P<0.01). C) Recruitment of MEF2A to cytoskeletal target genes during C2C12 differentiation. Values were calculated using the percent input method. SMA was used as a control (n=2). D) Efficiency of knockdown of MEF2A, Fra-2 and c-Jun in C2C12 myocytes (48 hr DM) using siRNA mediated gene silencing. C2C12 were transfected with siRNA and allowed to differentiate for 48 hr before western blot analysis. E) siRNA-mediated knockdown of MEF2A, Fra-2 and c-Jun at 48 hr DM. Data were analyzed as in B.

## **Age and dexamethasone induced atrophy causes changes in MEF2A/AP-1 cytoskeletal target genes**

The cytoskeleton is integrally linked to the contractile unit of the myofibril, the sarcomere which is made up of  $\alpha$ -actin and myosin. During muscle atrophy, a phenomenon observed in sarcopenia, cachexia and various genetic diseases, the cytoskeleton and components of the sarcomere become degraded resulting in overall muscle loss and weakness. Since these five proteins are involved, to varying degrees, in the actin cytoskeleton we wanted to determine whether expression of these MEF2/AP-1 target genes may change under atrophic conditions. To determine whether these genes were differentially expressed in aging muscle we isolated RNA from the gastrocnemius and quadriceps of 8- and 63-week old mice (Figure 4A). In the gastrocnemius Hspb7 was upregulated with age. In the quadriceps Dstn, Flnc and Hspb7 were upregulated. In cell culture, muscle atrophy can be replicated using Dexamethasone (Dex), a synthetic glucocorticoid. To model glucocorticoid induced atrophy C2C12 were allowed to differentiate for 72 hr in DM, and then treated with Dex (Figure 4B). In this analysis we included two E3 ubiquitin ligases, MAFbx and MURF1 which are associated with muscle atrophy and serve as positive controls. These E3 ligases promote atrophy and ubiquitinate proteins for degradation. In muscle, MuRF1 directly targets myosin and myosin binding proteins for degradation, contributing to loss of the sarcomere (270, 271). After 6 or 24 hr treatment of Dex MAFbx and MuRF1 were upregulated. Six hour Dex treatment increased Dstn and Hspb7 expression and decreased Flnc. Lmod3 and Plekhh2 expression were unchanged. After 24 hr treatment with Dex these trends were similar, however, Hspb7 was upregulated by five-fold, equivalent to the degree of MAFbx and MuRF1 induction.

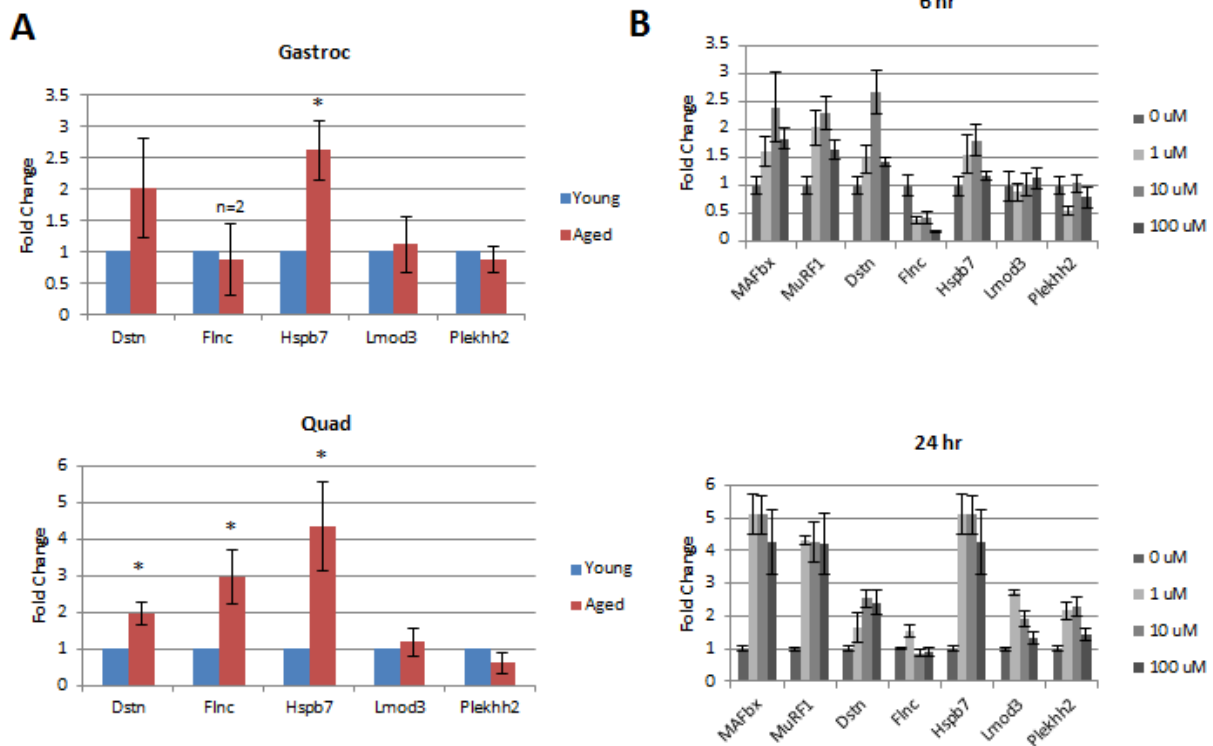


**Figure 4. Aging and dexamethasone-induced atrophy cause changes in MEF2A/AP-1 cytoskeletal target genes.** A) The RNA from the gastrocnemius and quadriceps of 8- and 63-week old CB57/J mice was isolated for qRT-PCR analysis. Values were calculated using the  $\Delta\Delta C_t$  method and normalized to Gapdh (n=3 unless otherwise indicated, \*P<0.05). B) Dexamethasone treatment of myotubes induces atrophy and the expression of MEF2A/AP-1 target genes. C2C12 were allowed to differentiate for 72 hr and then treated with Dexamethasone for 6 hr (upper graph) or 24 hr (lower graph) at the indicated concentrations. Values were calculated as in A.

### **MEF2 and AP-1 regulate atrophy-induced Hspb7 expression**

Since Hspb7 expression was induced by Dex, increased during aging and is regulated by MEF2A and AP-1 (Figure 3) we chose to study the regulation of this gene in more detail. Using ChIP-seq, GR binding sites were identified in C2C12 myotubes treated with Dex (407). Interestingly, GR was found to bind to an intron of Hspb7. Using UCSC browser we plotted the MEF2A, c-Jun, Fra-1 and AP-1 peaks and compared them to GR recruitment from Kuo et al. (407) within the Hspb7 gene (Figure 5A). Where GR was recruited following Dex treatment was within the second intron of Hspb7 which contained c-Jun and Fra-1 enrichment peaks. We utilized Dex treatment to further determine how MEF2A, AP-1 and GR might be contributing to Hspb7 expression.

At the protein level, Dex treatment upregulated Hspb7 expression in the late stages of differentiation but not under growth conditions (Figure 5B). The effect of exogenous expression of MEF2A, Fra-2 or c-Jun in combination with Dex treatment was assessed in growth conditions and 72 hr myotubes. Under growth conditions, Hspb7 expression was only enhanced by the combined overexpression of MEF2A and Dex treatment. Dex treatment alone could not induce induction of Hspb7 (Figure 5C). In myotubes, Dex treatment consistently upregulated Hspb7 expression, with the exception of c-Jun overexpression (Figure 5D). In differentiation conditions, overexpression of MEF2A alone could upregulate Hspb7 expression, and this was enhanced by Dex treatment.

Finally, to determine whether MEF2 and AP-1 were necessary for Dex-induced upregulation of Hspb7, C2C12 were transfected with siRNA targeting MEF2A, Fra-2 or c-Jun, allowed to differentiate for 48 hr and then treated with Dex (10  $\mu$ M, 6 hr) to determine whether Hspb7 expression was affected (Figure 5E). Under Dex treatment, loss of MEF2A prevented Dex-dependent induction of Hspb7 expression, however, loss of Fra-2 or c-Jun upregulated Hspb7 and this was enhanced upon Dex treatment. Together this indicates that Hspb7 is repressed by AP-1 factors c-Jun and Fra-2 and upregulated by a combination of MEF2A and GR recruitment.

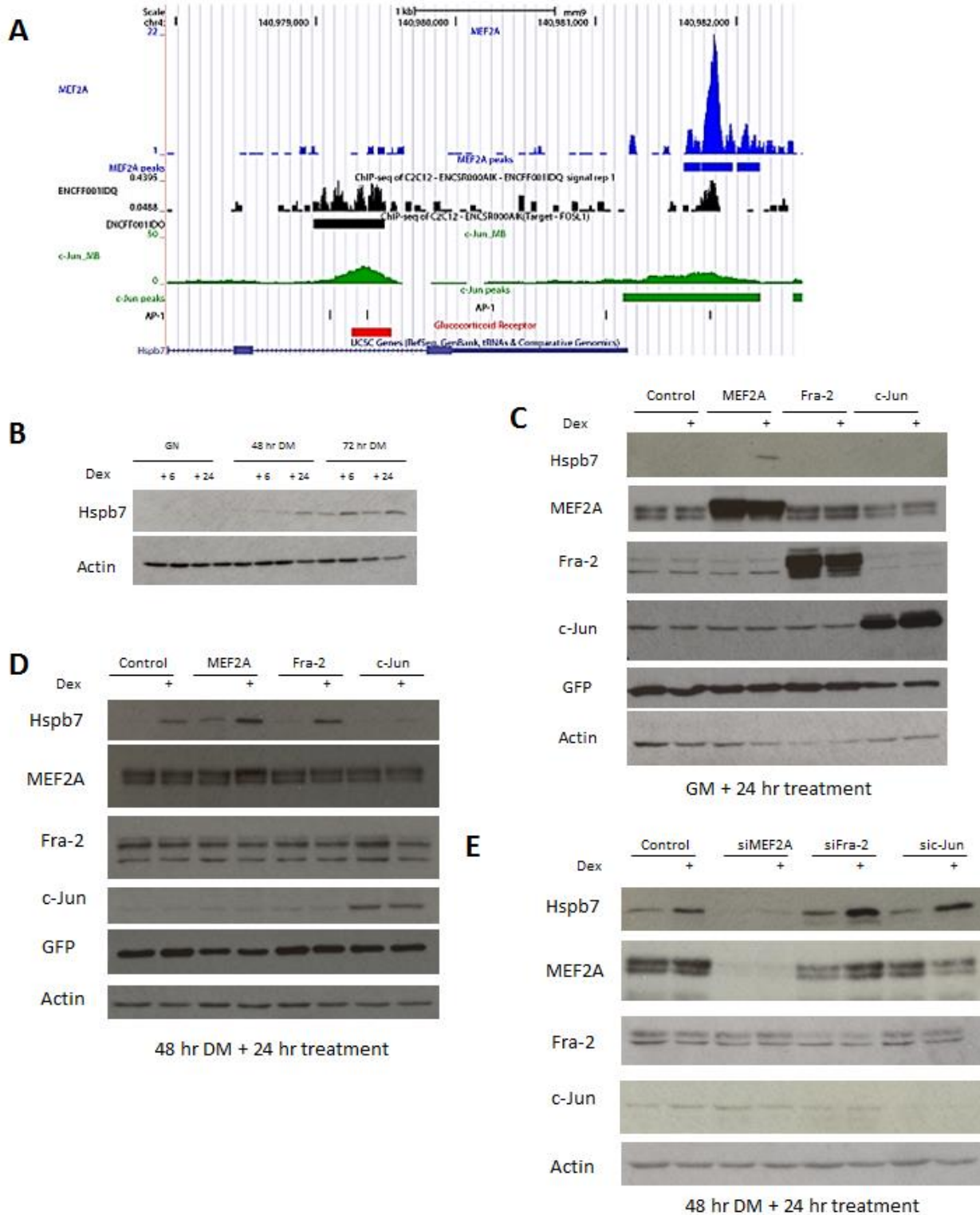


**Figure 5.**

**Figure 5. MEF2 and AP-1 regulate atrophy induced Hspb7 expression.** A) UCSC genome browser image depicting recruitment of MEF2A (blue), Fra-1 (black), c-Jun (green) and Glucocorticoid Receptor (GR, red) to Hspb7. AP-1 consensus sequences are indicated by vertical black lines. B) Dex treatment of myotubes strongly upregulated Hspb7 protein expression. C2C12 were treated with 10  $\mu$ M Dex for the indicated time. Actin was used as a loading control. C) Exogenous expression of MEF2A, Fra-2 or c-Jun in Dex treatment in growth conditions (C) or 72 hr (D). C2C12 were transfected with the indicated construct using calcium phosphate. Cells were treated with 10  $\mu$ M Dex for 24 hr. E) Loss of MEF2A, Fra-2 or c-Jun prevents the induction of Hspb7 expression by Dex treatment. Cells were transfected with the indicated siRNA and allowed to differentiate for 48 hr, after which they were treated with 10  $\mu$ M Dex for 24 hr.

## **Characterizing the role of Hspb7 in muscle atrophy**

Small heat shock proteins have a role in protecting the cytoskeleton during stress (408). Hspb7 (also known as cvHsp) is highly expressed in skeletal and cardiac muscle (409) and it has been linked to cardiac morphogenesis and cardiomyopathies (410, 411), but a role in skeletal muscle has thus far not been established. In other cell types Hspb7 has been shown to prevent protein aggregation (412) and to localize to nuclear speckles (405), a sub-nuclear location in which pre-mRNA is spliced.

First, Hspb7 expression was observed to be expressed late in myogenesis (Figure 6A). Secondly, we found that similar to the majority of literature on Hspb7, it is localized to the cytoplasm, and this is more pronounced under Dex treatment (Figure 6B). Occasionally we could detect Hspb7 as a doublet but the significance of this is unclear.

Using an HA tagged Hspb7 expression construct we observed that exogenous expression of Hspb7 did not influence myogenesis, as MyoG expression was unchanged (Figure 6C). Hspb7 has been associated with autophagy but the mechanism is unclear (413). Bag3 is a component of chaperone mediated autophagy that shows enriched expression in striated muscle and Bag3 null mice develop myopathies (414). Interestingly, Hspb7 and Bag3 SNPs have been associated with heart failure (415). Hspb7 has also been shown to interact with Hspb8 (416), an autophagy related protein that interacts with Bag3 (417). Therefore we decided to look at whether Hspb7 could affect autophagy using LC3B as a readout. We observed that with Hspb7 overexpression, LC3B-II levels were not significantly affected, however Hspb7 protein turnover occurred within 24 hr in spite of maintained GFP expression (Figure 6C). Many proteins that contribute to autophagy are degraded with the autophagic vesicle, such as p62 which shows a reduction in expression in response to increased autophagy. To induce autophagy we treated C2C12 myotubes with Rapamycin, an mTOR inhibitor. We saw an accumulation of LC3B-II in Rapamycin treated cells indicative of enhanced autophagy. This was accompanied by downregulation of Hspb7 after 24hr Rapamycin treatment (Figure 6D), indicating that Hspb7 may be degraded with the autophagosome or involved in autophagy.



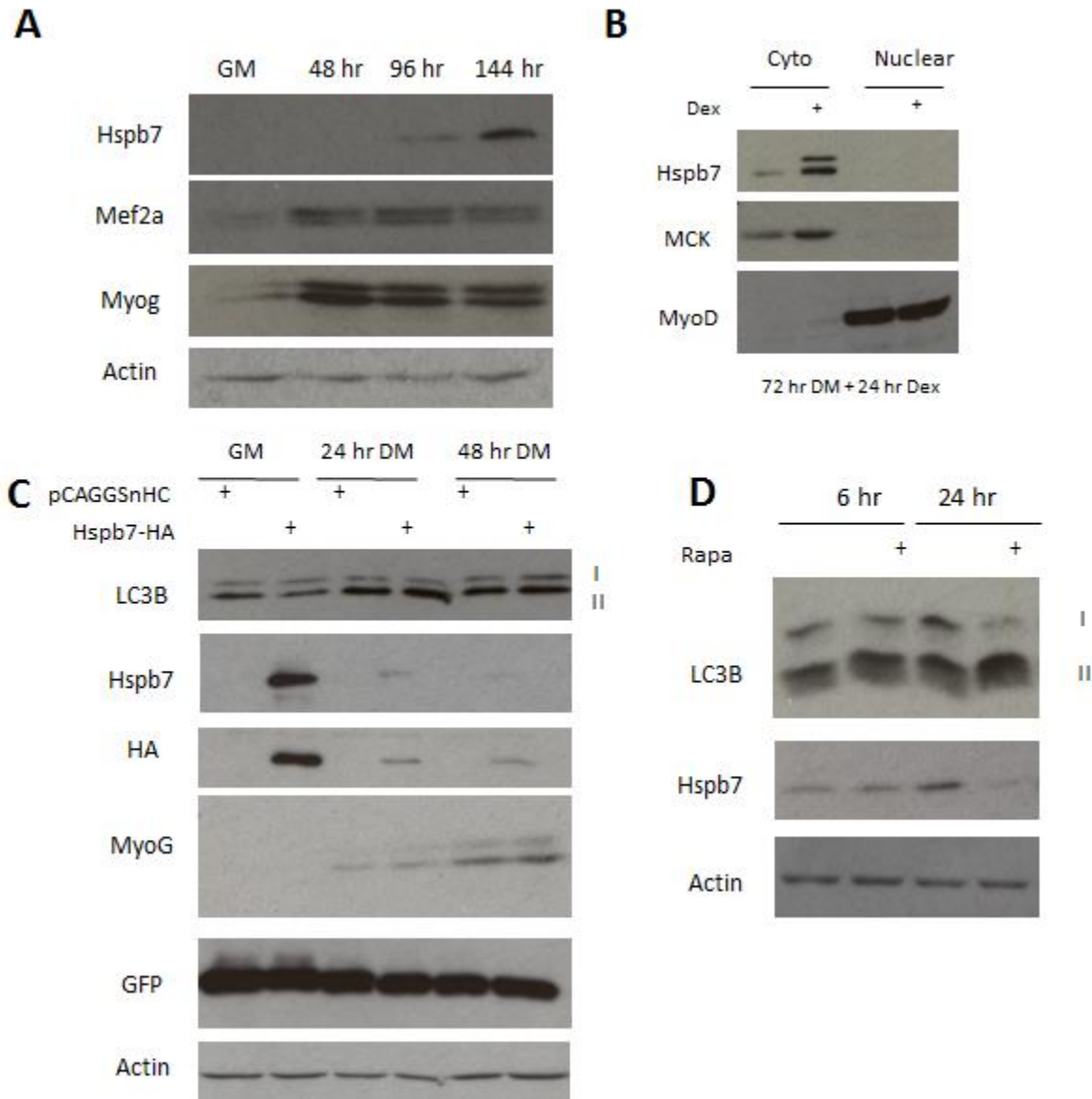


**Figure 6. Role of Hspb7 in skeletal muscle atrophy.** A) Hspb7 during myogenesis. Protein extracts were collected from differentiating C2C12 at the indicated time and prepared for western blot analysis. B) Cyto-Nuclear fractionation in Dex-treated C2C12 myotubes. Cells at 72 hr DM were treated with 10  $\mu$ M Dex for 24 hr and prepared for fractionation. MCK was used as a cytoplasmic control. MyoD was used as a nuclear control. C) Overexpression of Hspb7 in differentiating C2C12. Cells were transfected with Hspb7-HA and allowed to differentiate for the indicated time. Extracts were prepared for western blot. D) Rapamycin treatment decreases Hspb7 expression. Myotubes (72 hr) were treated with Rapamycin (10  $\mu$ g/ml) for the indicated time.

### **Hspb7 expression *in vivo***

These data indicate that Hspb7 is induced under muscle atrophy and may also have a role in autophagy. To determine whether Hspb7 has any correlation to autophagy *in vivo* we induced autophagy via fasting (24 hr). Twenty-four hours prior to fasting, colchicine (0.4mg/kg/day) was injected to serve as an autophagic block and this treatment was maintained throughout fasting. Colchicine+Fast reduced overall weight of the quadriceps and gastrocnemius (Figure 7A). The tibialis anterior (TA) was also affected but this reduction was not as dramatic. Induction of autophagy via fasting and colchicine treatment upregulated Map1lc3b, p62, MyoG Atg7, Foxo1, Foxo3 and Hspb7 in the TA ( $P<0.01$ ) (Figure 7B). Hspb7 expression was also increased ( $P<0.05$ ) in the quadriceps and gastrocnemius but not the heart (Figure 7C).

To determine whether Hspb7 may have a protective role during muscle atrophy we exogenously expressed an HA tagged Hspb7 construct into the TA muscle. Under control conditions, Hspb7-HA did not affect Map1lc3b or p62 expression, however, in response to colchicine and fasting, Hspb7-HA prevented induction of these autophagic genes (Figure 8A, B). The level of Hspb7-HA expression is shown in Figure 8C.

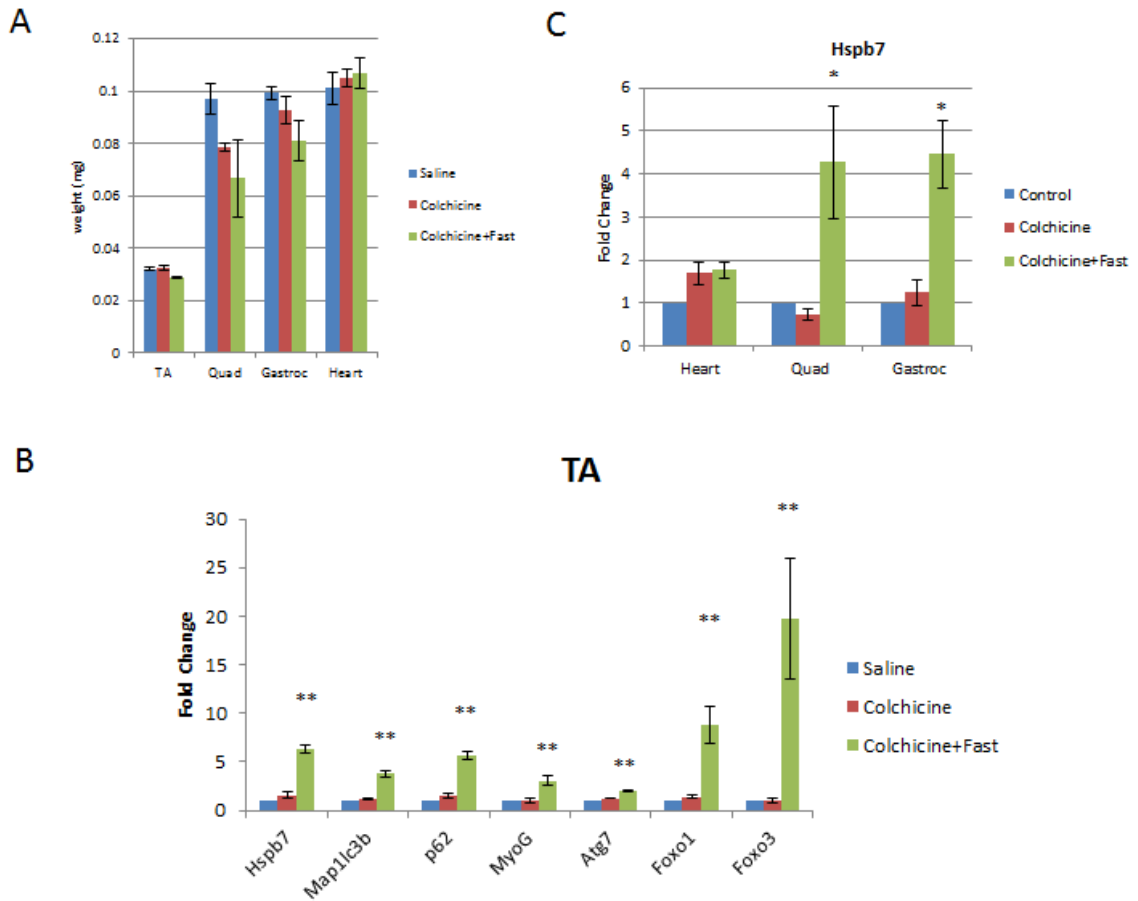


**Figure 7. *Hspb7* expression is associated with autophagy.** A) Total muscle mass of 6-8week old CB57/J mice treated with saline, colchicine (0.4mg/kg/day) or Colchicine+Fast (n=3). B) Changes in autophagy genes in response to fasting. RNA was isolated for qRT-PCR analysis from the TA. Values were calculated using the  $\Delta\Delta C_t$  method and normalized to Gapdh (n=3, \*P<0.05, \*\*P<0.01). C) *Hspb7* in the Heart, Quadriceps (Quad) and Gastrocnemius (Gastroc). Data were analyzed as in B.

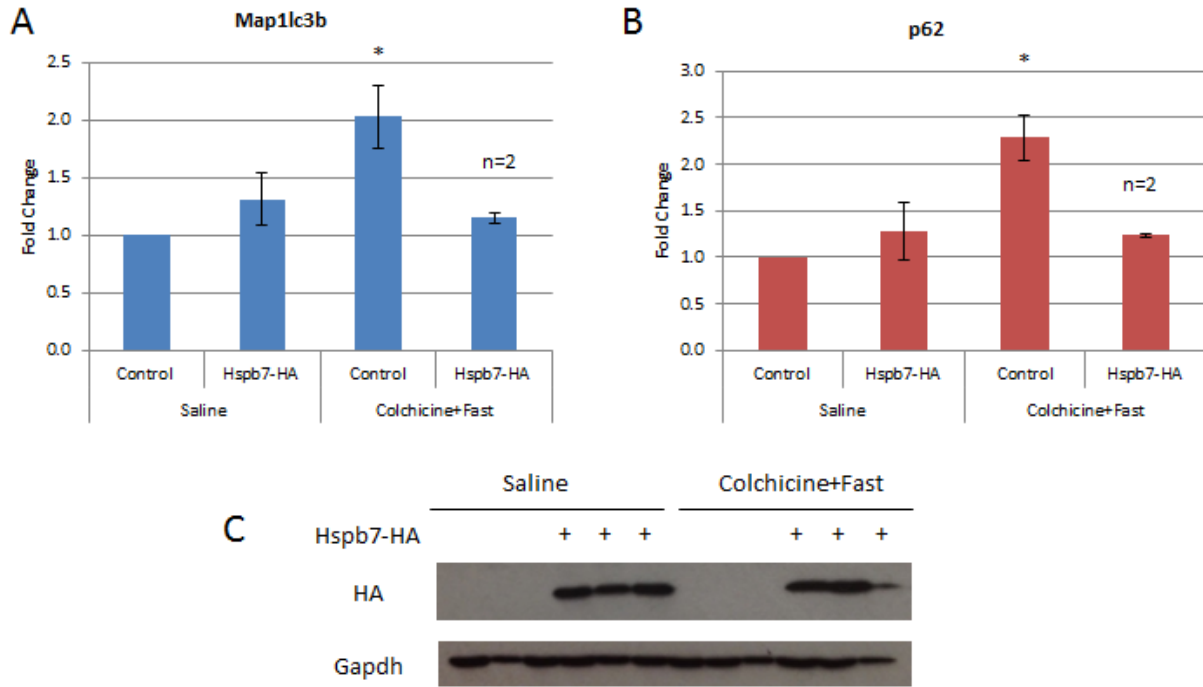


**Figure 8. Hspb7 expression prevents induction of autophagy markers in response to fasting.** A) Hspb7-HA or control (pCAGGSnHC) was electroporated into the TA muscle on Day 1. On Day 3 daily colchicine injections began and on Day 4, colchicine fasting began. Values were calculated using the  $\Delta\Delta C_t$  method and normalized to the geometric mean of  $\beta$ -actin, Gapdh, Tbp and Rps26 (n=3 unless otherwise indicated, \*P<0.05). Panel A shows expression of Map1lc3b while Panel B shows p62 expression. C) Samples were analyzed using western blot analysis to determine level of exogenous expression of Hspb7-HA.

## **Discussion**

From our previous study which identified novel MEF2A target genes in skeletal and cardiac muscle (225) we observed that AP-1 consensus sequences were enriched with MEF2A binding events, and there was strong indication that MEF2A regulates the actin cytoskeleton based on GO term analysis (136, 225). Based on the inverse expression pattern of MEF2 and most AP-1 components (Figure 3A), we hypothesized that MEF2 and AP-1 may regulate the actin cytoskeleton in a competitive manner. In the work presented here we show, through bioinformatic and biochemical analysis that MEF2 and AP-1 share common target genes related to the actin cytoskeleton. Our study presents a mechanism by which changes in gene expression during muscle atrophy directly involve both MEF2 and AP-1. Using Dexamethasone as a model of muscle atrophy we further provide evidence that AP-1 and MEF2 regulate a novel target gene, *Hspb7*, in a Dex-dependent manner. Additionally, we show a novel role for *Hspb7* muscle atrophy that may have implications in autophagy (Figure 9).

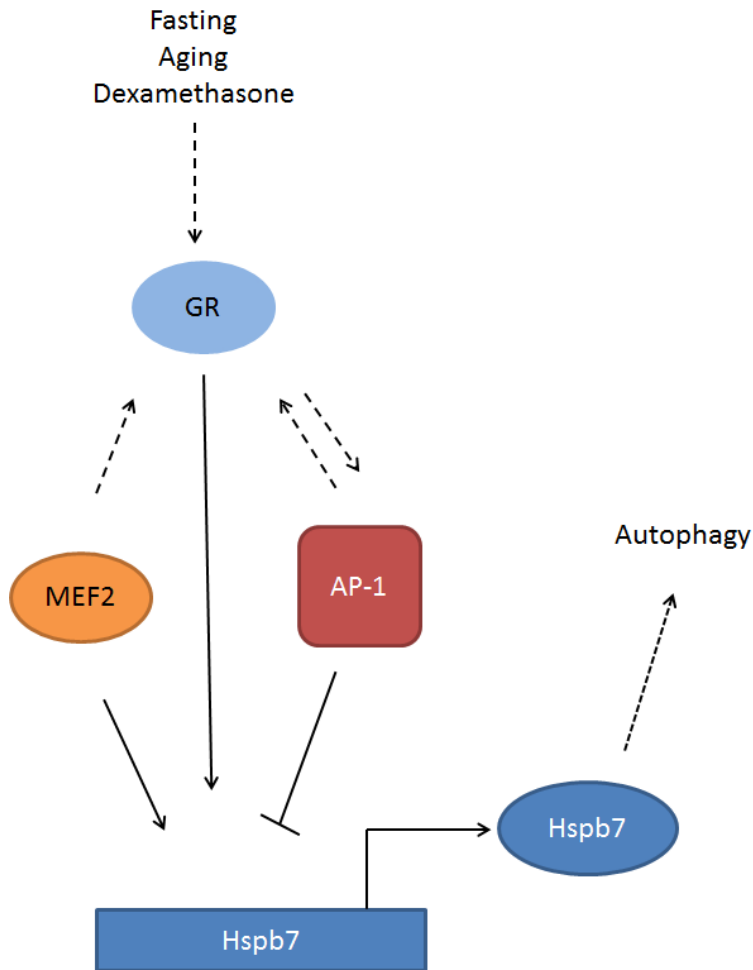


**Figure 9. Model for the regulation and role of Hspb7 in atrophic conditions.** Glucocorticoid signaling (e.g Dexamethasone), aging and fasting induces Hspb7 expression. Activation of Hspb7 requires glucocorticoid receptor (GR) and MEF2A which co-operatively regulate Hspb7 expression. AP-1 inhibits Hspb7 expression by repressing GR activity.

### **MEF2 and AP-1 regulation of the actin cytoskeleton and muscle atrophy**

MEF2 and AP-1 are ubiquitous transcription factors yet their potential interaction at the transcriptional level has not been studied. Based on our results, MEF2 and AP-1 appear to inversely regulate Hspb7 wherein MEF2 promotes expression and AP-1 represses it. We also identified several other potential common target genes that MEF2 and AP-1 may co-operatively or competitively regulate. Based on GO term analysis, Fra-1 and MEF2A do not share a significant number of target genes compared to MEF2A and c-Jun (Figure 1). This may indicate that Fra-1 and MEF2 have fundamentally different functions and also that Fra-1 associates with another Jun family member such as Junb or Jund to target differential AP-1 genes. MEF2 and c-

Jun were enriched for several muscle-related GO terms. This likely reflects the role of c-Jun in priming muscle specific enhancers with MyoD (379), whereby c-Jun and MyoD could prime DNA binding for MEF2A. Fra-1/c-Jun exclusive targets were mainly associated with angiogenesis and the response to bacterium, the latter of which is associated with inflammation and cytokine production, one of the traditional roles of AP-1 (418, 419). This bioinformatic analysis demonstrates that analysis of differential transcription factors can reveal distinct roles of co-operative and exclusive biological functions.

A striking feature of Fra-1 and c-Jun recruitment was that the anti-inflammatory GR also binds within the same location of the second intron of Hspb7 (Figure 5A). GR and AP-1 competitive regulation is not a new phenomenon and was observed several decades ago on the collagenase I gene (420). Subsequently, many other genes were shown to be regulated by GR and AP-1, and interestingly GR co-operates with a Jun homodimer but inhibits Jun:Fos heterodimers (421, 422). Additionally AP-1 has been shown to potentiate GR recruitment by promoting accessible chromatin in epithelial cells (423). In the case of Hspb7 we showed that loss of c-Jun or Fra-2 induces Hspb7 expression upon Dex treatment, indicating a Jun:Fos dimer is involved in regulation of this gene.

In striated muscle the actin cytoskeleton stabilizes the sarcomere in concert with the costamere which tether the Z-line of the sarcomere to the sarcolemma (424). This link facilitates sarcomere stabilization and connects the actin cytoskeleton to the extracellular matrix via the costamere, but it also has roles in other cell processes including migration, adhesion and gene expression (425). Therefore, identifying pathways that mediate actin cytoskeletal gene expression have implications across different type of disease. MEF2 has a well-established role in sarcomere organization as it regulates key target genes associated with the costamere and sarcomeric proteins (136, 137, 297). There are fewer studies that have investigated the role of AP-1 in sarcomere integrity, however, in cardiomyocytes c-Jun has been shown to have an important role in promoting sarcomere gene expression and sarcomere integrity (396). Interestingly, destabilization of actin cytoskeleton triggers c-Jun activity *in vitro* and represses glucocorticoid receptor activity (426). The myofibers in mouse models of cachexia is associated with a defective sarcolemma similar to those seen in muscular dystrophies (307), therefore common structural and cytoskeletal defects may contribute to various pathologies. In cancer cachexia, expression of the dominant negative AP-1 factor Tam67 or AP-1/NF-kappaB double

inhibitor can prevent loss of muscle mass (427, 428). In contrast, Junb was found to be universally downregulated in models of atrophy (264) and loss of AP-1 factors in denervation-induced muscle atrophy prevents upregulation of MAFbx and MURF1 (429). Dysregulation of AP-1 in cancer (430) could therefore not only modulate proliferation and metastasis but also muscle health, which is modulated in cancer cachexia.

### **A role for Hspb7 in muscle disease and sarcopenia.**

The role of small heat shock proteins to date has largely been to interact with and stabilize the cytoskeleton under stress conditions. Hspb7 has been shown to interact with  $\alpha$ -filamin (409) and to stabilize the cytoskeleton in tachypaced cardiomyocytes through co-localization with other heat shock proteins to F-actin, preventing polymerization (431). Along with other small heat shock proteins, Hspb7 moves from the cytosol to myofibrils in response to cardiac ischemia (432). A critical role for Hspb7 in heart development has been shown in zebrafish (411) and an increasing amount of evidence exists that correlates mutations in Hspb7 to cardiomyopathies (415, 433). Co-incidentally Hspb7 SNPs within the second intron where GR and AP-1 recruitment was observed are associated with cardiomyopathies (433). Although Hspb7 was induced in skeletal muscles in response to fasting it was not upregulated in the heart (Figure 7). This may indicate that Hspb7 is induced to protect tissues in response to different forms of stress.

The molecular function of Hspb7 in the stress response, aside from stabilization of the cytoskeleton, has been unclear. Hspb7 does not chaperone misfolded proteins like other small heat shock proteins but instead has been linked to autophagy as a mechanism to clear polyQ protein aggregates (405, 413). In our model of skeletal muscle autophagy, Hspb7 protein levels decrease with Rapamycin, yet expression of mRNA is highly inducible with Dex, aging and fasting. The function of Hspb7 may be similar to one of its co-factors, Hspb8, which interacts with the CASA complex via protein Bag3. The decrease of endogenous Hspb7 in response to Rapamycin treatment likely indicates that Hspb7 is degraded via the autophagy pathway, perhaps as it chaperones muscle proteins. Also Hspb7 has been reported to be located in sub-nuclear speckles in HL-1 and HeLa cells using a tagged Hspb7 construct (405) however in our data, Hspb7 was localized exclusively to the cytosol.

Doran et al. (403) observed increased expression of Hspb7 and Cryab in rat models of sarcopenia aged 30 months. In our model, Hspb7 also increased with age. Since autophagy



impairment is believed to be associated with sarcopenia (434), Hspb7 maybe a protective response as suggested by Doran et al. (403). Decreased satellite cell number has recently been associated with decreased autophagy (435), which could also mean there is a role for Hspb7 in satellite cell quiescence.

In conclusion, MEF2 and AP-1 each have distinct functions, yet both are involved in regulation of skeletal muscle development and the actin-cytoskeleton. Furthermore these transcription factor families may regulate some genes in an inverse manner, such as Hspb7. The precise role of Hspb7 still requires further characterization but so far our experiments indicate that Hspb7 is involved in autophagy which may be of particular importance for muscle function and pathology.

**Table S1. MEF2A target genes that contain AP-1 consensus sequences within the enriched DNA fragment. Results here are limited to  $\pm 10$ kb of TSS.**

Gene Symbol	Gene ID	Peak Location
1700001K19Rik	RIKEN cDNA 1700001K19 gene	MACS_peak_671 (-5250)
1700034E13Rik	RIKEN cDNA 1700034E13 gene	MACS_peak_1317 (-6521)
4930564D02Rik	RIKEN cDNA 4930564D02 gene	MACS_peak_1802 (-6871)
4931408C20Rik	RIKEN cDNA 4931408C20 gene	MACS_peak_15 (+1371)
Acta1	actin, alpha 1, skeletal muscle	MACS_peak_2612 (+9788)
Actr3	ARP3 actin-related protein 3 homolog (yeast)	MACS_peak_143 (+6940)
Aebp2	AE binding protein 2	MACS_peak_2324 (-1642)
Aldoa1	predicted gene 8659; aldolase 1, A isoform, retrogene 1	MACS_peak_1974 (+9501)
Anxa11	annexin A11; predicted gene 2260; predicted gene 2274	MACS_peak_831 (-9585)
Aqp1	aquaporin 1	MACS_peak_2246 (+8468)
Bbc3	BCL2 binding component 3	MACS_peak_2351 (+4483)
Bhlhe40	basic helix-loop-helix family, member e40	MACS_peak_2288 (+5093)
Birc5	baculoviral IAP repeat-containing 5	MACS_peak_575 (-5521)
Bmf	BCL2 modifying factor	MACS_peak_1621 (+8695)
C030005K15Rik	RIKEN cDNA C030005K15 gene	MACS_peak_371 (+55)
Capn2	calpain 2	MACS_peak_248 (-2987)
Ccr3	chemokine (C-C motif) receptor 3	MACS_peak_2728 (+1247)
Cd300lb	CD300 antigen like family member B	MACS_peak_567 (+4643)
Cdh17	cadherin 17	MACS_peak_1905 (+9238)
Chst3	carbohydrate (chondroitin 6/keratan) sulfotransferase 3	MACS_peak_319 (+9824)
Cldn20	claudin 20	MACS_peak_1175 (-760)
Cspg4	chondroitin sulfate proteoglycan 4	MACS_peak_2665 (+8160)
Ctps	cytidine 5'-triphosphate synthase	MACS_peak_2027 (-898)
Cxcr6	chemokine (C-X-C motif) receptor 6	MACS_peak_2727 (+9716)
Diras1	DIRAS family, GTP-binding RAS-like 1	MACS_peak_351 (-2159)
Dstn	destrin	MACS_peak_1668 (-359)
Ephb2	Eph receptor B2	MACS_peak_2045 (+1959)
Fadd	Fas (TNFRSF6)-associated via death domain	MACS_peak_2460 (+4321)
Flnc	filamin C, gamma	MACS_peak_2215 (-2395)
Gas2	growth arrest specific 2	MACS_peak_2376 (+9357)
Gata2	GATA binding protein 2	MACS_peak_2264 (+9663)
Git1	G protein-coupled receptor kinase-interactor 1	MACS_peak_491 (-1334)
Gpc6	predicted gene 4672; glypican 6; similar to Glypican 6	MACS_peak_899 (+3069)
Gtf3c5	general transcription factor IIIC, polypeptide 5	MACS_peak_1486 (-8235)
H3f3b	H3 histone, family 3B	MACS_peak_569 (+3721)
Hspb7	heat shock protein family, member 7 (cardiovascular)	MACS_peak_2052 (+5169)
Ifnlr1	interferon, lambda receptor 1	MACS_peak_2041 (-9676)
Il20	interleukin 20	MACS_peak_151 (-7486)
Itgbl1	integrin, beta-like 1	MACS_peak_903 (+2644)
Jup	junction plakoglobin	MACS_peak_544 (+9544)
Klhl41	kelch like family member 41	MACS_peak_1541 (-342)
Lmod3	leiomodrin 3 (fetal)	MACS_peak_2277 (-51)
Lsm4	LSM4 homolog, U6 small nuclear RNA associated (S. cerevisiae)	MACS_peak_2552 (+9194)
Mall	mal, T-cell differentiation protein-like	MACS_peak_1642 (+7295)
Man2a2	mannosidase 2, alpha 2	MACS_peak_2395 (-5837)
Nav1	neuron navigator 1	MACS_peak_165 (-8842), MACS_peak_164 (-5605)
Necap1	NECAP endocytosis associated 1	MACS_peak_2307 (-2794)
Npas4	neuronal PAS domain protein 4	MACS_peak_1381 (-2966)
Olf432	olfactory receptor 432	MACS_peak_238 (+2806)
Orai1	ORAI calcium release-activated calcium modulator 1	MACS_peak_2169 (-5772)
Plec	plectin 1	MACS_peak_1032 (-7521)
Plekhh2	pleckstrin homology domain containing, family H (with MyTH4 domain) member 2	MACS_peak_1250 (-1476)
Ppap2a	phosphatidic acid phosphatase type 2A	MACS_peak_799 (+2938)
Prkag3	protein kinase, AMP-activated, gamma 3 non-catalytic subunit	MACS_peak_77 (-260)
Prnp	prion protein	MACS_peak_1655 (-6982)
Rapgef1	Rap guanine nucleotide exchange factor (GEF) 1	MACS_peak_1487 (+5135)
Rcc2	regulator of chromosome condensation 2; hypothetical protein LOC100047340	MACS_peak_2050 (-4012)
Sil1	endoplasmic reticulum chaperone SIL1 homolog (S. cerevisiae)	MACS_peak_1284 (-185)
Slc30a4	solute carrier family 30 (zinc transporter), member 4	MACS_peak_1628 (-2027)
Smtnl1	smoothelin-like 1	MACS_peak_1563 (+2568)
Sp2	Sp2 transcription factor	MACS_peak_535 (-4416)
Spata4	spermatogenesis associated 4	MACS_peak_2533 (+8876)
Stambpl1	STAM binding protein like 1	MACS_peak_1428 (+3047)
Stmn4	stathmin-like 4	MACS_peak_864 (-3371)
Supt3	suppressor of Ty 3	MACS_peak_1207 (-6125)
Tlr4	toll-like receptor 4	MACS_peak_1970 (+1251)
Trem1	triggering receptor expressed on myeloid cells-like 1	MACS_peak_1212 (-3847)
Wisp1	WNT1 inducible signaling pathway protein 1	MACS_peak_1017 (-7370), MACS_peak_1021 (+2803)
Xcl1	chemokine (C motif) ligand 1	MACS_peak_222 (+8518)
Xirp1	xin actin-binding repeat containing 1	MACS_peak_2720 (-673)
Ybx3	Y-box binding protein 3	MACS_peak_2318 (+5898)
Zbtb42	predicted gene 5188	MACS_peak_672 (+4714)
Zc3h18	predicted gene 5939; zinc finger CCCH-type containing 18	MACS_peak_2609 (-7767)
Zfp46	zinc finger protein 46	MACS_peak_2044 (-1687)
Zfp516	zinc finger protein 516	MACS_peak_1375 (-310)
Zfp697	zinc finger protein 697	MACS_peak_1795 (-7835)

**Table S2. siRNA oligonucleotides.**

Target	Product Number
scr	SIC001
Mef2a	SASI_Mm01_00120788
c-Jun	SASI_Mm01_00046358
Fra-2	SASI_Mm01_00201001

**Table S3. Primers used in qRT-PCR and ChIP-qPCR.**

Gene	Forward 5'-3'	Reverse 5'-3'
Atg7	TTTCTGTCACGGTTCGATAATG	TGAATCCTTCTCGCTCGTACT
Dstn	CACCAGAACCAAGCACCTCTG	AGCCACCTAGCTTTTCAGCA
Flnc	TTAACCGAGACTGGCAGGAC	CCTCTCTGGCATTCTGCAC
Foxo1	ACG AGT GGA TGG TGA AGA GC	TGC TGT GAA GGG ACA GAT TG
Foxo3	AGT GGA TGG TGC GCT GTG T	CTG TGC AGG GAC AGG TTG T
Hspb7	TGTCACCACCTTCAACAACCAC	TCATGACTGTGCCATCAGCTG
Lmod3	TGACTCTGCCAGAAAACCT	GTTGAGCTGCTGGGAGTGAC
Plekhh2	AATTCCGAGTTCAAGCAAGC	CCGCTCTGCATCGATAACTT
MAFbx	GCAGAGAGTCGGCAA GTC	CAGGTCGGTGATCGTGAG
Murf1	AGTGTCCATGTCTGGAGGTCGTTT	ACTGGAGCACTCCTGCTTGTAGAT
Map1lc3b	GCTTGCAGCTCAATGCTAAC	CCTGCGAGGCATAAACCATGTA
Myogenin	CAGCTCCCTCAACCAGGAG	GACTGCAGGAGGCGCTGT
Rps26	GCCATCCATAGCAAGGTTGT	GCCTCTTTACATGGGCTTTG
Sqstm1/p62	TGTGGTGGGAACTCGCTATAA	CAGCGGCTATGAGAGAAGCTAT
Tbp	TCATGGACCAGAACAACAGC	GCTGTGGAGTAAGTCCTGTGC
$\beta$ -Actin	AAGTGTGACGTTGACATCCGTAA	TGCCTGGGTACATGGTGGTA
Gapdh	ACCCCAATGTATCCGTTGT	TACTCCTTGGAGGCCATGTA

## CHAPTER V: Summary of Dissertation

The complex role that MEF2 has during embryogenesis and in adult diseases in both skeletal and cardiac muscle has been difficult to fully characterize. Genetic knockout mouse models have shown critical roles for individual MEF2 genes yet their redundancy in function may hide physiological outcomes as seen in MEF2A, C, and D triple knockout models during skeletal muscle regeneration (140). To better identify the functions of MEF2A we utilized high throughput ChIP-sequencing in skeletal and cardiac cells to find new target genes. Bioinformatic analysis showed that MEF2A is recruited to a loosely conserved set of binding sites (~300) in both cell types. Using Gene Ontology analysis it was found that across cell types MEF2A recruited genes were mutually associated with functions related to the actin cytoskeleton but in myoblasts, MEF2A was also associated with functions related to the regulation of MAPK activity while in cardiomyocytes, enriched genes were associated with the induction of apoptosis. Enriched consensus sequences within these cell types included MEF2 and AP-1.

We also used a loss of function approach via siRNA-mediated gene silencing to find differentially expressed genes in MEF2A depleted myoblasts. The majority of downregulated genes were associated with muscle system processes and upregulated genes were related to cellular locomotion. Additionally, the location of MEF2A recruitment may dictate function: 20% of downregulated genes corresponded to MEF2A enrichment within  $\pm 5$  kb of the transcription start site, compared to upregulated genes which had less than 5% of total gene recruitment within  $\pm 5$  kb of the TSS. We then validated five genes (*Dusp6*, *Hspb7*, *Kitl*, *Lmod3*, *Prrx1*) that were differentially expressed in the RNA-seq analysis and also bound by MEF2A in both cardiomyocytes and myoblasts. Loss of function analysis of the genes modulated *MyoG* expression in myoblasts, indicating a functional role for these genes in myogenesis. Further characterization of DUSP6 showed that MEF2 inhibits expression of this gene in both cardiac and skeletal muscle. We observed that during myoblast differentiation, DUSP6 becomes dramatically decreased as p38MAPK activity increases. Using p38MAPK inhibitor SB 203580 in combination with MEF2 gene silencing we found that p38 activity contributes to DUSP6 repression in a MEF2D-dependent manner. Therefore this research established a model whereby MEF2 repression of DUSP6, a MAPK phosphatase, depends on MAPK activity.

From this bioinformatic analysis it was observed that AP-1 consensus sequences are enriched in MEF2A bound DNA in striated muscle. MEF2A recruitment in myoblasts was

compared to Fra-1 and c-Jun ChIP-seq datasets in an exploratory bioinformatic screen. Of the 2783 MEF2A enriched binding sites, approximately 69% were enriched with only MEF2A, not c-Jun or Fra-1. Interestingly, this analysis showed MEF2A and c-Jun share more binding sites than MEF2A and Fra-1, although there were sites enriched for all three factors. Fra-1 rarely showed recruitment without c-Jun. As many AP-1 factors could be interacting with MEF2A, we reasoned that mapping AP-1 consensus sequence (TGAGTCA) to MEF2A-enriched DNA could be a less-biased approach to finding shared MEF2A/AP-1 target genes. Many of the MEF2A/AP-1 target genes were associated with Gene Ontology terms related to the actin cytoskeleton. Five were chosen for further study: *Dstn*, *Flnc*, *Hspb7*, *Lmod3* and *Plekhh2*. *Hspb7* was found to be upregulated in aging skeletal muscle and also in response to atrophic signaling mediated by Dexamethasone, a synthetic glucocorticoid. Using gain and loss of function approaches it was found that MEF2A positively regulates *Hspb7* expression, and Dex-mediated upregulation of *Hspb7* requires MEF2A. In contrast, AP-1 factors Fra-2 and c-Jun repress *Hspb7* expression. *Hspb7* has been linked to autophagy by others, but not studied in skeletal muscle. Using *in vivo* models of autophagy we found that *Hspb7* is induced in skeletal muscle but not the heart. Exogenous expression of *Hspb7* may offer protection from atrophy as this reduced upregulation of *Map1lc3b* and *p62* in response to fasting.

Together, this thesis identified the common and divergent MEF2A target genes in skeletal and cardiac muscle using high throughput sequencing. Furthermore, *Dusp6* and *Hspb7* were identified as two MEF2A target genes in skeletal and cardiac muscle that have implications in cardiac hypertrophy, myogenesis, and atrophy.

## CHAPTER VI: Future Directions and Conclusions

Broad scale high throughput approaches, such as those used in this thesis, are useful in identifying transcription factor target genes, and several thousands of studies have been compiled and released into public databases that often remain underutilized. Future work will need to take into account existing high throughput data and transform it into a more complex, integrated network. In this thesis we compared ChIP-seq data from MEF2A and AP-1 components Fra-1 and c-Jun. Based on the differential regulation of MEF2A and MEF2D by p38MAPK on DUSP6 expression shown in Manuscript I it is clear that MEF2 proteins have different capacities in gene regulation that are dependent on post-translational modifications which was not considered in Manuscript II. As MEF2A and MEF2D are the predominant MEF2 dimer found in the adult heart and skeletal muscle (134, 146), it would be interesting to compare MEF2A recruitment to MEF2D to determine whether MEF2A or D homodimers have different effects on gene expression and whether this is related to differential AP-1 recruitment. Furthermore alternative splicing of MEF2 may determine their potential for co-factor interactions. A skeletal muscle specific MEF2D splice variant was shown to evade PKA signaling and in addition it did not interact with HDAC4 (148). To fully understand how muscle responds to stress it will be necessary to have a complete genomic understanding of temporal recruitment of MEF2 proteins and their co-factors. With these considerations in mind, the complexity of understanding gene regulation can seem overwhelming. It will therefore be important in the future to fully utilize available research using bioinformatic approaches.

DUSP6 has been shown to inhibit ERK1/2 activity and thereby regulate proliferation of the satellite pool in skeletal muscle regeneration (364) and hypertrophy in cardiac pressure overload (363, 436). We studied the upstream factors that regulate MEF2 activity in myoblasts and found p38MAPK to have an important role in this pathway, but did not investigate possible mechanisms in cardiomyocytes. As cardiomyocyte hypertrophy is known to be regulated by MEF2, and loss of DUSP6 has a protective effect on pressure overload (363), it may be useful to study the regulation of DUSP6 by MEF2 in cardiomyocytes in more detail.

There is a significant body of literature that identifies a role for Hspb7 in heart development (411), cell stress (397, 413, 431), and aging in muscle (403), yet aside from zebrafish, a genetic knockout model of Hspb7 has not yet been generated. It would be useful to create a floxed Hspb7 mouse to conditionally delete Hspb7 from certain tissues. Studying Hspb7

*in vitro* was particularly difficult since it is expressed only in mature myotubes, therefore the effect of siRNA mediated gene silencing was difficult to achieve. Generating Hspb7 knockout mice could be used to understand aging models of autophagy, as Hspb7 is upregulated in skeletal muscle with age and has a definite but unclear role in autophagy. Also, data from our lab indicates Hspb7 may have a pro-survival role in the heart, as loss of Hspb7 *in vitro* upregulated a variety of stress related genes such as ANF, MAFbx and cleaved Caspase-3 (data not shown). Loss of function of Hspb7 in experimental animal models of myocardial infarct and pressure overload would elucidate whether this small heat shock protein has a function in adult myopathy.

More broadly speaking, the regulation of MEF2 is implicated in many types of disease. Models of cancer cachexia show disturbed myofiber membranes and have similar properties to muscular dystrophies (307). Characterizing the activity of MEF2 in cancer has been done only in a few studies and looks primarily at the role of MEF2 in EMTs of the invasive tissue. Tumor-bearing mice show reduced muscle stability and MEF2 expression (295), therefore implicating MEF2 activity in cancer cachexia. Examining how MEF2 is downregulated in cancer cachexia could lead to the development of beneficial treatment options to improve muscle health and quality of life in the chronically ill.

Genome editing via TALENs and CRISPR/Cas9 has become an integral part of experimental design in many labs, and it is possible that in the future, human diseases will also be treated using this technology. Recently a child in the United Kingdom with leukemia was, for the first time, “cured” using genome editing, although official results are awaiting publication. With respect to MEF2, various diseases in which MEF2 signaling is maladaptive could be blocked by a reversible single nucleotide deletion from the MEF2 consensus sequence in specific tissues. For example in pathological hypertrophy, shutting down MEF2 recruitment to genes associated with remodelling would slow the progression to heart failure. Another possibility would be to activate MEF2 by swapping out the class II HDAC interacting domain in MEF2 in satellite cells to promote myofiber repair in muscle atrophy.

If genome editing of human tissues *in vivo* is undesirable, then manipulating MEF2 activity prior to stem cell transplantation could also be considered. Stem cell transplantation has already been done for several years in cardiac and skeletal muscle in which fibroblasts that have been reprogrammed to behave as cardiac stem cells or satellite cells are added to damaged tissue. Instead of treating the problem after the fact, stem cells should be prepared as protective reagents

and transplanted prior to injury. For example, creating PKA-resistant MEF2D cardiomyocytes and transplanting these into patients predisposed to have heart attacks may prevent cardiomyocyte death and fare better than with  $\beta$ -blocker treatment. Or athletes, astronauts or the elderly may take a dose of super-activated MEF2 satellite cells prior to strenuous workout, returning to earth or going for a walk, to temporarily increase Type I fibers.

There is still much to be determined about MEF2 in disease. Future experiments related to MEF2 must utilize a combination of bioinformatics, *in vivo* and biochemical analyses to further elucidate gene regulation in striated muscle disease.



## REFERENCES

1. Grubb BJ (2006) Developmental Biology, Eighth Edition. Scott F. Gilbert, editor. *Integr Comp Biol* 46(5):652–653.
2. Rossant J, Tam PPL (2009) Blastocyst lineage formation, early embryonic asymmetries and axis patterning in the mouse. *Development* 136(5):701–713.
3. Stern CD, Downs KM (2012) The hypoblast (visceral endoderm): an evo-devo perspective. *Development* 139(6):1059–69.
4. Tam PP., Behringer RR (1997) Mouse gastrulation: the formation of a mammalian body plan. *Mech Dev* 68(1-2):3–25.
5. Tam PP, Williams EA, Chan WY (1993) Gastrulation in the mouse embryo: ultrastructural and molecular aspects of germ layer morphogenesis. *Microsc Res Tech* 26(4):301–28.
6. Schoenwolf GC, Smith JL (1990) Mechanisms of neurulation: traditional viewpoint and recent advances. *Development* 109(2):243–70.
7. Copp AJ, Greene NDE, Murdoch JN (2003) The genetic basis of mammalian neurulation. *Nat Rev Genet* 4(10):784–93.
8. Shyamala K, Yanduri S, Girish HC, Murgod S Neural crest: The fourth germ layer. *J Oral Maxillofac Pathol* 19(2):221–229.
9. Christ B, Ordahl CP (1995) Early stages of chick somite development. *Anat Embryol (Berl)* 191(5):381–96.
10. Gilbert SF (2000) Paraxial Mesoderm: The Somites and Their Derivatives. Available at: <http://www.ncbi.nlm.nih.gov/books/NBK10085/> [Accessed January 9, 2016].
11. Jiang YJ, et al. (2000) Notch signalling and the synchronization of the somite segmentation clock. *Nature* 408(6811):475–9.
12. Dubrulle J, McGrew MJ, Pourquié O (2001) FGF Signaling Controls Somite Boundary Position and Regulates Segmentation Clock Control of Spatiotemporal Hox Gene

- Activation. *Cell* 106(2):219–232.
13. Carapuco M (2005) Hox genes specify vertebral types in the presomitic mesoderm. *Genes Dev* 19(18):2116–2121.
  14. Harms M, Seale P (2013) Brown and beige fat: development, function and therapeutic potential. *Nat Med* 19(10):1252–63.
  15. Buckingham M, et al. (2003) The formation of skeletal muscle: from somite to limb. *J Anat* 202(1):59–68.
  16. Rios AC, Serralbo O, Salgado D, Marcelle C (2011) Neural crest regulates myogenesis through the transient activation of NOTCH. *Nature* 473(7348):532–5.
  17. Epstein DJ, Vekemans M, Gros P (1991) Splotch (Sp2H), a mutation affecting development of the mouse neural tube, shows a deletion within the paired homeodomain of Pax-3. *Cell* 67(4):767–74.
  18. Conway S (1997) Development of a lethal congenital heart defect in the splotch (Pax3) mutant mouse. *Cardiovasc Res* 36(2):163–173.
  19. Bober E, Franz T, Arnold HH, Gruss P, Tremblay P (1994) Pax-3 is required for the development of limb muscles: a possible role for the migration of dermomyotomal muscle progenitor cells. *Development* 120(3):603–12.
  20. Tremblay P, et al. (1998) A crucial role for Pax3 in the development of the hypaxial musculature and the long-range migration of muscle precursors. *Dev Biol* 203(1):49–61.
  21. WILLIAMS B, ORDAHL C (1994) PAX-3 EXPRESSION IN SEGMENTAL MESODERM MARKS EARLY STAGES IN MYOGENIC CELL SPECIFICATION. *DEVELOPMENT* 120(4):785–796.
  22. Daston G, Lamar E, Olivier M, Goulding M (1996) Pax-3 is necessary for migration but not differentiation of limb muscle precursors in the mouse. *Development* 122(3):1017–27.
  23. Mansouri A, Stoykova A, Torres M, Gruss P (1996) Dysgenesis of cephalic neural crest derivatives in Pax7<sup>-/-</sup> mutant mice. *Development* 122(3):831–8.

24. Seale P, et al. (2000) Pax7 is required for the specification of myogenic satellite cells. *Cell* 102(6):777–86.
25. Galili N, et al. (1993) Fusion of a fork head domain gene to PAX3 in the solid tumour alveolar rhabdomyosarcoma. *Nat Genet* 5(3):230–5.
26. DAVIS R, DCRUZ C, LOVELL M, BIEGEL J, BARR F (1994) FUSION OF PAX7 TO FKHR BY THE VARIANT T(1,13)(P36,Q14) TRANSLOCATION IN ALVEOLAR RHABDOMYOSARCOMA. *CANCER Res* 54(11):2869–2872.
27. Jostes B, Walther C, Gruss P (1990) The murine paired box gene, Pax7, is expressed specifically during the development of the nervous and muscular system. *Mech Dev* 33(1):27–37.
28. Tajbakhsh S, Rocancourt D, Cossu G, Buckingham M (1997) Redefining the genetic hierarchies controlling skeletal myogenesis: Pax-3 and Myf-5 act upstream of MyoD. *Cell* 89(1):127–38.
29. Lassar AB, et al. (1991) Functional activity of myogenic HLH proteins requires hetero-oligomerization with E12/E47-like proteins in vivo. *Cell* 66(2):305–315.
30. Braun T, Rudnicki MA, Arnold H-H, Jaenisch R (1992) Targeted inactivation of the muscle regulatory gene Myf-5 results in abnormal rib development and perinatal death. *Cell* 71(3):369–382.
31. Rudnicki MA, Braun T, Hinuma S, Jaenisch R (1992) Inactivation of MyoD in mice leads to up-regulation of the myogenic HLH gene Myf-5 and results in apparently normal muscle development. *Cell* 71(3):383–390.
32. BRAUN T, ARNOLD H (1995) INACTIVATION OF MYF-6 AND MYF-5 GENES IN MICE LEADS TO ALTERATIONS IN SKELETAL-MUSCLE DEVELOPMENT. *EMBO J* 14(6):1176–1186.
33. PATAPOUTIAN A, et al. (1995) DISRUPTION OF THE MOUSE MRF4 GENE IDENTIFIES MULTIPLE WAVES OF MYOGENESIS IN THE MYOTOME. *DEVELOPMENT* 121(10):3347–3358.
34. Rudnicki MA, et al. (1993) MyoD or Myf-5 is required for the formation of skeletal muscle. *Cell* 75(7):1351–1359.

35. Rawls A, et al. (1998) Overlapping functions of the myogenic bHLH genes MRF4 and MyoD revealed in double mutant mice. *Development* 125(13):2349–58.
36. Kassam-Duchossoy L, et al. (2004) Mrf4 determines skeletal muscle identity in Myf5:MyoD double-mutant mice. *Nature* 431(7007):466–71.
37. Maroto M, et al. (1997) Ectopic Pax-3 activates MyoD and Myf-5 expression in embryonic mesoderm and neural tissue. *Cell* 89(1):139–48.
38. Bajard L, et al. (2006) A novel genetic hierarchy functions during hypaxial myogenesis: Pax3 directly activates Myf5 in muscle progenitor cells in the limb. *Genes Dev* 20(17):2450–64.
39. Kassam-Duchossoy L, et al. (2005) Pax3/Pax7 mark a novel population of primitive myogenic cells during development. *Genes Dev* 19(12):1426–31.
40. Delfini MC, Hirsinger E, Pourquié O, Duprez D (2000) Delta 1-activated notch inhibits muscle differentiation without affecting Myf5 and Pax3 expression in chick limb myogenesis. *Development* 127(23):5213–24.
41. Kopan R, Nye JS, Weintraub H (1994) The intracellular domain of mouse Notch: a constitutively activated repressor of myogenesis directed at the basic helix-loop-helix region of MyoD. *Development* 120(9):2385–96.
42. Nabeshima Y, et al. (1993) Myogenin gene disruption results in perinatal lethality because of severe muscle defect. *Nature* 364(6437):532–5.
43. Grifone R, et al. (2005) Six1 and Six4 homeoproteins are required for Pax3 and Mrf expression during myogenesis in the mouse embryo. *Development* 132(9):2235–49.
44. Grifone R, et al. (2007) Eya1 and Eya2 proteins are required for hypaxial somitic myogenesis in the mouse embryo. *Dev Biol* 302(2):602–16.
45. Giordani J, et al. (2007) Six proteins regulate the activation of Myf5 expression in embryonic mouse limbs. *Proc Natl Acad Sci* 104(27):11310–11315.
46. Relaix F, et al. (2013) Six homeoproteins directly activate MyoD expression in the gene

- regulatory networks that control early myogenesis. *PLoS Genet* 9(4):e1003425.
47. Potthoff MJ, Olson EN (2007) MEF2: a central regulator of diverse developmental programs. *Development* 134(23):4131–40.
  48. Ge Y, Chen J (2011) MicroRNAs in skeletal myogenesis. *Cell Cycle* 10(3):441–8.
  49. Saccone V, Puri PL Epigenetic regulation of skeletal myogenesis. *Organogenesis* 6(1):48–53.
  50. Buckingham M, Rigby PWJ (2014) Gene regulatory networks and transcriptional mechanisms that control myogenesis. *Dev Cell* 28(3):225–38.
  51. Relaix F, Rocancourt D, Mansouri A, Buckingham M (2005) A Pax3/Pax7-dependent population of skeletal muscle progenitor cells. *Nature* 435(7044):948–53.
  52. Ben-Yair R, Kalcheim C (2005) Lineage analysis of the avian dermomyotome sheet reveals the existence of single cells with both dermal and muscle progenitor fates. *Development* 132(4):689–701.
  53. McKinnell IW, et al. (2008) Pax7 activates myogenic genes by recruitment of a histone methyltransferase complex. *Nat Cell Biol* 10(1):77–84.
  54. Kuang S, Kuroda K, Le Grand F, Rudnicki MA (2007) Asymmetric self-renewal and commitment of satellite stem cells in muscle. *Cell* 129(5):999–1010.
  55. Olguin HC, Olwin BB (2004) Pax-7 up-regulation inhibits myogenesis and cell cycle progression in satellite cells: a potential mechanism for self-renewal. *Dev Biol* 275(2):375–388.
  56. Olguin HC, Yang Z, Tapscott SJ, Olwin BB (2007) Reciprocal inhibition between Pax7 and muscle regulatory factors modulates myogenic cell fate determination. *J Cell Biol* 177(5):769–779.
  57. Kuroda K, Kuang S, Taketo MM, Rudnicki MA (2013) Canonical Wnt signaling induces BMP-4 to specify slow myofibrogenesis of fetal myoblasts. *Skelet Muscle* 3(1):5.
  58. Jones AE, Price, VD, Dick SA, Megeney LA, Rudnicki MA Wnt/ $\beta$ -catenin controls

- follistatin signalling to regulate satellite cell myogenic potential. *Skelet Muscle* 5:14.
59. Le Grand F, Jones AE, Seale V, Scimè A, Rudnicki MA (2009) Wnt7a activates the planar cell polarity pathway to drive the symmetric expansion of satellite stem cells. *Cell Stem Cell* 4(6):535–47.
  60. Bentzinger CF, et al. (2013) Fibronectin Regulates Wnt7a Signaling and Satellite Cell Expansion. *Cell Stem Cell* 12(1):75–87.
  61. Conboy IM, Rando TA (2002) The regulation of Notch signaling controls satellite cell activation and cell fate determination in postnatal myogenesis. *Dev Cell* 3(3):397–409.
  62. Cheung TH, et al. (2012) Maintenance of muscle stem-cell quiescence by microRNA-489. *Nature* 482(7386):524–U247.
  63. Conboy IM, Conboy MJ, Smythe GM, Rando TA (2003) Notch-mediated restoration of regenerative potential to aged muscle. *Science* 302(5650):1575–7.
  64. Xin M, Olson EN, Bassel-Duby R (2013) Mending broken hearts: cardiac development as a basis for adult heart regeneration and repair. *Nat Rev Mol Cell Biol* 14(8):529–41.
  65. Gilbert SF (2000) Lateral Plate Mesoderm. Available at: <http://www.ncbi.nlm.nih.gov/books/NBK9982/> [Accessed January 12, 2016].
  66. Yutzey KE, Kirby ML (2002) Wherefore heart thou? Embryonic origins of cardiogenic mesoderm. *Dev Dyn* 223(3):307–20.
  67. Abu-Issa R, Kirby ML (2007) Heart field: from mesoderm to heart tube. *Annu Rev Cell Dev Biol* 23:45–68.
  68. Black BL (2007) Transcriptional pathways in second heart field development. *Semin Cell Dev Biol* 18(1):67–76.
  69. Waldo KL, et al. (2001) Conotruncal myocardium arises from a secondary heart field. *Development* 128(16):3179–88.
  70. Lyons I, et al. (1995) Myogenic and morphogenetic defects in the heart tubes of murine embryos lacking the homeo box gene Nkx2-5. *Genes Dev* 9(13):1654–1666.

71. Molkenin JD, Lin Q, Duncan S a., Olson EN (1997) Requirement of the transcription factor GATA4 for heart tube formation and ventral morphogenesis. *Genes Dev* 11(8):1061–1072.
72. Takeuchi JK (2003) Tbx5 specifies the left/right ventricles and ventricular septum position during cardiogenesis. *Development* 130(24):5953–5964.
73. Kuo CT, et al. (1997) GATA4 transcription factor is required for ventral morphogenesis and heart tube formation. *Genes Dev* 11(8):1048–60.
74. Moorman A, Webb S, Brown N a, Lamers W, Anderson RH (2003) Development of the heart: (1) formation of the cardiac chambers and arterial trunks. *Heart* 89(7):806–814.
75. Thomas T, Yamagishi H, Overbeek P a, Olson EN, Srivastava D (1998) The bHLH factors, dHAND and eHAND, specify pulmonary and systemic cardiac ventricles independent of left-right sidedness. *Dev Biol* 196(2):228–236.
76. Srivastava D, et al. (1997) Regulation of cardiac mesodermal and neural crest development by the bHLH transcription factor, dHAND. *Nat Genet* 16(2):154–160.
77. Meno C, et al. (1998) Lefty-1 Is Required for Left-Right Determination As a Regulator of Lefty-2 and Nodal. *Cell* 94(3):287–297.
78. Lin Q, Schwarz J, Bucana C, Olson EN (1997) Control of mouse cardiac morphogenesis and myogenesis by transcription factor MEF2C. *Science* (80- ) 276(5317):1404–1407.
79. Parlakian A, et al. (2004) Targeted inactivation of serum response factor in the developing heart results in myocardial defects and embryonic lethality. *Mol Cell Biol* 24(12):5281–5289.
80. Evans SM, Yelon D, Conlon FL, Kirby ML (2010) Myocardial lineage development. *Circ Res* 107(12):1428–44.
81. Beltrami AP, et al. (2001) Evidence that human cardiac myocytes divide after myocardial infarction. *N Engl J Med* 344(23):1750–7.
82. Oh H, et al. (2003) Cardiac progenitor cells from adult myocardium: homing,

- differentiation, and fusion after infarction. *Proc Natl Acad Sci U S A* 100(21):12313–12318.
83. Beltrami AP, et al. (2003) Adult cardiac stem cells are multipotent and support myocardial regeneration. *Cell* 114(6):763–776.
  84. van Berlo JH, et al. (2014) C-Kit+ Cells Minimally Contribute Cardiomyocytes To the Heart. *Nature* 509(7500):337–41.
  85. Krijnen PAJ, et al. (2002) Apoptosis in myocardial ischaemia and infarction. *J Clin Pathol* 55(11):801–11.
  86. Frey N, Olson EN (2003) Cardiac hypertrophy: the good, the bad, and the ugly. *Annu Rev Physiol* 65:45–79.
  87. Chien KR, Knowlton KU, Zhu H, Chien S (1991) Regulation of cardiac gene expression during myocardial growth and hypertrophy: molecular studies of an adaptive physiologic response. *FASEB J* 5(15):3037–3046.
  88. Ervasti JM (2003) Costameres: the Achilles' heel of Herculean muscle. *J Biol Chem* 278(16):13591–4.
  89. Peter AK, Cheng H, Ross RS, Knowlton KU, Chen J (2011) The costamere bridges sarcomeres to the sarcolemma in striated muscle. *Prog Pediatr Cardiol* 31(2):83–88.
  90. Rayment I, et al. (1993) Structure of the actin-myosin complex and its implications for muscle contraction. *Science* 261(5117):58–65.
  91. Holmes KC, Geeves MA (2000) The structural basis of muscle contraction. *Philos Trans R Soc Lond B Biol Sci* 355(1396):419–31.
  92. Au Y (2004) The muscle ultrastructure: a structural perspective of the sarcomere. *Cell Mol Life Sci* 61(24):3016–33.
  93. Spudich JA, Watt S (1971) The Regulation of Rabbit Skeletal Muscle Contraction. I. BIOCHEMICAL STUDIES OF THE INTERACTION OF THE TROPOMYOSIN-TROPONIN COMPLEX WITH ACTIN AND THE PROTEOLYTIC FRAGMENTS OF MYOSIN. *J Biol Chem* 246(15):4866–4871.



94. Hirsch NP (2007) Neuromuscular junction in health and disease. *Br J Anaesth* 99(1):132–8.
95. Irnagawaso T, Smitholi JS, Coronadolijj R, Campbellsii KP (1987) Purified Ryanodine Receptor from Skeletal Muscle ~ a r c o p l a s ~ i c Reticulum Is the Ca<sup>2+</sup> -permeable Pore of the Calcium Release Channel”. 16636–16643.
96. F. anthony Lai, Harold P. Erickson, Eric Rousseau, Qu-Yi Liu GM (1988) © 1988 Nature Publishing Group. *Nature* 331(28):315–.
97. Tanabe T, Takeshima H, Mikami a (1986) Primary structure of the receptor for calcium channel blockers from skeletal muscle. *Nature* 328:313–318.
98. Marsden CD, Meadows JC (1970) The effect of adrenaline on the contraction of human muscle. *J Physiol* 207(2):429–48.
99. Williams JH, Barnes WS (1989) The positive inotropic effect of epinephrine on skeletal muscle: a brief review. *Muscle Nerve* 12(12):968–75.
100. Schiaffino S, Reggiani C (2011) Fiber types in mammalian skeletal muscles. *Physiol Rev* 91(4):1447–531.
101. Peter JB, Barnard RJ, Edgerton VR, Gillespie CA, Stempel KE (1972) Metabolic profiles of three fiber types of skeletal muscle in guinea pigs and rabbits. *Biochemistry* 11(14):2627–2633.
102. Lin J, et al. (2002) Transcriptional co-activator PGC-1 alpha drives the formation of slow-twitch muscle fibres. *Nature* 418(6899):797–801.
103. Ng S, Wong C, Tsang S (2010) Differential gene expressions in atrial and ventricular myocytes: insights into the road of applying embryonic stem cell-derived cardiomyocytes for future. *Am J ...* (158):1234–1249.
104. Aronsen JM, Swift F, Sejersted OM (2013) Cardiac sodium transport and excitation-contraction coupling. *J Mol Cell Cardiol* 61:11–9.
105. Beuckelmann DJ, Wier WG (1988) Mechanism of release of calcium from sarcoplasmic reticulum of guinea-pig cardiac cells. *J Physiol* 405:233–255.

106. López-López JR, Shacklock PS, Balke CW, Wier WG (1995) Local calcium transients triggered by single L-type calcium channel currents in cardiac cells. *Science* 268(5213):1042–1045.
107. Lytton J, Westlin M, Hanley MR (1991) Thapsigargin inhibits the sarcoplasmic or endoplasmic reticulum Ca-ATPase family of calcium pumps. *J Biol Chem* 266(26):17067–17071.
108. Lytton J, Westlin M, Burk SE, Shull GE, MacLennan DH (1992) Functional comparisons between isoforms of the sarcoplasmic or endoplasmic reticulum family of calcium pumps. *J Biol Chem* 267(20):14483–14489.
109. Pollock R, Treisman R (1991) Human Srf-Related Proteins - Dna-Binding Properties and Potential Regulatory Targets. *Genes Dev* 5(12A):2327–2341.
110. Gossett LA, Kelvin DJ, Sternberg EA, Olson EN (1989) A New Myocyte-Specific Enhancer-Binding Factor that Recognizes a Conserved Element Associated with Multiple Muscle-Specific Genes. *Mol Cell Biol* 9(11):5022–5033.
111. L'honore A, et al. (2007) Identification of a new hybrid serum response factor and myocyte enhancer factor 2-binding element in MyoD enhancer required for MyoD expression during myogenesis. *Mol Biol Cell* 18(6):1992–2001.
112. Andres Vd, Cervera M, Mahdavi V (1995) Determination of the Consensus Binding-Site for Mef2 Expressed in Muscle and Brain Reveals Tissue-Specific Sequence Constraints. *J Biol Chem* 270(40):23246–23249.
113. Fickett JW (1996) Quantitative discrimination of MEF2 sites. *Mol Cell Biol* 16(1):437–41.
114. Naidu PS, Ludolph DC, To RQ, Hinterberger TJ, Konieczny SF (1995) Myogenin and MEF2 function synergistically to activate the MRF4 promoter during myogenesis. *Mol Cell Biol* 15(5):2707–18.
115. Clark RI, et al. (2013) MEF2 Is an In Vivo Immune-Metabolic Switch. *Cell* 155(2):435–447.
116. Yu YT, et al. (1992) Human Myocyte-Specific Enhancer Factor-Ii Comprises a Group of Tissue-Restricted Mads Box Transcription Factors. *Genes Dev* 6(9):1783–1798.

117. Edmondson DG, Cheng TC, Cserjesi P, Chakraborty T, Olson EN (1992) Analysis of the Myogenin Promoter Reveals an Indirect Pathway for Positive Autoregulation Mediated by the Muscle-Specific Enhancer Factor Mef-2. *Mol Cell Biol* 12(9):3665–3677.
118. Salminen M, et al. (1995) Myotube-specific activity of the human aldolase A M-promoter requires an overlapping binding site for NF1 and MEF2 factors in addition to a binding site (M1) for unknown proteins. *J Mol Biol* 253(1):17–31.
119. Chambers AE, et al. (1994) The RSRF/MEF2 protein SL1 regulates cardiac muscle-specific transcription of a myosin light-chain gene in *Xenopus* embryos. *Genes Dev* 8(11):1324–34.
120. Kuisk IR, Li H, Tran D, Capetanaki Y (1996) A single MEF2 site governs desmin transcription in both heart and skeletal muscle during mouse embryogenesis. *Dev Biol* 174(1):1–13.
121. Nakayama M, et al. (1996) Common core sequences are found in skeletal muscle slow- and fast-fiber-type-specific regulatory elements. *Mol Cell Biol* 16(5):2408–17.
122. Lilly B, et al. (1995) Requirement of MADS domain transcription factor D-MEF2 for muscle formation in *Drosophila*. *Science* 267(5198):688–93.
123. Lin Q, et al. (1998) Requirement of the MADS-box transcription factor MEF2C for vascular development. *Development* 125(22):4565–4574.
124. LYONS GE, MICALES BK, SCHWARZ J, MARTIN JF, OLSON EN (1995) Expression of Mef2 Genes in the Mouse Central-Nervous-System Suggests a Role in Neuronal Maturation. *J Neurosci* 15(8):5727–5738.
125. Youn HD, Sun L, Prywes R, Liu JO (1999) Apoptosis of T cells mediated by Ca<sup>2+</sup>-induced release of the transcription factor MEF2. *Science* (80- ) 286(5440):790–793.
126. Edmondson DG, Lyons GE, Martin JF, Olson EN (1994) Mef2 Gene-Expression Marks the Cardiac and Skeletal-Muscle Lineages during Mouse Embryogenesis. *Development* 120(5):1251–1263.
127. Lin X, Shah S, Bulleit RF (1996) The expression of MEF2 genes is implicated in CNS neuronal differentiation. *Mol Brain Res* 42(2):307–316.

128. Wilker PR, et al. (2008) Transcription factor Mef2c is required for B cell proliferation and survival after antigen receptor stimulation. *Nat Immunol* 9(6):603–612.
129. Arnold MA, et al. (2007) MEF2C transcription factor controls chondrocyte hypertrophy and bone development. *Dev Cell* 12(3):377–89.
130. Herglotz J, et al. (2015) Essential control of early B-cell development by Mef2 transcription factors. *Blood*. doi:10.1182/blood-2015-04-643270.
131. Molkenin JD, Black BL, Martin JF, Olson EN (1996) Mutational analysis of the DNA binding, dimerization, and transcriptional activation domains of MEF2C. *Mol Cell Biol* 16(6):2627–36.
132. Yu YT (1996) Distinct domains of myocyte enhancer binding factor-2A determining nuclear localization and cell type-specific transcriptional activity. *J Biol Chem* 271(40):24675–83.
133. Molkenin J, et al. (1996) MEF2B is a potent transactivator expressed in early myogenic lineages. *Mol Cell Biol* 16(7):3814–3824.
134. Naya FJ, et al. (2002) Mitochondrial deficiency and cardiac sudden death in mice lacking the MEF2A transcription factor. *Nat Med* 8(11):1303–1309.
135. Kim Y, et al. (2008) The MEF2D transcription factor mediates stress-dependent cardiac remodeling in mice. *J Clin Invest* 118(1):124–132.
136. Potthoff MJ, et al. (2007) Regulation of skeletal muscle sarcomere integrity and postnatal muscle function by Mef2c. *Mol Cell Biol* 27(23):8143–8151.
137. Hinits Y, Hughes SM (2007) Mef2s are required for thick filament formation in nascent muscle fibres. *Development* 134(13):2511–2519.
138. Ornatsky OI, Andreucci JJ, McDermott JC (1997) A dominant-negative form of transcription factor MEF2 inhibits myogenesis. *J Biol Chem* 272(52):33271–33278.
139. Snyder CM, et al. (2013) MEF2A regulates the Gtl2-Dio3 microRNA mega-cluster to modulate WNT signaling in skeletal muscle regeneration. *Development* 140(1):31–42.

140. Liu N, et al. (2014) Requirement of MEF2A, C, and D for skeletal muscle regeneration. *Proc Natl Acad Sci U S A* 111(11):4109–4114.
141. Calvo S, Venepally P, Cheng J, Buonanno A (1999) Fiber-type-specific transcription of the troponin I slow gene is regulated by multiple elements. *Mol Cell Biol* 19(1):515–25.
142. Shield MA, Haugen HS, Clegg CH, Hauschka SD (1996) E-box sites and a proximal regulatory region of the muscle creatine kinase gene differentially regulate expression in diverse skeletal muscles and cardiac muscle of transgenic mice. *Mol Cell Biol* 16(9):5058–5068.
143. Tai PW, et al. (2011) Differentiation and fiber type-specific activity of a muscle creatine kinase intronic enhancer. *Skelet Muscle* 1:25.
144. Wu H, et al. (2001) Activation of MEF2 by muscle activity is mediated through a calcineurin-dependent pathway. *EMBO J* 20(22):6414–23.
145. Potthoff MJ, et al. (2007) Histone deacetylase degradation and MEF2 activation promote the formation of slow-twitch myofibers. *J Clin Invest* 117(9):2459–2467.
146. Ornatsky OI, McDermott JC (1996) MEF2 protein expression, DNA binding specificity and complex composition, and transcriptional activity in muscle and non-muscle cells. *J Biol Chem* 271(40):24927–24933.
147. Du M, et al. (2008) Protein kinase a represses skeletal myogenesis by targeting myocyte enhancer factor 2D. *Mol Cell Biol* 28(9):2952–2970.
148. Sebastian S, et al. (2013) Tissue-specific splicing of a ubiquitously expressed transcription factor is essential for muscle differentiation. *Genes Dev* 27(11):1247–1259.
149. Molkenin JD, Black BL, Martin JF, Olson EN (1995) Cooperative activation of muscle gene expression by MEF2 and myogenic bHLH proteins. *Cell* 83(7):1125–1136.
150. Kaushal S, Schneider JW, Nadal-Ginard B, Mahdavi V (1994) Activation of the myogenic lineage by MEF2A, a factor that induces and cooperates with MyoD. *Science* 266(5188):1236–40.
151. Creemers EE, Sutherland LB, Oh J, Barbosa AC, Olson EN (2006) Coactivation of MEF2 by the SAP domain proteins myocardin and MASTR. *Mol Cell* 23(1):83–96.

152. Long X, Creemers EE, Wang D-Z, Olson EN, Miano JM (2007) Myocardin is a bifunctional switch for smooth versus skeletal muscle differentiation. *Proc Natl Acad Sci U S A* 104(42):16570–16575.
153. Mokalled MH, Johnson AN, Creemers EE, Olson EN (2012) MASTR directs MyoD-dependent satellite cell differentiation during skeletal muscle regeneration. *Genes Dev* 26(2):190–202.
154. Morin S, Charron F, Robitaille L, Nemer M (2000) GATA-dependent recruitment of MEF2 proteins to target promoters. *EMBO J* 19(9):2046–55.
155. Ghosh TK, et al. (2009) Physical interaction between TBX5 and MEF2C is required for early heart development. *Mol Cell Biol* 29(8):2205–18.
156. Bai XL, et al. (2015) Myocyte enhancer factor 2C regulation of hepatocellular carcinoma via vascular endothelial growth factor and Wnt/ $\beta$ -catenin signaling. *Oncogene* 34(31):4089–97.
157. Ehyai S, et al. (2015) A p38 MAPK regulated MEF2: $\beta$ -catenin interaction enhances canonical Wnt signalling. *Mol Cell Biol*:MCB.00832–15–.
158. Otto A, et al. (2008) Canonical Wnt signalling induces satellite-cell proliferation during adult skeletal muscle regeneration. *J Cell Sci* 121(Pt 17):2939–50.
159. Mirotsov M, et al. (2007) Secreted frizzled related protein 2 (Sfrp2) is the key Akt-mesenchymal stem cell-released paracrine factor mediating myocardial survival and repair. *Proc Natl Acad Sci U S A* 104(5):1643–8.
160. Wilson-Rawls J, Molkentin JD, Black BL, Olson EN (1999) Activated Notch Inhibits Myogenic Activity of the MADS-Box Transcription Factor Myocyte Enhancer Factor 2C. *Mol Cell Biol* 19(4):2853–2862.
161. Shen H, et al. (2006) The Notch coactivator, MAML1, functions as a novel coactivator for MEF2C-mediated transcription and is required for normal myogenesis. *Genes Dev* 20(6):675–88.
162. Yang CC, Ornatsky OI, McDermott JC, Cruz TF, Prody CA (1998) Interaction of myocyte enhancer factor 2 (MEF2) with a mitogen-activated protein kinase,

ERK5/BMK1. *Nucleic Acids Res* 26(20):4771–7.

163. Coyle-Thompson CA, Banerjee U (1993) The strawberry notch gene functions with Notch in common developmental pathways. *Development* 119(2):377–95.
164. Pallavi SK, Ho DM, Hicks C, Miele L, Artavanis-Tsakonas S (2012) Notch and Mef2 synergize to promote proliferation and metastasis through JNK signal activation in *Drosophila*. *EMBO J* 31(13):2895–2907.
165. Cusella-De Angelis MG, et al. (1994) Differential response of embryonic and fetal myoblasts to TGF beta: a possible regulatory mechanism of skeletal muscle histogenesis. *Development* 120(4):925–33.
166. Allen RE, Boxhorn LK (1987) Inhibition of skeletal muscle satellite cell differentiation by transforming growth factor-beta. *J Cell Physiol* 133(3):567–572.
167. Trendelenburg AU, et al. (2009) Myostatin reduces Akt/TORC1/p70S6K signaling, inhibiting myoblast differentiation and myotube size. *Am J Physiol Physiol* 296(6):C1258–C1270.
168. Sinha M, et al. (2014) Restoring systemic GDF11 levels reverses age-related dysfunction in mouse skeletal muscle. *Science* 344(6184):649–52.
169. Egerman MA, et al. (2015) GDF11 Increases with Age and Inhibits Skeletal Muscle Regeneration. *Cell Metab* 22(1):164–74.
170. Quinn ZA, Yang CC, Wrana JL, McDermott JC (2001) Smad proteins function as co-modulators for MEF2 transcriptional regulatory proteins. *Nucleic Acids Res* 29(3):732–42.
171. Liu D, Kang JS, Derynck R (2004) TGF-beta-activated Smad3 represses MEF2-dependent transcription in myogenic differentiation. *EMBO J* 23(7):1557–66.
172. Thomas JO, Kornberg RD (1975) An octamer of histones in chromatin and free in solution. *Proc Natl Acad Sci U S A* 72(7):2626–30.
173. Luger K, Mäder AW, Richmond RK, Sargent DF, Richmond TJ (1997) Crystal structure of the nucleosome core particle at 2.8 Å resolution. *Nature* 389(6648):251–60.

174. Whitlock JP, Simpson RT (1976) Removal of histone H1 exposes a fifty base pair DNA segment between nucleosomes. *Biochemistry* 15(15):3307–14.
175. Thoma F, Koller T (1977) Influence of histone H1 on chromatin structure. *Cell* 12(1):101–107.
176. McArthur M, Thomas JO (1996) A preference of histone H1 for methylated DNA. *EMBO J* 15(7):1705–14.
177. Levine A, Yeivin A, Ben-Asher E, Aloni Y, Razin A (1993) Histone H1-mediated inhibition of transcription initiation of methylated templates in vitro. *J Biol Chem* 268(29):21754–9.
178. Laurent BC, Treich I, Carlson M (1993) The yeast SNF2/SWI2 protein has DNA-stimulated ATPase activity required for transcriptional activation. *Genes Dev* 7(4):583–91.
179. Tsukiyama T, Wu C (1995) Purification and properties of an ATP-dependent nucleosome remodeling factor. *Cell* 83(6):1011–20.
180. Kuo MH, Zhou JX, Jambeck P, Churchill MEA, Allis CD (1998) Histone acetyltransferase activity of yeast Gcn5p is required for the activation of target genes in vivo. *Genes Dev* 12(5):627–639.
181. Kuo MH, et al. (1996) Transcription-linked acetylation by Gcn5p of histones H3 and H4 at specific lysines. *Nature* 383(6597):269–72.
182. Young MD, et al. (2011) ChIP-seq analysis reveals distinct H3K27me3 profiles that correlate with transcriptional activity. *Nucleic Acids Res* 39(17):7415–7427.
183. Santos-Rosa H, et al. (2002) Active genes are tri-methylated at K4 of histone H3. *Nature* 419(6905):407–11.
184. Nakayama J, Rice JC, Strahl BD, Allis CD, Grewal SI (2001) Role of histone H3 lysine 9 methylation in epigenetic control of heterochromatin assembly. *Science* 292(5514):110–3.
185. Lu JR, McKinsey TA, Zhang CL, Olson EN (2000) Regulation of skeletal myogenesis by association of the MEF2 transcription factor with class II histone deacetylases. *Mol Cell* 6(2):233–244.



186. Lu J, McKinsey TA, Nicol RL, Olson EN (2000) Signal-dependent activation of the MEF2 transcription factor by dissociation from histone deacetylases. *Proc Natl Acad Sci U S A* 97(8):4070–5.
187. Wang AH, et al. (2000) Regulation of histone deacetylase 4 by binding of 14-3-3 proteins. *Mol Cell Biol* 20(18):6904–12.
188. Grozinger CM, Schreiber SL (2000) Regulation of histone deacetylase 4 and 5 and transcriptional activity by 14-3-3-dependent cellular localization. *Proc Natl Acad Sci* 97(14):7835–7840.
189. McKinsey T, Zhang C, Lu J, Olson E (2000) Signal-dependent nuclear export of a histone deacetylase regulates muscle differentiation. *Nature* 408(6808):106–111.
190. Passier R, et al. (2000) CaM kinase signaling induces cardiac hypertrophy and activates the MEF2 transcription factor in vivo. *J Clin Invest* 105(10):1395–1406.
191. Zhang CL, et al. (2002) Class II histone deacetylases act as signal-responsive repressors of cardiac hypertrophy. *Cell* 110(4):479–488.
192. Haberland M, et al. (2007) Regulation of HDAC9 gene expression by MEF2 establishes a negative-feedback loop in the transcriptional circuitry of muscle differentiation. *Mol Cell Biol* 27(2):518–525.
193. Sparrow DB, et al. (1999) MEF-2 function is modified by a novel co-repressor, MITR. *Embo J* 18(18):5085–5098.
194. Backs J, et al. (2011) Selective repression of MEF2 activity by PKA-dependent proteolysis of HDAC4. *J Cell Biol* 195(3):403–415.
195. Eckner R, Yao TP, Oldread E, Livingston DM (1996) Interaction and functional collaboration of p300/CBP and bHLH proteins in muscle and B-cell differentiation. *Genes Dev* 10(19):2478–2490.
196. Yuan W, Condorelli G, Caruso M, Felsani A, Giordano A (1996) Human p300 protein is a coactivator for the transcription factor MyoD. *J Biol Chem* 271(15):9009–9013.

197. Sartorelli V, Huang J, Hamamori Y, Kedes L (1997) Molecular mechanisms of myogenic coactivation by p300: Direct interaction with the activation domain of MyoD and with the MADS box of MEF2C. *Mol Cell Biol* 17(2):1010–1026.
198. Zhuang Q, et al. (2013) Class IIa Histone Deacetylases and Myocyte Enhancer Factor 2 Proteins Regulate the Mesenchymal-to-Epithelial Transition of Somatic Cell Reprogramming. *J Biol Chem* 288(17):12022–12031.
199. Hagiwara H, et al. (2011) Histone deacetylase inhibitor trichostatin A enhances myogenesis by coordinating muscle regulatory factors and myogenic repressors. *Biochem Biophys Res Commun* 414(4):826–31.
200. Jayathilaka N, et al. (2012) Inhibition of the function of class IIa HDACs by blocking their interaction with MEF2. *Nucleic Acids Res* 40(12):5378–88.
201. Choi M-C, et al. (2014) HDAC4 promotes Pax7-dependent satellite cell activation and muscle regeneration. *EMBO Rep* 15(11):1175–1183.
202. Asp P, et al. (2011) Genome-wide remodeling of the epigenetic landscape during myogenic differentiation. *Proc Natl Acad Sci U S A* 108(22):E149–E158.
203. Zhang CL, McKinsey TA, Olson EN (2002) Association of class II histone deacetylases with heterochromatin protein 1: Potential role for histone methylation in control of muscle differentiation. *Mol Cell Biol* 22(20):7302–7312.
204. Rampalli S, et al. (2007) p38 MAPK signaling regulates recruitment of Ash2L-containing methyltransferase complexes to specific genes during differentiation. *Nat Struct Mol Biol* 14(12):1150–1156.
205. Simone C, et al. (2004) p38 pathway targets SWI-SNF chromatin-remodeling complex to muscle-specific loci. *Nat Genet* 36(7):738–743.
206. Ohkawa Y, Marfella CGA, Imbalzano AN (2006) Skeletal muscle specification by myogenin and Mef2D via the SWI/SNF ATPase Brg1. *Embo J* 25(3):490–501.
207. Diao Y, et al. (2012) Pax3/7BP Is a Pax7- and Pax3-Binding Protein that Regulates the Proliferation of Muscle Precursor Cells by an Epigenetic Mechanism. *Cell Stem Cell* 11(2):231–241.

208. Kawabe Y, Wang YX, McKinnell IW, Bedford MT, Rudnicki MA (2012) *Carm1* Regulates Pax7 Transcriptional Activity through MLL1/2 Recruitment during Asymmetric Satellite Stem Cell Divisions. *Cell Stem Cell* 11(3):333–345.
209. Tao Y, et al. (2011) The histone methyltransferase Set7/9 promotes myoblast differentiation and myofibril assembly. *J Cell Biol* 194(4):551–565.
210. Seenundun S, et al. (2010) UTX mediates demethylation of H3K27me3 at muscle-specific genes during myogenesis. *EMBO J* 29(8):1401–11.
211. Shi Y, et al. (2004) Histone demethylation mediated by the nuclear amine oxidase homolog LSD1. *Cell* 119(7):941–53.
212. Choi J, et al. (2010) Histone demethylase LSD1 is required to induce skeletal muscle differentiation by regulating myogenic factors. *Biochem Biophys Res Commun* 401(3):327–332.
213. Sandmann T, et al. (2006) A temporal map of transcription factor activity: Mef2 directly regulates at all stages of muscle target genes development. *Dev Cell* 10(6):797–807.
214. Blais A, et al. (2005) An initial blueprint for myogenic differentiation. *Genes Dev* 19(5):553–569.
215. Paris J (2004) Identification of MEF2-regulated genes during muscle differentiation. *Physiol Genomics* 20(1):143–151.
216. Cao Y, et al. (2010) Genome-wide MyoD Binding in Skeletal Muscle Cells: A Potential for Broad Cellular Reprogramming. *Dev Cell* 18(4):662–674.
217. Han J, Jiang Y, Li Z, Kravchenko V V, Ulevitch RJ (1997) Activation of the transcription factor MEF2C by the MAP kinase p38 in inflammation. *Nature* 386(6622):296–299.
218. Ornatsky OI, et al. (1999) Post-translational control of the MEF2A transcriptional regulatory protein. *Nucleic Acids Res* 27(13):2646–2654.
219. Kato Y, et al. (1997) BMK1/ERK5 regulates serum-induced early gene expression through transcription factor MEF2C. *Embo J* 16(23):7054–7066.

220. de la Vega L, Hornung J, Kremmer E, Milanovic M, Schmitz ML (2013) Homeodomain-interacting protein kinase 2-dependent repression of myogenic differentiation is relieved by its caspase-mediated cleavage. *Nucleic Acids Res* 41(11):5731–5745.
221. Al Madhoun AS, et al. (2011) Skeletal myosin light chain kinase regulates skeletal myogenesis by phosphorylation of MEF2C. *Embo J* 30(12):2477–2489.
222. Satoh K, et al. (2007) Nemo-like kinase-myocyte enhancer factor 2A signaling regulates anterior formation in xenopus development. *Mol Cell Biol* 27(21):7623–7630.
223. Perry RLS, et al. (2009) Direct Interaction between Myocyte Enhancer Factor 2 (MEF2) and Protein Phosphatase 1 alpha Represses MEF2-Dependent Gene Expression. *Mol Cell Biol* 29(12):3355–3366.
224. Zhao M, et al. (1999) Regulation of the MEF2 family of transcription factors by p38. *Mol Cell Biol* 19(1):21–30.
225. Wales S, Hashemi S, Blais A, McDermott JC (2015) Global MEF2 target gene analysis in cardiac and skeletal muscle reveals novel regulation of DUSP6 by p38MAPK-MEF2 signaling. *Nucleic Acids Res* 42(18):11349–11362.
226. Zetser A, Gredinger E, Bengal E (1999) p38 Mitogen-activated Protein Kinase Pathway Promotes Skeletal Muscle Differentiation: PARTICIPATION OF THE MEF2C TRANSCRIPTION FACTOR. *J Biol Chem* 274(8):5193–5200.
227. de Angelis L, et al. (2005) Regulation of vertebrate myotome development by the p38 MAP kinase-MEF2 signaling pathway. *Dev Biol* 283(1):171–9.
228. Kolodziejczyk SM, et al. (1999) MEF2 is upregulated during cardiac hypertrophy and is required for normal post-natal growth of the myocardium. *Curr Biol* 9(20):1203–1206.
229. Dadson K, et al. (2015) Adiponectin is required for cardiac MEF2 activation during pressure overload induced hypertrophy. *J Mol Cell Cardiol* 86:102–9.
230. Gordon JW, et al. (2009) Protein Kinase A-regulated Assembly of a MEF2.HDAC4 Repressor Complex Controls c-Jun Expression in Vascular Smooth Muscle Cells. *J Biol Chem* 284(28):19027–19042.
231. Salma J, McDermott JC (2012) Suppression of a MEF2-KLF6 Survival Pathway by PKA

- Signaling Promotes Apoptosis in Embryonic Hippocampal Neurons. *J Neurosci* 32(8):2790–2803.
232. Hashemi S, Salma J, Wales S, McDermott J (2015) Pro-survival function of MEF2 in cardiomyocytes is enhanced by  $\beta$ -blockers. *Cell Death Discov* 1:15019.
233. Callis TE, Chen J-F, Wan D-Z (2007) MicroRNAs in skeletal and cardiac muscle development. *DNA Cell Biol* 26(4):219–225.
234. Liu N, et al. (2007) An intragenic MEF2-dependent enhancer directs muscle-specific expression of microRNAs 1 and 133. *Proc Natl Acad Sci U S A* 104(52):20844–20849.
235. Kim HK, Lee YS, Sivaprasad U, Malhotra A, Dutta A (2006) Muscle-specific microRNA miR-206 promotes muscle differentiation. *J Cell Biol* 174(5):677–687.
236. Dey BK, Gagan J, Dutta A (2011) miR-206 and -486 Induce Myoblast Differentiation by Downregulating Pax7. *Mol Cell Biol* 31(1):203–214.
237. Williams AH, et al. (2009) MicroRNA-206 Delays ALS Progression and Promotes Regeneration of Neuromuscular Synapses in Mice. *Science* (80- ) 326(5959):1549–1554.
238. Gagan J, Dey BK, Layer R, Yan Z, Dutta A (2012) Notch3 and Mef2c Proteins Are Mutually Antagonistic via Mkp1 Protein and miR-1/206 MicroRNAs in Differentiating Myoblasts. *J Biol Chem* 287(48):40360–40370.
239. Kondoh K, Sunadome K, Nishida E (2007) Notch signaling suppresses p38 MAPK activity via induction of MKP-1 in myogenesis. *J Biol Chem* 282(5):3058–3065.
240. Cesana M, et al. (2011) A long noncoding RNA controls muscle differentiation by functioning as a competing endogenous RNA. *Cell* 147(2):358–69.
241. Bryant NJ, Govers R, James DE (2002) Regulated transport of the glucose transporter GLUT4. *Nat Rev Mol Cell Biol* 3(4):267–277.
242. Ren JM, Semenkovich CF, Gulve EA, Gao J, Holloszy JO (1994) Exercise induces rapid increases in GLUT4 expression, glucose transport capacity, and insulin-stimulated glycogen storage in muscle. *J Biol Chem* 269(20):14396–401.

243. Tsao TS, Burcelin R, Katz EB, Huang L, Charron MJ (1996) Enhanced insulin action due to targeted GLUT4 overexpression exclusively in muscle. *Diabetes* 45(1):28–36.
244. DeFronzo RA, Bonadonna RC, Ferrannini E (1992) Pathogenesis of NIDDM. A balanced overview. *Diabetes Care* 15(3):318–68.
245. Garvey WT, et al. (1998) Evidence for defects in the trafficking and translocation of GLUT4 glucose transporters in skeletal muscle as a cause of human insulin resistance. *J Clin Invest* 101(11):2377–86.
246. Garvey WT, Maianu L, Hancock JA, Golichowski AM, Baron A (1992) Gene expression of GLUT4 in skeletal muscle from insulin-resistant patients with obesity, IGT, GDM, and NIDDM. *Diabetes* 41(4):465–75.
247. Hales CN, Barker DJP (1992) Type 2 (non-insulin-dependent) diabetes mellitus: the thrifty phenotype hypothesis. *Diabetologia* 35(7):595–601.
248. Phillips DI, Barker DJ, Hales CN, Hirst S, Osmond C (1994) Thinness at birth and insulin resistance in adult life. *Diabetologia* 37(2):150–4.
249. Martin-Gronert MS, Ozanne SE (2007) Experimental IUGR and later diabetes. *J Intern Med* 261(5):437–452.
250. Thai M V, Guruswamy S, Cao KT, Pessin JE, Olson AL (1998) Myocyte enhancer factor 2 (MEF2)-binding site is required for GLUT4 gene expression in transgenic mice. Regulation of MEF2 DNA binding activity in insulin-deficient diabetes. *J Biol Chem* 273(23):14285–92.
251. Liu ML, Olson AL, Edgington NP, Moye-Rowley WS, Pessin JE (1994) Myocyte enhancer factor 2 (MEF2) binding site is essential for C2C12 myotube-specific expression of the rat GLUT4/muscle-adipose facilitative glucose transporter gene. *J Biol Chem* 269(45):28514–21.
252. Mora S (2000) The MEF2A Isoform Is Required for Striated Muscle-specific Expression of the Insulin-responsive GLUT4 Glucose Transporter. *J Biol Chem* 275(21):16323–16328.
253. Knight JB, Eyster CA, Griesel BA, Olson AL (2003) Regulation of the human GLUT4 gene promoter: interaction between a transcriptional activator and myocyte enhancer

- factor 2A. *Proc Natl Acad Sci U S A* 100(25):14725–30.
254. Santalucía T, et al. (2001) A novel functional co-operation between MyoD, MEF2 and TR $\alpha$ 1 is sufficient for the induction of GLUT4 gene transcription. *J Mol Biol* 314(2):195–204.
  255. Zheng S, Rollet M, Pan Y-X (2012) Protein restriction during gestation alters histone modifications at the glucose transporter 4 (GLUT4) promoter region and induces GLUT4 expression in skeletal muscle of female rat offspring. *J Nutr Biochem* 23(9):1064–1071.
  256. Thamotharan M, et al. (2005) GLUT4 expression and subcellular localization in the intrauterine growth-restricted adult rat female offspring. *Am J Physiol Endocrinol Metab* 288(5):E935–47.
  257. Raychaudhuri N, Raychaudhuri S, Thamotharan M, Devaskar SU (2008) Histone Code Modifications Repress Glucose Transporter 4 Expression in the Intrauterine Growth-restricted Offspring. *J Biol Chem* 283(20):13611–13626.
  258. McGee SL, Hargreaves M (2004) Exercise and myocyte enhancer factor 2 regulation in human skeletal muscle. *Diabetes* 53(5):1208–14.
  259. McGee SL (2005) Exercise increases MEF2- and GEF DNA-binding activities in human skeletal muscle. *FASEB J* 20(2):348–9.
  260. Wu H, et al. (2002) Regulation of mitochondrial biogenesis in skeletal muscle by CaMK. *Science* 296(5566):349–52.
  261. Czubryt MP, McAnally J, Fishman GI, Olson EN (2003) Regulation of peroxisome proliferator-activated receptor gamma coactivator 1 alpha (PGC-1 alpha ) and mitochondrial function by MEF2 and HDAC5. *Proc Natl Acad Sci U S A* 100(4):1711–6.
  262. Mootha VK, et al. (2003) PGC-1alpha-responsive genes involved in oxidative phosphorylation are coordinately downregulated in human diabetes. *Nat Genet* 34(3):267–73.
  263. Michael LF, et al. (2001) Restoration of insulin-sensitive glucose transporter (GLUT4) gene expression in muscle cells by the transcriptional coactivator PGC-1. *Proc Natl Acad Sci U S A* 98(7):3820–5.

264. Lecker SH, et al. (2004) Multiple types of skeletal muscle atrophy involve a common program of changes in gene expression. *FASEB J* 18(1):39–51.
265. Demand J, Alberti S, Patterson C, Höhfeld J (2001) Cooperation of a ubiquitin domain protein and an E3 ubiquitin ligase during chaperone/proteasome coupling. *Curr Biol* 11(20):1569–77.
266. Ballinger CA, et al. (1999) Identification of CHIP, a novel tetratricopeptide repeat-containing protein that interacts with heat shock proteins and negatively regulates chaperone functions. *Mol Cell Biol* 19(6):4535–45.
267. Zhang C, Xu Z, He X-R, Michael LH, Patterson C (2005) CHIP, a cochaperone/ubiquitin ligase that regulates protein quality control, is required for maximal cardioprotection after myocardial infarction in mice. *Am J Physiol Heart Circ Physiol* 288(6):H2836–42.
268. Bodine SC, et al. (2001) Identification of ubiquitin ligases required for skeletal muscle atrophy. *Science* 294(5547):1704–8.
269. Mearini G, et al. (2009) Atrogin-1 and MuRF1 regulate cardiac MyBP-C levels via different mechanisms. *Cardiovasc Res* 85(2):357–366.
270. Clarke BA, et al. (2007) The E3 ligase MuRF1 degrades myosin heavy chain protein in dexamethasone-treated skeletal muscle. *Cell Metab* 6(5):376–385.
271. Cohen S, et al. (2009) During muscle atrophy, thick, but not thin, filament components are degraded by MuRF1-dependent ubiquitylation. *J Cell Biol* 185(6):1083–1095.
272. Lagirand-Cantaloube J, et al. (2008) The initiation factor eIF3-f is a major target for Atrogin1/MAFbx function in skeletal muscle atrophy. *EMBO J* 27(8):1266–1276.
273. Lagirand-Cantaloube J, et al. (2009) Inhibition of Atrogin-1/MAFbx Mediated MyoD Proteolysis Prevents Skeletal Muscle Atrophy In Vivo. *PLoS One* 4(3):e4973.
274. Kabeya Y, et al. (2000) LC3, a mammalian homologue of yeast Apg8p, is localized in autophagosome membranes after processing. *EMBO J* 19(21):5720–8.
275. Tanida I, Ueno T, Kominami E (2004) LC3 conjugation system in mammalian autophagy. *Int J Biochem Cell Biol* 36(12):2503–18.



276. Pankiv S, et al. (2007) p62/SQSTM1 binds directly to Atg8/LC3 to facilitate degradation of ubiquitinated protein aggregates by autophagy. *J Biol Chem* 282(33):24131–45.
277. Kim I, Rodriguez-Enriquez S, Lemasters JJ (2007) Selective degradation of mitochondria by mitophagy. *Arch Biochem Biophys* 462(2):245–53.
278. Chiang HL, Terlecky SR, Plant CP, Dice JF (1989) A role for a 70-kilodalton heat shock protein in lysosomal degradation of intracellular proteins. *Science* 246(4928):382–5.
279. Kaushik S, Cuervo AM (2012) Chaperone-mediated autophagy: a unique way to enter the lysosome world. *Trends Cell Biol* 22(8):407–17.
280. Cuervo AM, Dice JF (1996) A receptor for the selective uptake and degradation of proteins by lysosomes. *Science* 273(5274):501–3.
281. Gamerding M, et al. (2009) Protein quality control during aging involves recruitment of the macroautophagy pathway by BAG3. *EMBO J* 28(7):889–901.
282. Arndt V, et al. (2010) Chaperone-Assisted Selective Autophagy Is Essential for Muscle Maintenance. *Curr Biol* 20(2):143–148.
283. Gamerding M, Kaya AM, Wolfrum U, Clement AM, Behl C (2011) BAG3 mediates chaperone-based aggresome-targeting and selective autophagy of misfolded proteins. *EMBO Rep* 12(2):149–56.
284. Mammucari C, et al. (2007) FoxO3 controls autophagy in skeletal muscle in vivo. *Cell Metab* 6(6):458–71.
285. Zhao J, et al. (2007) FoxO3 Coordinately Activates Protein Degradation by the Autophagic/Lysosomal and Proteasomal Pathways in Atrophying Muscle Cells. *Cell Metab* 6(6):472–483.
286. Sandri M, et al. (2006) PGC-1alpha protects skeletal muscle from atrophy by suppressing FoxO3 action and atrophy-specific gene transcription. *Proc Natl Acad Sci U S A* 103(44):16260–5.
287. Raffaello A, et al. (2010) JunB transcription factor maintains skeletal muscle mass and promotes hypertrophy. *J Cell Biol* 191(1):101–13.

288. Bentzinger CF, Wang YX, Dumont NA, Rudnicki MA (2013) Cellular dynamics in the muscle satellite cell niche. *EMBO Rep* 14(12):1062–72.
289. Briggs D, Morgan JE (2013) Recent progress in satellite cell/myoblast engraftment -- relevance for therapy. *FEBS J* 280(17):4281–93.
290. Day K, Shefer G, Shearer A, Yablonka-Reuveni Z (2010) The depletion of skeletal muscle satellite cells with age is concomitant with reduced capacity of single progenitors to produce reserve progeny. *Dev Biol* 340(2):330–43.
291. Lambert JC, et al. (2013) Meta-analysis of 74,046 individuals identifies 11 new susceptibility loci for Alzheimer's disease. *Nat Genet* 45(12):1452–8.
292. Le Meur N, et al. (2010) MEF2C haploinsufficiency caused by either microdeletion of the 5q14.3 region or mutation is responsible for severe mental retardation with stereotypic movements, epilepsy and/or cerebral malformations. *J Med Genet* 47(1):22–9.
293. Mao ZX, Bonni A, Xia F, Nadal-Vicens M, Greenberg ME (1999) Neuronal activity-dependent cell survival mediated by transcription factor MEF2. *Science (80- )* 286(5440):785–790.
294. Zheng H-F, et al. (2013) Meta-analysis of genome-wide studies identifies MEF2C SNPs associated with bone mineral density at forearm. *J Med Genet* 50(7):473–8.
295. Shum AMY, et al. (2012) Disruption of MEF2C signaling and loss of sarcomeric and mitochondrial integrity in cancer-induced skeletal muscle wasting. *Aging (Albany NY)* 4(2):133–43.
296. Konno T, et al. (2010) Heterogeneous myocyte enhancer factor-2 (Mef2) activation in myocytes predicts focal scarring in hypertrophic cardiomyopathy. *Proc Natl Acad Sci U S A* 107(42):18097–102.
297. Ewen EP, Snyder CM, Wilson M, Desjardins D, Naya FJ (2011) The Mef2A Transcription Factor Coordinately Regulates a Costamere Gene Program in Cardiac Muscle. *J Biol Chem* 286(34):29644–29653.
298. Potthoff MJ, et al. (2007) Regulation of skeletal muscle sarcomere integrity and postnatal muscle function by Mef2c. *Mol Cell Biol* 27(23):8143–8151.

299. Gao C, et al. (2015) RBFox1-mediated RNA splicing regulates cardiac hypertrophy and heart failure. *J Clin Invest*. doi:10.1172/JCI84015.
300. Bachinski LL, et al. (2010) Altered MEF2 isoforms in myotonic dystrophy and other neuromuscular disorders. *Muscle Nerve* 42(6):856–63.
301. Yuen M, et al. (2014) Leiomodlin-3 dysfunction results in thin filament disorganization and nemaline myopathy. *J Clin Invest* 124(11):4693–4708.
302. Cenik BK, et al. (2015) Severe myopathy in mice lacking the MEF2/SRF-dependent gene leiomodlin-3. *J Clin Invest* 125(4):1569–78.
303. Ahn AH, Kunkel LM (1993) The structural and functional diversity of dystrophin. *Nat Genet* 3(4):283–91.
304. Goldstein JA, McNally EM (2010) Mechanisms of muscle weakness in muscular dystrophy. *J Gen Physiol* 136(1):29–34.
305. Gussoni E, et al. (1992) Normal dystrophin transcripts detected in Duchenne muscular dystrophy patients after myoblast transplantation. *Nature* 356(6368):435–8.
306. Filareto A, et al. (2013) An ex vivo gene therapy approach to treat muscular dystrophy using inducible pluripotent stem cells. *Nat Commun* 4:1549.
307. Acharyya S, et al. (2005) Dystrophin glycoprotein complex dysfunction: a regulatory link between muscular dystrophy and cancer cachexia. *Cancer Cell* 8(5):421–32.
308. Long C, et al. (2014) Prevention of muscular dystrophy in mice by CRISPR/Cas9-mediated editing of germline DNA. *Science* 752429(August):1–34.
309. Long C, et al. (2015) Postnatal genome editing partially restores dystrophin expression in a mouse model of muscular dystrophy. *Science*:science.aad5725–.
310. Tabebordbar M, et al. (2015) In vivo gene editing in dystrophic mouse muscle and muscle stem cells. *Science*:science.aad5177–.
311. Angus LM, et al. (2005) Calcineurin-NFAT signaling, together with GABP and peroxisome PGC-1{alpha}, drives utrophin gene expression at the neuromuscular

- junction. *Am J Physiol Cell Physiol* 289(4):C908–17.
312. Handschin C, et al. (2007) PGC-1 regulates the neuromuscular junction program and ameliorates Duchenne muscular dystrophy. *Genes Dev* 21(7):770–783.
  313. Kalsotra A, et al. (2014) The Mef2 transcription network is disrupted in myotonic dystrophy heart tissue, dramatically altering miRNA and mRNA expression. *Cell Rep* 6(2):336–45.
  314. Wu H, Olson EN (2002) Activation of the MEF2 transcription factor in skeletal muscles from myotonic mice. *J Clin Invest* 109(10):1327–33.
  315. Garg A, et al. (2014) KLHL40 deficiency destabilizes thin filament proteins and promotes nemaline myopathy. *J Clin Invest* 124(8):3529–3539.
  316. Chereau D, et al. (2008) Leiomodins are actin filament nucleators in muscle cells. *Science* 320(5873):239–43.
  317. Nanda V, Miano JM (2012) Leiomodins are novel serum response factor-dependent target genes expressed preferentially in differentiated smooth muscle cells. *J Biol Chem* 287(4):2459–2467.
  318. Cenik BK, et al. (2015) Severe myopathy in mice lacking the MEF2/SRF-dependent gene leiomodins. *J Clin Invest* 125(4):1569–1578.
  319. Estrella NL, Clark AL, Desjardins CA, Nocco SE, Naya FJ (2015) MEF2D deficiency in neonatal cardiomyocytes triggers cell cycle re-entry and programmed cell death in vitro. *J Biol Chem* 290(40):24367–24380.
  320. Woronicz JD, et al. (1995) Regulation of the Nur77 orphan steroid-receptor in activation-induced apoptosis. *Mol Cell Biol* 15(11):6364–6376.
  321. Yang Q, et al. (2009) Regulation of neuronal survival factor MEF2D by chaperone-mediated autophagy. *Science* 323(5910):124–7.
  322. Zhang L, et al. (2014) Disruption of chaperone-mediated autophagy-dependent degradation of MEF2A by oxidative stress-induced lysosome destabilization. *Autophagy* 10(6):1015–35.

323. Rourke BC, Yokoyama Y, Milsom WK, Caiozzo VJ Myosin isoform expression and MAFbx mRNA levels in hibernating golden-mantled ground squirrels (*Spermophilus lateralis*). *Physiol Biochem Zool* 77(4):582–93.
324. Rourke BC, Cotton CJ, Harlow HJ, Caiozzo VJ (2006) Maintenance of slow type I myosin protein and mRNA expression in overwintering prairie dogs (*Cynomys leucurus* and *ludovicianus*) and black bears (*Ursus americanus*). *J Comp Physiol B* 176(7):709–20.
325. Tessier SN, Storey KB (2010) Expression of myocyte enhancer factor-2 and downstream genes in ground squirrel skeletal muscle during hibernation. *Mol Cell Biochem* 344(1-2):151–62.
326. Kamei Y, et al. (2004) Skeletal muscle FOXO1 (FKHR) transgenic mice have less skeletal muscle mass, down-regulated Type I (slow twitch/red muscle) fiber genes, and impaired glycemic control. *J Biol Chem* 279(39):41114–23.
327. Yamakuchi M, et al. (2000) Type I muscle atrophy caused by microgravity-induced decrease of myocyte enhancer factor 2C (MEF2C) protein expression. *FEBS Lett* 477(1-2):135–40.
328. Baskin KK, Taegtmeyer H (2011) AMP-activated protein kinase regulates E3 ligases in rodent heart. *Circ Res* 109(10):1153–61.
329. Forbes SJ, Rosenthal N (2014) Preparing the ground for tissue regeneration: from mechanism to therapy. *Nat Med* 20(8):857–69.
330. Wallace GQ, McNally EM (2009) Mechanisms of muscle degeneration, regeneration, and repair in the muscular dystrophies. *Annu Rev Physiol* 71:37–57.
331. van Hall G (2012) Cytokines: muscle protein and amino acid metabolism. *Curr Opin Clin Nutr Metab Care* 15(1):85–91.
332. Li Y-P, et al. (2005) TNF- $\alpha$  acts via p38 MAPK to stimulate expression of the ubiquitin ligase atrogin1/MAFbx in skeletal muscle. *FASEB J* 19(3):362–70.
333. Palacios D, et al. (2010) TNF/p38  $\alpha$ /Polycomb Signaling to Pax7 Locus in Satellite Cells Links Inflammation to the Epigenetic Control of Muscle Regeneration. *Cell Stem Cell* 7(4):455–469.

334. Chesley A, et al. (2000) The beta(2)-adrenergic receptor delivers an antiapoptotic signal to cardiac myocytes through G(i)-dependent coupling to phosphatidylinositol 3'-kinase. *Circ Res* 87(12):1172–9.
335. Nikolaev VO, et al. (2010) Beta2-adrenergic receptor redistribution in heart failure changes cAMP compartmentation. *Science* 327(5973):1653–7.
336. Lehman JJ, Kelly DP (2002) Transcriptional activation of energy metabolic switches in the developing and hypertrophied heart. *Clin Exp Pharmacol Physiol* 29(4):339–45.
337. Antos CL, et al. (2001) Dilated Cardiomyopathy and Sudden Death Resulting From Constitutive Activation of Protein Kinase A. *Circ Res* 89(11):997–1004.
338. Ha CH, et al. (2010) PKA phosphorylates histone deacetylase 5 and prevents its nuclear export, leading to the inhibition of gene transcription and cardiomyocyte hypertrophy. *Proc Natl Acad Sci U S A* 107(35):15467–72.
339. Castaldi A, et al. (2014) MicroRNA-133 modulates the  $\beta$ 1-adrenergic receptor transduction cascade. *Circ Res* 115(2):273–83.
340. Chang S, et al. (2004) Histone deacetylases 5 and 9 govern responsiveness of the heart to a subset of stress signals and play redundant roles in heart development. *Mol Cell Biol* 24(19):8467–76.
341. Passier R, et al. (2000) CaM kinase signaling induces cardiac hypertrophy and activates the MEF2 transcription factor in vivo. *J Clin Invest* 105(10):1395–1406.
342. Zhang T, et al. (2003) The deltaC isoform of CaMKII is activated in cardiac hypertrophy and induces dilated cardiomyopathy and heart failure. *Circ Res* 92(8):912–9.
343. Zhang R, et al. (2005) Calmodulin kinase II inhibition protects against structural heart disease. *Nat Med* 11(43):409–417.
344. Backs J, Song K, Bezprozvannaya S, Chang S, Olson EN (2006) CaM kinase II selectively signals to histone deacetylase 4 during cardiomyocyte hypertrophy. *J Clin Invest* 116(7):1853–64.
345. el Azzouzi H, et al. (2010) MEF2 transcriptional activity maintains mitochondrial adaptation in cardiac pressure overload. *Eur J Heart Fail* 12(1):4–12.

346. Ieda M, et al. (2010) Direct Reprogramming of Fibroblasts into Functional Cardiomyocytes by Defined Factors. *Cell* 142(3):375–386.
347. Inagawa K, et al. (2012) Induction of Cardiomyocyte-Like Cells in Infarct Hearts by Gene Transfer of Gata4, Mef2c, and Tbx5. *Circ Res* 111(9):1147–1156.
348. Miska EA, et al. (1999) HDAC4 deacetylase associates with and represses the MEF2 transcription factor. *Embo J* 18(18):5099–5107.
349. Naya FJ, Wu CZ, Richardson JA, Overbeek P, Olson EN (1999) Transcriptional activity of MEF2 during mouse embryogenesis monitored with a MEF2-dependent transgene. *Development* 126(10):2045–2052.
350. Vega RB, et al. (2004) Protein kinases C and D mediate agonist-dependent cardiac hypertrophy through nuclear export of histone deacetylase 5. *Mol Cell Biol* 24(19):8374–8385.
351. Sartorelli V, Kurabayashi M, Kedes L (1993) Muscle-Specific Gene-Expression - a Comparison of Cardiac and Skeletal-Muscle Transcription Strategies. *Circ Res* 72(5):925–931.
352. Schlesinger J, et al. (2011) The Cardiac Transcription Network Modulated by Gata4, Mef2a, Nkx2.5, Srf, Histone Modifications, and MicroRNAs. *Plos Genet* 7(2):e1001313–e1001313.
353. Wilker PR, et al. (2008) Transcription factor Mef2c is required for B cell proliferation and survival after antigen receptor stimulation. *Nat Immunol* 9(6):603–12.
354. Rhee HS, Pugh BF (2011) Comprehensive Genome-wide Protein-DNA Interactions Detected at Single-Nucleotide Resolution. *Cell* 147(6):1408–1419.
355. Ekerot M, et al. (2008) Negative-feedback regulation of FGF signalling by DUSP6/MKP-3 is driven by ERK1/2 and mediated by Ets factor binding to a conserved site within the DUSP6/MKP-3 gene promoter. *Biochem J* 412:287–298.
356. Dionyssiou MG, et al. (2013) Kruppel-like factor 6 (KLF6) promotes cell proliferation in skeletal myoblasts in response to TGFbeta/Smad3 signaling. *Skelet Muscle* 3(1):7.

357. Zhang Y, et al. (2008) Model-based Analysis of ChIP-Seq (MACS). *Genome Biol* 9(9):R137–R137.
358. Kent WJ, et al. (2002) The human genome browser at UCSC. *Genome Res* 12(6):996–1006.
359. McLean CY, et al. (2010) GREAT improves functional interpretation of cis-regulatory regions. *Nat Biotechnol* 28(5):495–501.
360. Zhang Z, Chang CW, Goh WL, Sung W-K, Cheung E (2011) CENTDIST: discovery of co-associated factors by motif distribution. *Nucleic Acids Res* 39:W391–W399.
361. Boyle EI, et al. (2004) GO::TermFinder - open source software for accessing Gene Ontology information and finding significantly enriched Gene Ontology terms associated with a list of genes. *Bioinformatics* 20(18):3710–3715.
362. Robinson JT, et al. (2011) Integrative genomics viewer. *Nat Biotechnol* 29(1):24–26.
363. Maillet M, et al. (2008) DUSP6 (MKP3) Null Mice Show Enhanced ERK1/2 Phosphorylation at Baseline and Increased Myocyte Proliferation in the Heart Affecting Disease Susceptibility. *J Biol Chem* 283(45):31246–31255.
364. Le Grand F, et al. (2012) Six1 regulates stem cell repair potential and self-renewal during skeletal muscle regeneration. *J Cell Biol* 198(5):815–832.
365. Groom LA, Sneddon AA, Alessi DR, Dowd S, Keyse SM (1996) Differential regulation of the MAP, SAP and RK/p38 kinases by Pyst1, a novel cytosolic dual-specificity phosphatase. *Embo J* 15(14):3621–3632.
366. Muda M, et al. (1996) The dual specificity phosphatases M3/6 and MKP-3 are highly selective for inactivation of distinct mitogen-activated protein kinases. *J Biol Chem* 271(44):27205–27208.
367. Li C, Scott DA, Hatch E, Tian X, Mansour SL (2007) Dusp6 (Mkp3) is a negative feedback regulator of FGF-stimulated ERK signaling during mouse development. *Development* 134(1):167–176.
368. Cox DM, et al. (2003) Phosphorylation motifs regulating the stability and function of myocyte enhancer factor 2A. *J Biol Chem* 278(17):15297–15303.



369. Yang S-H, Kalkan T, Morrisroe C, Smith A, Sharrocks AD (2012) A Genome-Wide RNAi Screen Reveals MAP Kinase Phosphatases as Key ERK Pathway Regulators during Embryonic Stem Cell Differentiation. *Plos Genet* 8(12):e1003112–e1003112.
370. Auger-Messier M, et al. (2013) Unrestrained p38 MAPK activation in *Dusp1/4* double-null mice induces cardiomyopathy (vol 112, pg 48, 2013). *Circ Res* 112(3):E32–E32.
371. Wu ZG, et al. (2000) P38 and Extracellular Signal-Regulated Kinases Regulate the Myogenic Program at Multiple Steps. *Mol Cell Biol* 20(11):3951–3964.
372. Bennett AM, Tonks NK (1997) Regulation of distinct stages of skeletal muscle differentiation by mitogen-activated protein kinases. *Science* (80- ) 278(5341):1288–1291.
373. Li J, Johnson SE (2006) ERK2 is required for efficient terminal differentiation of skeletal myoblasts. *Biochem Biophys Res Commun* 345(4):1425–1433.
374. Youn HD, Liu JO (2000) Cabin1 represses MEF2-dependent Nur77 expression and T cell apoptosis by controlling association of histone deacetylases and acetylases with MEF2. *Immunity* 13(1):85–94.
375. Weston AD, Sampaio A V, Ridgeway AG, Underhill TM (2003) Inhibition of p38 MAPK signaling promotes late stages of myogenesis. *J Cell Sci* 116(14):2885–2893.
376. Papait R, et al. (2013) Genome-wide analysis of histone marks identifying an epigenetic signature of promoters and enhancers underlying cardiac hypertrophy. *Proc Natl Acad Sci U S A* 110(50):20164–20169.
377. Bengal E, et al. (1992) Functional Antagonism between C-Jun and Myod Proteins - a Direct Physical Association. *Cell* 68(3):507–519.
378. Li L, Chambard JC, Karin M, Olson EN (1992) Fos and Jun Repress Transcriptional Activation by Myogenin and Myod - the Amino Terminus of Jun can Mediate Repression. *Genes Dev* 6(4):676–689.
379. Blum R, Vethantham V, Bowman C, Rudnicki M, Dynlacht BD (2012) Genome-wide identification of enhancers in skeletal muscle: the role of MyoD1. *Genes Dev* 26(24):2763–2779.

380. Romanick M, Thompson L V, Brown-Borg HM (2013) Murine models of atrophy, cachexia, and sarcopenia in skeletal muscle. *Biochim Biophys Acta* 1832(9):1410–20.
381. Morley JE, Baumgartner RN, Roubenoff R, Mayer J, Nair KS (2001) Sarcopenia. *J Lab Clin Med* 137(4):231–243.
382. Kotler DP (2000) Cachexia. *Ann Intern Med* 133(8):622–634.
383. Kadar L, Albertsson M, Areberg J, Landberg T, Mattsson S (2000) The prognostic value of body protein in patients with lung cancer. *Ann N Y Acad Sci* 904:584–591.
384. Prado CMM, et al. (2009) Sarcopenia as a Determinant of Chemotherapy Toxicity and Time to Tumor Progression in Metastatic Breast Cancer Patients Receiving Capecitabine Treatment. *Clin Cancer Res* 15(8):2920–2926.
385. Sandri M, et al. (2004) Foxo transcription factors induce the atrophy-related ubiquitin ligase atrogin-1 and cause skeletal muscle atrophy. *Cell* 117(3):399–412.
386. Stitt TN, et al. (2004) The IGF-1/PI3K/Akt pathway prevents short article expression of muscle atrophy-induced ubiquitin ligases by inhibiting FOXO transcription factors. *Mol Cell* 14(3):395–403.
387. Lach-Trifilieff E, et al. (2014) An Antibody Blocking Activin Type II Receptors Induces Strong Skeletal Muscle Hypertrophy and Protects from Atrophy. *Mol Cell Biol* 34(4):606–618.
388. Zhou X, et al. (2010) Reversal of Cancer Cachexia and Muscle Wasting by ActRIIB Antagonism Leads to Prolonged Survival. *Cell* 142(4):531–543.
389. Raben N, et al. (2008) Suppression of autophagy in skeletal muscle uncovers the accumulation of ubiquitinated proteins and their potential role in muscle damage in Pompe disease. *Hum Mol Genet* 17(24):3897–908.
390. Masiero E, et al. (2009) Autophagy Is Required to Maintain Muscle Mass. *Cell Metab* 10(6):507–515.
391. Demontis F, Perrimon N (2010) FOXO/4E-BP signaling in Drosophila muscles regulates organism-wide proteostasis during aging. *Cell* 143(5):813–25.

392. Angel P, et al. (1987) Phorbol ester-inducible genes contain a common cis element recognized by a TPA-modulated trans-acting factor. *Cell* 49(6):729–39.
393. Nagy G, Dániel B, Jónás D, Nagy L, Barta E (2013) A novel method to predict regulatory regions based on histone mark landscapes in macrophages. *Immunobiology* 218(11):1416–1427.
394. Ma Q, Telese F (2015) Genome-wide epigenetic analysis of MEF2A and MEF2C transcription factors in mouse cortical neurons. *Commun Integr Biol*:00–00.
395. Alli NS, et al. (2013) Signal-dependent fra-2 regulation in skeletal muscle reserve and satellite cells. *Cell Death Dis* 4:e692–e692.
396. Windak R, et al. (2013) The AP-1 transcription factor c-Jun prevents stress-imposed maladaptive remodeling of the heart. *PLoS One* 8(9):e73294.
397. Lin J, et al. (2014) Downregulation of the tumor suppressor HSPB7, involved in the p53 pathway, in renal cell carcinoma by hypermethylation. *Int J Oncol* 44(5):1490–8.
398. Ju J-S, Varadhachary AS, Miller SE, Wehl CC (2010) Quantitation of “autophagic flux” in mature skeletal muscle. *Autophagy* 6(7):929–35.
399. Eferl R, et al. (2004) The Fos-related antigen Fra-1 is an activator of bone matrix formation. *EMBO J* 23(14):2789–99.
400. Fleischmann A (2000) Fra-1 replaces c-Fos-dependent functions in mice. *Genes Dev* 14(21):2695–2700.
401. Carlier MF, et al. (1997) Actin depolymerizing factor (ADF/cofilin) enhances the rate of filament turnover: Implication in actin-based motility. *J Cell Biol* 136(6):1307–1322.
402. Thompson TG, et al. (2000) Filamin 2 (FLN2): A muscle-specific sarcoglycan interacting protein. *J Cell Biol* 148(1):115–126.
403. Doran P, Gannon J, O’Connell K, Ohlendieck K (2007) Aging skeletal muscle shows a drastic increase in the small heat shock proteins alpha B-crystallin/HspB35 and cvHsp/HspB7. *Eur J Cell Biol* 86(10):629–640.

404. Perisic L, et al. (2012) Plekhh2, a novel podocyte protein downregulated in human focal segmental glomerulosclerosis, is involved in matrix adhesion and actin dynamics. *Kidney Int* 82(10):1071–1083.
405. Vos MJ, Kanon B, Kampinga HH (2009) HSPB7 is a SC35 speckle resident small heat shock protein. *Biochim Biophys Acta-Molecular Cell Res* 1793(8):1343–1353.
406. Andreucci JJ, et al. (2002) Composition and function of AP-1 transcription complexes during muscle cell differentiation. *J Biol Chem* 277(19):16426–32.
407. Kuo T, et al. (2012) Genome-wide analysis of glucocorticoid receptor-binding sites in myotubes identifies gene networks modulating insulin signaling. *Proc Natl Acad Sci U S A* 109(28):11160–11165.
408. Garrido C, Paul C, Seigneuric R, Kampinga HH (2012) The small heat shock proteins family: The long forgotten chaperones. *Int J Biochem Cell Biol* 44(10):1588–1592.
409. Krief S, et al. (1999) Identification and characterization of cvHsp. A novel human small stress protein selectively expressed in cardiovascular and insulin-sensitive tissues. *J Biol Chem* 274(51):36592–600.
410. Chiu T-F, et al. (2012) Association of Plasma Concentration of Small Heat Shock Protein B7 With Acute Coronary Syndrome. *Circ J* 76(9):2226–2233.
411. Rosenfeld GE, Mercer EJ, Mason CE, Evans T (2013) Small heat shock proteins Hspb7 and Hspb12 regulate early steps of cardiac morphogenesis. *Dev Biol* 381(2):389–400.
412. Minoia M, Grit C, Kampinga HH (2014) HSPA1A-Independent Suppression of PARK2 C289G Protein Aggregation by Human Small Heat Shock Proteins. *Mol Cell Biol* 34(19):3570–3578.
413. Vos MJ, et al. (2010) HSPB7 is the most potent polyQ aggregation suppressor within the HSPB family of molecular chaperones. *Hum Mol Genet* 19(23):4677–4693.
414. Homma S, et al. (2006) BAG3 Deficiency Results in Fulminant Myopathy and Early Lethality. *Am J Pathol* 169(3):761–773.
415. Garnier S, et al. (2015) Involvement of BAG3 and HSPB7 loci in various etiologies of systolic heart failure: Results of a European collaboration assembling more than 2000

- patients. *Int J Cardiol* 189:105–7.
416. Sun X, et al. (2004) Interaction of human HSP22 (HSPB8) with other small heat shock proteins. *J Biol Chem* 279(4):2394–402.
  417. Carra S, Seguin SJ, Landry J (2008) HspB8 and Bag3: a new chaperone complex targeting misfolded proteins to macroautophagy. *Autophagy* 4(2):237–9.
  418. Shaulian E, Karin M (2002) AP-1 as a regulator of cell life and death. *Nat Cell Biol* 4(5):E131–E136.
  419. Hess J, Angel P, Schorpp-Kistner M (2004) AP-1 subunits: quarrel and harmony among siblings. *J Cell Sci* 117(Pt 25):5965–73.
  420. Jonat C (1990) Antitumor promotion and antiinflammation: Down-modulation of AP-1 (Fos/Jun) activity by glucocorticoid hormone. *Cell* 62(6):1189 – 1204.
  421. Herrlich P (2001) Cross-talk between glucocorticoid receptor and AP-1. *Oncogene* 20(19):2465–2475.
  422. Adcock IM, Caramori G (2001) Cross-talk between pro-inflammatory transcription factors and glucocorticoids. *Immunol Cell Biol* 79(4):376–384.
  423. Biddie SC, et al. (2011) Transcription factor AP1 potentiates chromatin accessibility and glucocorticoid receptor binding. *Mol Cell* 43(1):145–55.
  424. Ervasti JM, Campbell KP (1993) A role for the dystrophin-glycoprotein complex as a transmembrane linker between laminin and actin. *J Cell Biol* 122(4):809–23.
  425. Zheng B, Han M, Bernier M, Wen J (2009) Nuclear actin and actin-binding proteins in the regulation of transcription and gene expression. *FEBS J* 276(10):2669–85.
  426. Oren A, et al. (1999) The Cytoskeletal Network Controls c-Jun Expression and Glucocorticoid Receptor Transcriptional Activity in an Antagonistic and Cell-Type-Specific Manner. *Mol Cell Biol* 19(3):1742–1750.
  427. Moore-Carrasco R, et al. (2006) The AP-1/CJUN signaling cascade is involved in muscle differentiation: implications in muscle wasting during cancer cachexia. *FEBS Lett*

580(2):691–6.

428. Moore-Carrasco R, et al. (2007) The AP-1/NF-kappaB double inhibitor SP100030 can revert muscle wasting during experimental cancer cachexia. *Int J Oncol* 30(5):1239–45.
429. Choi M-C, et al. (2012) A Direct HDAC4-MAP Kinase Crosstalk Activates Muscle Atrophy Program. *Mol Cell* 47(1):122–132.
430. Eferl R, Wagner EF (2003) AP-1: a double-edged sword in tumorigenesis. *Nat Rev Cancer* 3(11):859–68.
431. Ke L, et al. (2011) HSPB1, HSPB6, HSPB7 and HSPB8 protect against RhoA GTPase-induced remodeling in tachypaced atrial myocytes. *PLoS One* 6(6):e20395.
432. Golenhofen N, Perng M Der, Quinlan RA, Drenckhahn D (2004) Comparison of the small heat shock proteins alphaB-crystallin, MKBP, HSP25, HSP20, and cvHSP in heart and skeletal muscle. *Histochem Cell Biol* 122(5):415–25.
433. Matkovich SJ, et al. (2010) Cardiac signaling genes exhibit unexpected sequence diversity in sporadic cardiomyopathy, revealing HSPB7 polymorphisms associated with disease. *J Clin Invest* 120(1):280–9.
434. Rubinsztein DC, Mariño G, Kroemer G (2011) Autophagy and aging. *Cell* 146(5):682–95.
435. García-Prat L, et al. (2016) Autophagy maintains stemness by preventing senescence. *Nature* 529(7584):37–42.
436. Purcell NH, et al. (2007) Genetic inhibition of cardiac ERK1/2 promotes stress-induced apoptosis and heart failure but has no effect on hypertrophy in vivo. *Proc Natl Acad Sci U S A* 104(35):14074–9.

## APPENDIX

### Expanded Material and Methods

#### CaCl<sub>2</sub> Transfection in C2C12

##### Day 1

Seed  $12.5 \times 10^3$  cells/well for a 2 ml well.

Or  $1.0 \times 10^5$  cells/ plate for a 10 ml plate.

##### Day 2

3 hr prior to transfection add either 2 or 10 ml of fresh media to encourage proliferation.

At time of transfection cells should be at 40-50% confluency; i.e. cells should not be touching.

Cell contact causes differentiation and so does low serum.

##### Day 3

16 hr after transfection, wash 2X with PBS and add fresh medium.

Allow cells to recover for 24 hr (harvest 48 hr post-transfection).

#### Transfection Preparation

- 1) Aliquot HEBS from 2X stock (dilute to 1X).
  - Ex 300  $\mu$ l Hebes + 300ul CaCl<sub>2</sub>+DNA.
- 2) Make Master Mix in 2 ml tubes; Add DNA first!
  - Add the appropriate volumes of DNA. For C2C12 in a 10 ml plate this should be a total of 25  $\mu$ g DNA. For 2 ml well this should be 5  $\mu$ g of total DNA.
  - Add ddH<sub>2</sub>O – pipette up and down \*Beware: smaller pipette tips will shear DNA.
- 3) Add CaCl<sub>2</sub> mix to MM tubes.
  - Ensure mixing by tapping.
- 4) Vortex tube that has HEBS (2.8 M NaCl, 15 mM Na<sub>2</sub>HPO<sub>4</sub>, 50 mM HEPES at pH 7.15).
  - While vortexing add dropwise the complete MM solution.
  - Solution will become slightly cloudy as precipitate forms.
- 5) Give slight mix before adding transfection mixture to cell wells.
  - As you add, agitate plate and add in dropwise manner.

#### Lipofectamine Transfection in C2C12

##### Day 1

- 1) Seed cells at  $2.0 \times 10^5$  cells per 10 ml plate.

##### Day 2

- 1) Cell should be 80-90% confluent. Dilute DNA into final volume of 500  $\mu$ l in DMEM (serum free media).
  - Dilute 35  $\mu$ l Lipofectamine into final volume of 500  $\mu$ l in DMEM (serum free media).

- Incubate both solutions for 5 minutes.
- 2) Add 4 ml DMEM (SFM) to cells.
- Mix DNA mixture with Lipo mixture = 1 ml total. Incubate for 20 minutes at room temperature. After 20 minutes has passed, to this volume add an additional 3 ml DMEM (SFM).
- 3) Wash cells with DMEM (serum free media) 2X.
- 4) The 4 ml of DNA:lipo solution can now be added to the 4ml in the dish.
- 5) Total volume of 8 ml is incubated for 5 hours.
- 6) After 5 hours add 20% serum; i.e. 2 ml serum FBS (found in fridge in 50 ml aliquot).  
**Make sure** that this is thawed in advance!

### Day 3

- 1) In the morning wash cells 2X with PBS and add 10 ml 10% FBS (GM).
- 2) Check confluency and fluorescent signal. If the signal is not strong enough, let recover 5-8 hours or if they are ready, harvest or add DM.

## Chromatin Immunoprecipitation Protocol

**Cell Culture:** This protocol prepares four aliquots of chromatin for four possible IPs.

1. Plate cells: 2-4 confluent 100 mm dishes or 1-2 confluent 150 mm<sup>2</sup>
  - Collect approximately  $1 \times 10^7 - 5 \times 10^7$  cells per treatment.
  - Use a spare plate for counting if necessary.

### Day 1

#### A. Cross-link cells

- 1) At room temperature wash plate once with PBS.
- 2) Add 10 ml of PBS followed by 270  $\mu$ l of 37% Formaldehyde.
  - Final formaldehyde concentration of 1%.
  - Do not use formaldehyde past expiration date.
  - Do not over cross link.
- 3) Incubate at RT for 10 min.
  - Agitation of cells is not necessary, but slow rocking is ok.
- 4) Quench cross-linking reaction by adding 1.25 M glycine (10X Glycine) dropwise to each plate for a final concentration of 0.125 M glycine.
  - 1 ml per 10 ml dish.
  - Incubate for 5 min with slow rocking.
- 5) Place dishes on ice. Pour into formaldehyde waste. Wash with ice cold PBS 3X. Aspirate on last wash to remove as much PBS as possible.
- 6) On ice scrape cells into 1 ml of ice cold PBS containing Roche tablet and PMSF.
  - 1 Roche Tablet per 10.5 ml PBS + 105  $\mu$ l PMSF.
- 7) Pellet cells by centrifugation at 3000-5000 rpm for 5 minutes at 4 degrees.



- 8) Remove supernatant. Resuspend pellet with 1 ml of **Wash Buffer 1** (10mM HEPES pH 6.5, 0.5 mM EGTA, 10 mM EDTA, 0.25% Triton X-100, 1 Roche tablet, PMSF).
- 9) Incubate on ice for 5 minutes.
- 10) Centrifuge at 3000-5000 rpm for 5 min at 4 degrees.
- 11) Remove supernatant. Resuspend nuclei in 1 ml of **Wash Buffer 2** (10mM HEPES pH 6.5, 0.5 mM EGTA, 1 mM EDTA, 200mM NaCl, 1 Roche tablet, PMSF).
- 12) Incubate on ice for 10 minutes.
- 13) Centrifuge at 3000-5000 rpm for 5 minutes at 4 degrees.
- 14) Remove supernatant. Either continue to immediately to **Day 2** or nuclei can be frozen at -80 degrees.

## Day 2

### A. Nuclear lysis

1. To nuclei add 500  $\mu$ l of **SDS lysis buffer** (50mM Tris-HCl pH 8.1, 1-mM EDTA, 1% SDS, plus Roche tablet and PMSF).
  - Buffer must be prepared fresh.
  - Pipette gently, avoid forming bubbles, work quickly as SDS will precipitate on ice.
  - You may want to consider using 0.1% SDS if too many bubbles are forming.
2. Sonicate to break up DNA to approximately 500 bp fragments.
  - Gel sample should be run on 2.5-3% agarose to confirm fragment size following DNA purification.
  - \*\*\*Can remove an unsonicated sample to run alongside the sheared sample for a comparison.
  - Sonicate on ice as sonicating produces heat which can denature the DNA.
3. Centrifuge samples at 14000 rpm for 15 min at 4 degrees to remove insoluble materials. If SDS precipitates, leave briefly at RT.
4. Transfer **supernatant** to new tubes.
  - aliquot 4x100  $\mu$ l for IP (store at -80 for up to a few months; label as XLSC for crosslinked sheared chromatin).
  - 2 x 20  $\mu$ l aliquots for gel and input samples (store at -20) or proceed to Day 3 Step 12 to get DNA concentration.
  - avoid multiple freeze thawing.

\* Gel and input samples should be DNA purified (Day 3-4) and the chromatin concentration should be calculated prior to any IPs.

### B. Pre-blocked Protein G

Incubate 15 µl of protein G dynal beads (Invitrogen) with 20 µg of salmon sperm DNA for each IP in **IP dilution buffer**.

- 15 µl beads + 135 µl IP dilution buffer + 20 µg (2 µl of 10 mg/ml) salmon sperm per IP.
- Ex: for 10 IPs: 150ul beads + 1.35 ml IP dilution buffer + 20 µl salmon sperm DNA.
- Incubate O/N at 4 degrees.

\*Make 0.5 extra IP.

\* Protein G and Protein A have different affinities for different animal immunoglobulins. Use the appropriate one. A mix of the two can also be used.

### C. Lysate-antibody Incubation

1. Once the DNA concentration is known, an equivalent of 25 µg per IP is recommended.
2. Dilute sample 1:10 with IP dilution buffer (0.01% SDS, 1.1% Triton-X 100, 1.2 mM EDTA, 16.7 mM Tris-HCl pH 8.1, 167 mM NaCl) to 1 ml.
  - I.e. add 900 µl of **IP dilution buffer** to 100 µl of XLSC.
3. Add 1-2 µg of antibody. Some antibodies have recommended dilution of antibody: chromatin ratio. Some antibodies must have the appropriate concentration determined empirically. 1-10 µg of antibody per 25 µg of DNA often works well. Use the equivalent in the IgG control.
  - **Note:** A beads-only control can also be prepared but this requires more XLSC samples.
4. Rotate at 4 degrees O/N.

### Day 3

#### A. Incubation with Dynabeads and Recovering Bound DNA

1. Add 152 µl of pre-blocked beads (beads+buffer+salmon sperm DNA) to each IP reaction. Rotate at 4 degrees for 1 hour.
2. Using magnet remove supernatant.
3. Wash beads with 1 ml of **cold IP Low Salt Immune Complex Wash buffer 1** (20 mM Tris pH 8.1, 2mM EDTA, 150 mM NaCl, 1% Triton-X 100, 0.1% SDS). Rotate at 4 degrees for 5-10 minutes.
4. Using magnet remove supernatant.
5. Wash beads with 1 ml of **cold IP High Salt Immune Complex Wash buffer 2** (20 mM Tris pH 8.1, 2 mM EDTA, 500 mM NaCl, 1% Triton X-100, 0.1% SDS). Rotate at 4 degrees for 5-10 minutes.
6. Using magnet remove supernatant.
7. **Wash beads with 1 ml of cold LiCl Immune Complex Wash buffer 3** (10 mM Tris pH 8.1, 0.25M LiCl, 1 mM EDTA, 1% NP-40, 1% Deoxycholate). Rotate at 4 degrees for 5-10 minutes.
8. Wash beads with 2X with TE. Rotate at 4 degrees for 2 x 15 minute washes.
9. Using magnet, remove supernatant.

10. Elute Protein-DNA complexes from the beads by adding 300 µl of **freshly made Elution Buffer** (0.1 M NaHCO<sub>3</sub>, 1% SDS). Incubate with rotation for 30 minutes at RT.  
Use this elution buffer also for input and gel samples.
11. Using magnet collect supernatant in fresh tubes. **DO NOT THROW AWAY SUPERNATANT.**
12. For input and gel samples make up to 300 µl of **elution buffer** so it will have the same volume as the IP sample.
13. To recovered complexes (IP) add 12 µl of **5M NaCl**. Add the same amount of 5M NaCl to input and gel samples. (Reverses cross links).
14. Incubate at 65 degrees for 4-5 hours or O/N.

#### Day 4

##### **DNA Purification** (Using Qiagen PCR clean up kit)

1. Add 6 µl of 0.5 M EDTA, 12 µl of 1 M Tris-HCl pH 6.5, 1.2 µl of 10 mg/ml proteinase K, incubate for 1 hour at 45 degrees in the water bath.
  - proteinase K may have to be made up fresh.
2. Purify DNA using Qiagen PCR clean up kit. Elute into 50 µl of nuclease free water. For gel samples elute with 30 µl of elution buffer.

Eluate is now purified DNA and can be analyzed immediately or stored frozen at -20 degrees.

#### **Harvesting C2C12 Cells (Whole cell extracts)**

On Ice:

- Aspirate/dump old media out of dish.
- Wash 2X PBS; Add 700 µl of PBS onto plate; Scrape into tubes using rubber policeman.
- Pellet cells: 1.5g for 5 minutes.
- Aspirate PBS.
- Add 100 µl of (or 5x the pellet size) NP-40 lysis buffer or β-gal depending on protocol.
- Pipette up and down to break cells.
- Vortex for 10 sec, Incubate on ice 5 min. Repeat 3X.
- Spin at max speed 15 min.
- Store supernatant at -80°C.

Lysis Buffer Ingredients:

PMSF, Sodium Othrovanadate, Protease Inhibitor.

- Add to NP-40 lysis buffer in 1:100 ratio.

NP-40 Lysis Buffer: Make up to 100 ml, store at 4°C.

Volume	Stock	Take	Final Concentration
250 ml	1 M Tris pH 8.0	5 ml	50 mM

250 ml	5 M NaCl	3 ml	150 mM
50 ml	10% NP-40	5 ml	0.5 %
100 ml	0.5 M EDTA pH 8.0	400 $\mu$ l	2 mM
100 ml	0.5 M NaF	20 ml	100 mM
100 ml	0.1 M Na Pyrophos.	10 ml	10 mM

### Transformation

- 1) Stock expression plasmids should be diluted to 10ng/ $\mu$ l in a -20 freezer for easy transformation.
    - Carrier DNA (has no promoter): Bluescript (pBSK), etc.
    - Marker of transfection: ds Red, GFP.
    - Backbone: pMT2, pcDNA, etc.
    - DNA effectors: Mef2a, Mef2c, etc.
  
  - 2) Obtain competent cells: E. Coli XL1Blue.
    - Once thawed, can't reuse.
    - Thaw on ice.
    - Must be grown at a certain OD prior to freezing.
  
  - 3) Add 1  $\mu$ l (10ng) of expression plasmid to 50  $\mu$ l of E. Coli.
    - Add plasmid to tube first.
    - Pipette up and down once.
    - Incubate on ice for 30 minutes.
  
  - 4) Heat Shock: 1 min at 42°C water bath.
    - Follow up with 2 min on ice.
    - In the meantime take out LB plates and warm them in 37 degree room.
    - Put bacterial waste in a designated waste.
  
  - 5) At room temperature add 200  $\mu$ l of LB+0.1% glucose by open flame to the bacteria.
  - 6) Put in water bath or incubator at 37°C for 30 minutes.
  - 7) Spin at 7000 rpm for 5 minutes. Remove supernatant.
  - 8) Resuspend in 50 $\mu$ l LB and plate by an open flame.
  - 9) Place the plates facing down at 37 degrees overnight. Next day put in 4°C or select colony and proceed with maxiprep. Keep plates for 1 week.
- \*This protocol is ideal for cloning new plasmids. You can do a 5 minute transformation protocol (NEB website) if transforming a standard plasmid.

## **C2C12 Cell Culture**

### **Thawing C2C12 cells**

- 1) Thaw cells in 37 degree bath.
- 2) Mix with 10 ml fresh Growth Medium (GM; DMEM plus 10%FBS, 1%Pen-Strep, 1% glutamine).
- 3) Spin for 5 min at 1.5g.
- 4) Aspirate media. Tap remaining cells to dislodge pellet.
- 5) Replace with 10 ml fresh GM and add to dish. Check 24 hr later.

### **Culturing C2C12 cells**

C2C12 should not be cultured if they grow beyond 90% confluency as they may have lost their proliferative capacity. To pass cells every second day, at 80% confluency, pass cells in a 1:10 ratio:

- 1) Wash 1-2X with Versene (0.2 g EDTA in PBS).
- 2) Add 1ml 0.125% Trypsin. Swirl around the dish and remove the majority of Trypsin. Cells should start to lift off of the plate. Tap if necessary to expedite the process.
- 3) Add 10 ml GM. Pipette up and down several times, and then use as necessary.
- 4) To form myotubes, allow cells to reach 90% confluency and then change to Differentiation Media (DM; 2% Horse Serum, 1% Pen-Strep, 1% Glutatmine). Add fresh medium every two days.

### **Freezing C2C12 cells**

- 1) Grow cells to 80% confluency.
- 2) Dissociate cells from plate using Trypsin.
- 3) Prepare 1 ml Freezing Medium (GM+10%DMSO) for each plate of cells that is to be frozen.
- 4) Resuspend the cells in Freezing Medium and aliquot 1ml into cryotubes. Place in -80 freezer or in liquid nitrogen for long term storage.

## **Luciferase Assay**

- 1) On ice, wash cells 2X with PBS.
- 2) Add 300 µl Luciferase assay Lysis buffer (20 mM Tris, pH 7.4, 0.1% Triton-X 100) and scrape cells using a rubber policeman into labelled tubes.
- 3) Vortex 10 sec.
- 4) Spin at max speed for 15 minutes at 4 degrees.
- 5) Transfer the supernatant to new tubes. Use 25-50 µl of solution in the luciferase assay.

## Bioinformatic Analysis

### General workflow of RNA-seq processing

Done by MUGQIC:

- 1: Sequence trimming (trimomatic)
- 2: Genome alignment (tophat/bowtie)
- 3: Read and alignment statistics (RNAseQC)
- 4: FPKM (cufflinks)
- 5: De novo transcript estimation (CuffCompare)
- 6: Raw read counts (htseq-count)
- 7: Saturation and correlation analysis (R)
- 8: UCSC tracks (Wiggle)
- 9: exploratory analysis (R - gqSeqUtils)
- 10: Differential gene expression (**edgeR** & **DESeq**)
- 11: Differential transcript expression (cuffdiff)
- 12: Gene ontology analysis (goseq)
- 13: HTML report (nozzle)

**edgeR** or **DESeq** genes and/or transcripts were used for downstream analysis:

DAVID Gene Ontology:

- 1) First upload (paste) your gene list on the left-hand side bar. Select identifier: This is usually “OFFICIAL\_GENE\_SYMBOL”. List type: Gene List. Identify species (e.g. mouse)
- 2) Expand “Gene Ontology” from the list of options generated. GOTERM\_BP\_FAT will tell you GO terms for Biological Processes (BP). Other GO terms are available as well.
- 3) You can scroll down and use Functional annotation clustering to combine all potential annotations into clusters

oPossum 3.0: [opossum.cisreg.ca/](http://opossum.cisreg.ca/)

- 1) Upload gene list to find regulatory regions in silico
- 2) There are different genomes and analysis options available

### General workflow of ChIP-seq processing

- 1) Reads were aligned to mm10 or rn5 genome by Peconic

- 2) BAM files provided by Peconic were filtered using bedtools or samtools using functions to exclude reads with phred scores lower than 37 and to remove duplicates (Picard)
- 3) Resulting IgG or ChIP sequencing BAM files were used as inputs for MACS peak calling using “no model” option which generates bed files for downstream analysis

## Programs

- 1) MACS (Model-based analysis for ChIP-Seq) <http://liulab.dfci.harvard.edu/MACS/>
- 2) Picard <http://broadinstitute.github.io/picard/>
- 3) Samtools <http://samtools.sourceforge.net/>
- 4) Bedtools <http://bedtools.readthedocs.org/en/latest/>

## Definitions

Expanded definitions can be found under UCSC Frequently Asked Questions: Data File Formats at <https://genome.ucsc.edu/FAQ/FAQformat.html>

**BED files:** multiple data sets; format .bed (tabs) or .gz or .gff (general feature format, no tabs)

A header line gives a reference spot to examine in the genome. Therefore if you have two headers you can have two datasets to look at on the genome browser.

**BAM:** compressed binary file. Must be converted to sam to visualize with human eyes.

Blue and red alignments represent sequenced hits

Pink are maps at more than 1 place, low mapability

.bai: indexed bam file

**Redundant read:** maps to multiple places

**Non-mappable read:** Doesn't map to anywhere in the genome

**Duplicate read:** can be real or may be an experimental artefact from PCR

## Analysis of ChIP-seq data

Bed files generated by MACS were uploaded to different programs using DEFAULT setting unless otherwise indicated.

- 1) GREAT (Genomics regions enrichment of annotation tool): predicts associated genes and functions. Input is a bed file
- 2) Centdist: find cis elements in bed file (input)
- 3) UCSC Liftover function: lets you convert genome alignment files between species. To compare rat vs mouse (cardiac vs skeletal muscle) we used mm9. To compare AP-1 sites to MEF2A sites in skeletal muscle we also converted everything to mm9.

- 4) UCSC intersect: We found overlapping MEF2A (cardiac vs skeletal muscle) or MEF2A and AP-1 binding events using UCSC Table Browser, uploading custom tracks, and selecting intersection. DEFAULT settings were used
- 5) Integrative Genome Viewer (IGV): Similar to UCSC genome browser in the sense that you can visualize ChIP-seq data but works much faster and lets you move around the genome faster. Does not allow manipulation of data, only visualization